NORTHWESTERN UNIVERSITY

Modeling Filamin C Mutations Causing Cardiomyopathy

A DISSERTATION

SUBMITTED TO THE GRADUATE SCHOOL

IN PARTIAL FULFILLMENT OF THE REQUIREMENTS

for the degree

DOCTOR OF PHILOSOPHY

Field of Biochemistry and Molecular Genetics

By:

Joyce Chimdinma Ohiri

EVANSTON, ILLINOIS

SEPTEMBER 2023

ABSTRACT

Heart failure is a growing clinical problem, and inherited cardiomyopathies contribute significantly to heart failure. Among the many genes associated with inherited cardiomyopathies, mutations in *FLNC*, the gene encoding the cytoskeletal protein filamin C, associate with a range of cardiomyopathy and increased risk for arrhythmia and sudden cardiac death in patients. Filamin C consists of three distinct domains: an actin-binding domain (ABD), a rod domain (RD), and a dimerization domain (DD). As a cytoskeletal protein, filamin C plays an important role in maintaining the structural integrity of the sarcomere in cardiac and skeletal muscle. Filamin C localizes at the Z-disk, an anchoring site for both titin and actin, and also at the sarcolemma. Proteostasis in an essential cellular process to maintain healthy protein quality control. Bcl-2-associated athanogene 3 (BAG3) mediates the autophagy pathway through its interaction with several heat shock factor proteins as a mechanism for proteostasis. However, it is not known what role the BAG3/filamin C interaction plays in the etiology of *FLNC*-linked DCM and arrhythmogenesis. I created novel physiological cell lines from patients with mutated *FLNC* and cardiomyopathy as well as gene edited *FLNC* isogenic cell lines. These induced pluripotent stem cell lines were differentiated to cardiomyocytes to directly measure the effect of loss of Filamin C on phenotypic expression. Proteotoxic and mechanical stressors were applied, and electrophysiological properties were measured to model the physiological responses of stressed cardiomyocytes *in vitro*. These studies showed that filamin C was required for a normal response to proteotoxic stress, and that in the absence of filamin C, cellular surrogate markers for arrhythmia were increased. This study contributes to the definition of clinical and molecular findings associated with mutation in *FLNC*.

ACKNOWLEDGEMENTS

I would like to thank Elizabeth McNally for her support and guidance throughout this project. As a physician-scientist at the top of your field, you have shown what it means to be a leading woman in science despite adversity. Thank you for providing the resources to conduct innovative, groundbreaking science and the opportunity to work alongside some of the smartest people I have ever met. Your avid love for basketball has created a fun, competitive (in a good way), and collaborative environment that is as intellectually stimulating as it is fun. You have provided balance in the lab and put the heart into science (literally).

I would also like to thank my committee chair, Dr. Alfred George for his relentless support and helping drive my committee members. We have had a great bond since my individualized study sessions with you years ago and I am in awe of the mentor that you are and continue to be. Thank you to Dr. Lisa Wilsbacher, my committee member and other favorite physician-scientist. You have been consistently kind and gracious from the first day I met you and are a stand-up woman in science whose career will go as far as you believe. A special thanks to my committee members, Dr. Tsutomu Kume and Dr. Congcong He, for your incessant support and encouragement during my tenure at Northwestern.

Many thanks to Dr. Dominic Fullenkamp for establishing cell culture techniques in the lab that were pivotal for performing these experiments, helping me navigate my project to bring out its novelty and ensuring my experiments were thorough, and his continued mentorship in the lab both personally and professionally. A special thank you to Dr. Anthony Gacita, who was an instrumental piece in getting CRISPR off the ground in the lab and proving his expertise- I am grateful for having you as my lab buddy through it all. Many thanks to Dr. Tanner Monroe, my favorite troll, whose zeal for science keeps me on my toes and allows me to constantly think outside of the box. I would like to thank Dr. Ellis Kim and Dr. Eugene Wyatt for bringing the induced pluripotent stem cell technology into the lab- none of this would be possible without the initial hard work from you two. Thank you to Dr. David Barefield, Dr. Alexis Demonbreun and Dr. Megan Puckelwartz for stepping in during key moments to help with brainstorming

idea and data analysis. To team TC- our very own startup within the lab, for providing a safe space to laugh, cry and share scientific ideas (when we aren't laughing and crying). To my lab foodies- thank you for matching my love for freebies and going on scavenger hunts for free food with me as we continue to help Northwestern University become more sustainable through our healthy appetites. I am very appreciative of the forever friends I have gained in the lab, most especially Lauren Vaught and Kate Fallon, who have always provided a listening ear and been a solid source of support in the lab. I am very appreciative of the McNally lab, both old and new, for all the highs and the lows. This experience has undeniably made me a better scientist. For every entertaining lab meeting, Christmas party, Thanksgiving potluck, March Madness, lab outing, and kumbaya moment- I wouldn't change it for the world.

I would like to thank God for making me the woman I am today. Thank you for being my north star and giving me purpose every day to do the work I love. My unrelenting faith has gotten me through my toughest moments and is the sole reason I have made it this far. During my PhD, I became fully immersed in my community at St. Josephs Roman Catholic church and life group, which I am forever thankful for. In my last year, I took part in the Alpha program at church which has reshaped how I approach my faith in the most beautiful way. I have always said this is the most unique catholic church I have ever attended…and it is the perfect fit for me.

Thank you to the Nigerian community, both in the states and abroad. I am a very lucky gal to be a first-generation Nigerian-American and dual citizen who has had the privilege to go to the motherland several times, including two times during graduate school. Every visit is a new adventure and I have loved every moment of celebrating my ancestors, reconnecting with extended family, and cherishing new friendships. I look forward to visiting again soon, indulging in our rich culture through food, music, and dance, and becoming fluent in Igbo. Nigeria made me, America raised me, and I am truly a daughter of the soil. I meela.

My family is one of one, ten over ten, my rock and my hard place (just kidding!). You all are the reason I chose this journey in the first place and deserve this degree as much as me (but it'll be in my name). To

my father, king of kings, who came to America and made a man of himself. From working as an ice cream man to pay off your graduate school loans as a civil engineer, while we lived in a small two-bedroom apartment in Adelphi, you have laid the foundation for us. You are truly the American dream. Thank you for engraining your love for education into us and creating a warm environment to explore our creativity and athleticism from childhood- these memories have marvelously molded me. To my mother, the best woman I know hands down. She is my confidant, prayer partner, jokester, gister, dancing queen, and personal chef (quite literally the best cook I know). Your grace is effortless and your grit is unmatched. Thank you for all the sacrifices you had made for our family and for showing me how to be an amazing wife and mother. You are unconditional love personified. To my older sister- thank you for being my travel buddy and fellow fashionista and putting up with my annoyances throughout the years. To my older brother, the other PhD, thank you for providing the blueprint, mentoring me, cheering for me, and keeping me up to date on everything sports. To my little sister, aka my mini-me, you are the twin I always wished I had. I have so much to say, but only you can match my fire.

They say you are the company you keep, and I am proud to say I have lifelong friends that are now family. To my college roomies, thank you for providing a constant source of love, life, and laughter. We have gone through so many life changing moments together and I am happy to have had you two by my side through it all. I said it once and I'll say it again- the Marsala girls are undefeated. The best is yet to come. To my high school and college friends, you all mean the world to me. You all inspire me every day to chase after my dreams. Thank you for making me laugh until my stomach hurts and speaking life into me. I am so grateful for your kinship. The best is yet to come. To my sister-friends- the our mothers' friendship has brought us closer together and our friendship will last a lifetime. You all are some of the most enlightening, lovable, well-rounded, and cultured women I know. I look forward to our future family vacations together.

The road is long, but the journey continues. My story has just begun.

LIST OF ABBREVIATIONS

Actin-binding domain- ABD
Arrhythmogenic cardiomyopathy- ACM
Bcl-2-associated athanogene 3- BAG3
Cardiac Troponin- TNNT2, cTnT
Cardiovascular disease- CVD
Chaperone assisted selective autophagy- CASA
Conditional knockout- cKO
Desmin- DES
Dilated cardiomyopathy- DCM
Dimerization domain- DD
Duchenne Muscular Dystrophy- DMD
Dystrophin-glycoprotein complex- DGC
Human embryonic stem cell derived cardiomyocytes- hESC-CMs
Hypertrophic cardiomyopathy- HCM
Immunoglobin- Ig
iPSC- Induced pluripotent stem cells
iPSC-CMs- Induced pluripotent stem cell derived cardiomyocytes
Lamin- LMNA
Left ventricle- LV
Left ventricular ejection fraction- LVEF
Limb girdle muscular dystrophy- LGMD
Mammalian target of rapamycin- mTOR
Mitogen-activated protein kinase- MAPK
Multielectrode array- MEA
Myofibrillar Myopathy- MFM
Myosin binding protein C- MYBPC3
Myosin heavy chain 7- Myh7
Nonsense mediated decay- NMD
Nonsustained ventricular tachycardia- NSVT
Protein quality control- PQC
Restrictive cardiomyopathy- RCM
RNA binding motif protein 20- Rbm20
Rod domain- RD
Sudden cardiac death- SCD
Titin- TTN
Ubiquitin proteasome system- UPS
Ventricular arrhythmia- VA

DEDICATION

I would like to dedicate this dissertation to my late grandparents- the patriarch and matriarch of my family. You have left no stone unturned, and I am here to carry on your legacy. I also appreciate all of the patients who have been a source of inspiration to keep daring, keep doing, and keep dreaming.

TABLE OF CONTENTS

LIST OF FIGURES AND TABLES

Chapter 1.

Introduction

I. Prologue

Cardiovascular disease (CVD) is a leading cause of death worldwide. Cardiomyopathies are defined as a heterogenous group of diseases that result in electrical and/or mechanical dysfunction within the myocardium, the muscular tissue of the heart, and can eventually lead to progressive heart failure and sudden cardiac death (SCD) (*1*). In the cardiomyopathies, cardiac structural and functional abnormalities are characterized by clinical phenotypes. There are distinct forms of cardiomyopathy defined by the appearance of the heart. These forms include dilated cardiomyopathy (DCM), hypertrophic cardiomyopathy (HCM), arrhythmogenic cardiomyopathy (ACM), and restrictive cardiomyopathy (RCM). Many forms of cardiomyopathy arise from genetic mutations, which are mostly but not exclusively inherited in an autosomal dominant manner. Genetic cardiomyopathy can affect both the ventricle and atria, and the associated arrhythmias can also affect the atria and ventricles with variable expressivity.

Due to the heterogeneity and complexity of cardiomyopathy, understanding the genotype-phenotype relationship is useful to provide prognostic information and guide treatment. The genotype-phenotype relationship is important for predicting clinical outcomes (*2*). In a study evaluating 281 patients with pathogenic or likely pathogenic DCM, genotype classification was more predictive of SCD and major ventricular arrhythmias after adjusting for age and sex (*3*). Genotype is a substantial predictor of clinical outcomes and a compass for developing strategic treatment methods. Among the clinical symptoms associated with cardiomyopathy, early-onset atrial fibrillation, conduction system disease, and early ventricular contractions can be part of the clinical picture (*4*). Improved understanding of genotype and phenotype correlations can also provide mechanistic clues to how specific mutations cause cardiomyopathy.

II. DCM and HCM- Clinical Phenotypes

DCM is a common form of cardiomyopathy affecting both adults and children. Characterized by the thinning and dilation of the left ventricle (LV), DCM is often associated with reduced left ventricular contractility **(Figure 1.1)**. Additional DCM criteria specify the degree of left ventricular dilation indexed to body mass, the degree of systolic dysfunction, and left ventricular ejection fraction (LVEF) <40%, and

DCM contributes to 60% of cardiomyopathy cases (*5, 6*). DCM can arise from ischemic, toxic, or genetic insult, and multiple etiologies can be present in the same patient. Genetic DCM, which primarily presents with an autosomal dominant pattern and has variable expressivity and penetrance (*7*). Approximately 1:6 patients with variants in DCM genes presented with clinical features related to a DCM genotype (*7, 8*). DCM frequently overlaps with heart failure with reduced ejection fraction (HFrEF), and these conditions are treated by guideline directed medical therapy which relies on multiple medications. Genetic diagnoses can help predict clinical course and arrhythmia risk. With increased genetic definition, it is hoped that gene-based treatments will reach the heart of the problem.

HCM is defined as the thickening of the left ventricle with impaired filling and relaxation. It is seen in 1:500 people and is a heterogenous disease that can be attributed to both genetic and environmental effects (*9*). Similarly to DCM, genetic HCM is often inherited in an autosomal dominant pattern (*10*). Patients with HCM often have a history of arrhythmia, including atrial fibrillation, with an increased stroke rate and potential progression to heart failure; in HCM the heart often displays hyperdynamic contraction and impaired relaxation of the heart (*11*). HCM is associated with at least 18 genes, and genetic mutations within the sarcomere are correlated with an increase in heart failure (*11*). Along with an electrocardiography, which is a non-invasive test that records electrical activity in the heart to identify abnormal function, cardiac imaging including both MRI and echocardiography are used to diagnose HCM. Genetic testing is also used to stratify the type of HCM and to identify at-risk family members (*12*). More specifically, cardiac magnetic resonance imaging can also identify features of HCM cases like scarring in the myocardium, which is not as easily seen by echocardiography (*13*). HCM affects both men and women and can present in all age groups. HCM is divided into “sarcomeric HCM”, indicating a mutation in a sarcomere gene, and “non-sarcomeric” HCM. The Sarcomeric Human Cardiomyopathy Registry (SHaRe) is one of the largest cohort assessments of HCM patients consisting of >24,000 patient-years. In this registry, younger patients with sarcomere mutations were more at-risk for atrial fibrillation and heart failure, which became more prevalent with increasing age (*14*). These symptoms are consequential effects of disrupted cardiac remodeling that exacerbate as the patient gets older. The SHaRe study further validates the lifetime burden of HCM disease and suggests that early treatments that target

cardiac remodeling could slow progression of disease. Understanding the genetic context underlying HCM is critical because it identifies potential targets for genetically-directed treatments.

III. Genetic Landscape of DCM and HCM

There are more than 250 genes associated with DCM (*15*). Encoded by the *TTN* gene, a single titin molecule spans half the length of the sarcomeric protein, and titin provides structural support for the adult heart. Titin's extensible region exerts a passive force as the sarcomere lengthens (*16*). *TTN* truncating mutations account for 20-25% of familial cases of DCM (*17*). This protein is responsible for maintaining sarcomere structure and healthy cardiac muscle function. Truncating *TTN* mutations have been shown to associate with arrhythmia and heart failure in DCM patients (*18*). *RBM20* encodes RNA binding motif protein 20 and is another gene associated with DCM. *RBM20* mutations account for 3% of DCM cases and the RBM20 protein regulates the splicing of many developmentally regulated genes in the heart (*19, 20*). *RBM20*-associated DCM has an earlier onset than DCM caused by mutations in *TTN* (*20*). Mutations in *RBM20* affect the splicing of other cardiac genes, especially *TTN*, and trigger adverse events within DCM. Deletion of *Rbm20* in mice upregulated compliant titin and reduced diastolic chamber stiffness (*21*). *TTN* and *Rbm20* are therapeutic targets to restore cardiac function and improve clinical outcomes in these genetic forms of cardiomyopathy.

The *LMNA* gene encodes for lamin A/C and is involved in 5-10% of familial DCM cases, and mutations in the gene often present in patients from ages 30-40 years old, with greater prevalence at a younger age in males than females (*22, 23*). *LMNA*-associated DCM presents with a history of arrhythmia, systolic dysfunction, and impaired calcium signaling. Defects in calcium signaling further disrupt homeostasis and impair the heart's functionality. Many signaling pathways are involved in diseases caused by *LMNA* mutations, otherwise known as laminopathies. Mammalian target of rapamycin (mTOR) was one of the several genes identified as a key regulator in *Lmna*-deficient mice, which displayed cardiac dysfunction and defective autophagy (*24, 25*). The mTOR pathway regulates physiological and pathological responses in many settings including the heart. Additionally, mTOR complex 1 was shown to be hyperactivated with loss of *Lmna* in cardiac muscle of mice while aggregates were reduced and

autophagy was restored following rapamycin treatment (*25*). Another pathway affected by *Lmna* mutations is the mitogen-activated protein kinase (MAPK) pathway. In mice with mutated *Lmna,* the MAPK pathway was activated due to increased phosphorylation of kinases ERK1/2 and JNK as compared to control (*26*). The activation of the MAPK pathway when *Lmna* is reduced highlights this important downstream pathway in heart function. Interestingly, DCM caused by mutations in LMNA is caused by activation of other several signaling pathways, including the PDGF pathway, which plays a role in modulating cardiac fibrosis during heart failure (*23, 27*). Cellular modeling has been used to study these signaling pathways with attempts to restore functionality and identify novel pathways for potentially treating DCM. Furthermore, understanding the impact of *LMNA* haploinsufficiency on clinical phenotype will potentially enable gene therapy to restore the full lamin A/C content.

The *MYH7* gene encodes alpha myosin heavy chain 7 (αMyHC) and *MYBPC3* encodes cardiac myosin binding protein C (cMyBP-C). *MYH7* and *MYBPC3* are the most commonly mutated genes in patients with HCM. *MYH7* and *MYBPC3* account for nearly 50% of HCM cases (*28*). *MYH7* maps to chromosome 14 where it sits next to *MYH6*. Sarcomere modulators have been developed to inhibit aspects of myosin-mediated contractility (*29*). Sarcomere modulators have been developed that increase contractility (omecamtiv mecarbil) and decrease contractility (mavacamten). Mavacamten was FDA approved to treat obstructive HCM in 2022. However, not all HCM is associated with increased sarcomere function. For example, the HCM-associated *MYH7* mutation R712L was found to have impaired motility and stroke work in purified protein assays, and omecamtiv mecarbil was shown to rescue the defective working stroke in (*30*). Omecamtiv mecarbil improves cardiac muscle function by selectively binding to myosin and increasing its ability to initiate a power stroke at the beginning of systole (*30, 31*). In contrast, mavacamten inhibits myosin by decreasing contractility and myosin ATPase activity (*32*). Omecamtiv mecarbil activates myosin and increases force of contraction by sensitizing myofilaments to Ca^{2+} (*33*). Contrarily, mavacamten inhibits myosin and reduces force of contraction by desensitizing myofilaments to Ca^{2+} (*33*). Thus, small molecules can act in opposing directions to shift sarcomere and heart function.

MYBPC3 is located on chromosome 11 and its encoded protein, cMyBP-C, binds to both myosin heavy chain and titin (*34*). Human hearts with *MYBPC3* truncations show reduced cMyBP-C protein. However, mice engineered with an *Mybpc3* truncation have not shown hypertrophy, highlighting that mice are imperfect model for this human genetic disease. Typically in mice, additional stressors or a deletion of both copies of *Mybpc3* are needed to result in cardiac dysfunction, and mice lacking Mybpc3 homozygously develop DCM not HCM (*35*). *MYBPC3* is an important genetic target in patients with cardiomyopathy.

Understanding the dynamic differences within the genetic landscape of DCM and HCM is important for deciphering innovative mechanisms that can potentially lead to novel clinical treatments. Over the lifetime in individuals with genetic mutation, the heart can functionally decline over time, and the patient can progress to having heart failure. In the genetic cardiomyopathies, what causes the heart to develop altered function and when is not well understood. Additional stressors like untreated high blood pressure or coronary artery disease can cause heart failure to manifest sooner. Additionally, sex differences can contribute, where generally males are more likely to manifest with symptomatic cardiomyopathy. Why the male heart is more affected is not known but direct hormone levels, gene expression, and heart physiology can all impact clinical outcomes (*36, 37*). These genetic differences lead to differences in clinical presentations in males and females.

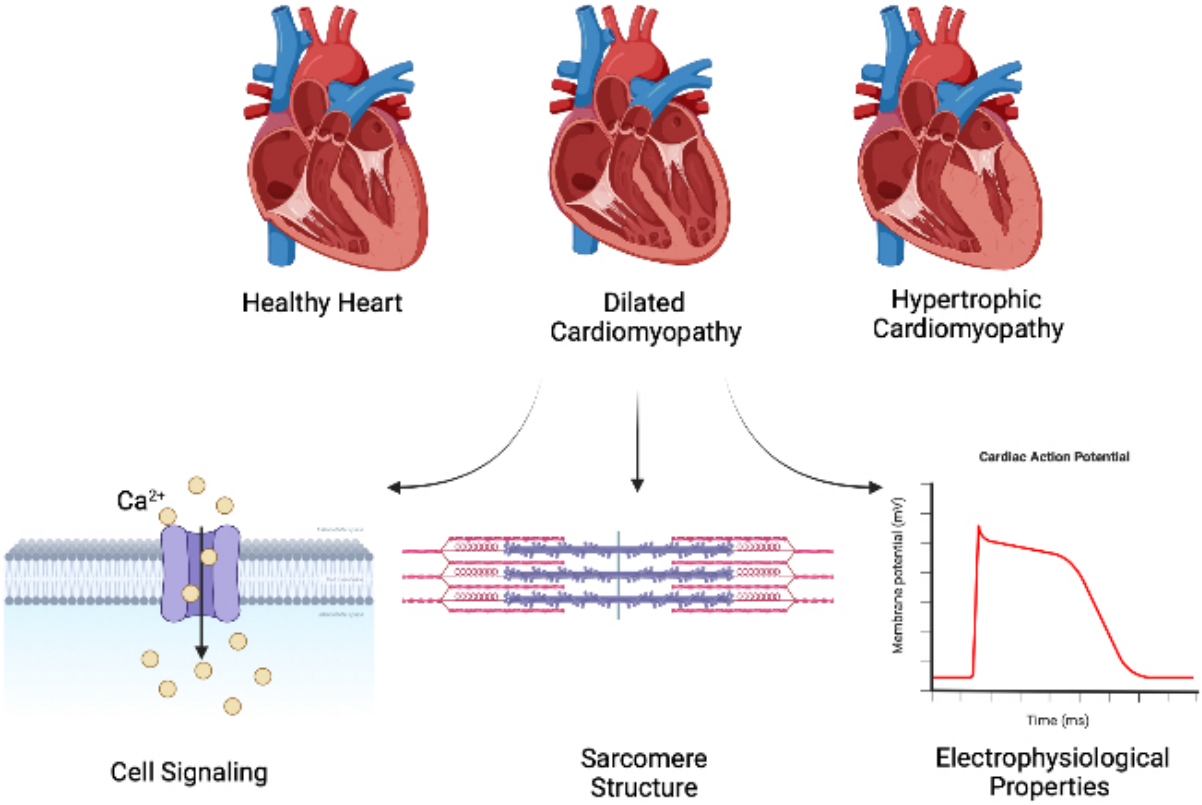

Figure 1.1. Types of cardiomyopathy and physiological characteristics in remodeling. Maintaining cell signaling, sarcomere structure and electrophysiological properties are essential to proper functioning of the heart. DCM is the thinning and widening of the ventricles causing the heart and is associated with increased volume within the heart chamber. HCM is the thickening of the myocardium, the heart muscle. Both DCM and HCM can limit cardiac output and have associated arrhythmias or even sudden cardiac death (SCD). Cardiomyopathic hearts can have impaired action potentials. Image created in Biorender.

IV. Filamin Family of Proteins

Filamins are a class of proteins that bind the actin cytoskeleton. The actin cytoskeleton is a dynamic network of proteins that regulates cell migration and motility, cell division, protein tracking and signal transduction and rearranges through cues in the microenvironment (*38*). Filamins are composed of two calponin homology domains in the actin binding domain (ABD) at the N-terminus, rod domain (RD) with 2 hinge regions, and the dimerization domain (DD) at the C-terminus (*39*). The ABD regulates the binding to actin filaments within the cytoskeleton (*40*). The RD modulates the changes in filamin conformation through its mechanochemical properties (*38*). Forces of 25-100 pN applied to the RD can promote unfolding and flexibility within the Ig-domains while the ABD at the N-terminus and DD at the C-terminus become stiffer. Due to the dynamic nature of the cytoskeleton, filamin is able to respond to different forces within this network through its RD. The DD is important for the crosslinking of actin at the C-terminus (*41*). The filamin family consists of filamin A, filamin B and filamin C **(Figure 1.2)**. These proteins are necessary for mediating structure and function within the actin filament.

The *FLNA* gene encodes the protein filamin A, and filamin A is composed of 2,647 amino acids, 48 exons, 24 immunoglobin (Ig) repeats. The *FLNA* gene is located on chromosome X, and the *FLNA* gene is highly enriched in smooth muscle-containing structures. During embryogenesis, filamin A is responsible for cell adhesion, cell migration, mechanical sensing, and cell signaling (*42*). Filamin A aids in cell adhesion, a process that happens following cellular interactions with extracellular matrix proteins, such as laminin, collagen, and fibronectin, and that is important for organ development and wound healing (*43*). Filamin A is localized at the intersection of stress fibers and isotropic actin filaments, regions that solely contain actin thin filaments, and a loss of filamin A results in more isolated and less interconnected stress fibers (*44, 45*). The absence of filamin A caused impaired initiation of motility and spreading, both of which were restored after restoring full-length filamin A (*45*). Filamin A impact cardiac function because it is highly expressed in vessels. When subjected to myocardial infarction, *Flna*-deficient mice displayed larger hearts, impaired biogenesis of blood cells, bigger scar areas, and reduced serum levels of secreted VEGF-A (*46*). In humans *FLNA* loss of function mutations can cause a range of vascular defects, including enlarged pulmonary arteries and dilatation of the thoracic and abdominal aorta (*47*).

Furthermore, the loss of functional *Flna* in mice resulted in cardiac and developmental defects, such as ventricular septal defects, and these features were seen in males leading to lethality, and skeletal abnormalities (*48*). Over 90 proteins have been shown to bind to filamin A during cellular signaling processes (*49*). Filamin A is highly enriched in vascular smooth muscle, and this expression impacts many developmental process (*50, 51*). As a key regulator of cell motility and signaling in different pathways, filamin A is an important regulator of vascular smooth muscle function.

Filamin B, encoded by the gene *FLNB*, is another filamin isoform that is widely expressed. The FLNB gene is located on chromosome 3, and the filamin B protein consists of 2,602 amino acids, 26 exons, and contains 24 Ig-like repeats. This isoform is important for skeletal development and regulates angiogenesis, muscle differentiation, and fibroblast motility (*52*). During myogenesis, *Flnb* variants encoding filamin B lacking the hinge 1 region localized to actin stress fibers produced fewer myotubes as compared to the control (*53*). Mutations in *FLNB* have been linked to several musculoskeletal disorders, such as Larsen syndrome, an autosomal dominant developmental disorder that affects bone development and muscle structure. Whole genome sequencing of patients with Larsen syndrome identified the *FLNB* missense mutations, p.Thr1616Ala and p.Ile2341R (*54*). These patients had bony skeletal abnormalities, and these variants differentially affected skeletal development. *Flnb*$^{-/-}$ mice die during embryonic development, and fibroblasts from these mice showed disorganized actin filaments, impaired cell motility, and hindered microvasculature and skeletal development (*55*). Although no filamin B protein was detected in these mice, this mutation if it were to produce protein would result in the termination of critical domains and interaction sites necessary for sustaining filamin structure and function. The rod domain is important for modulating conformational changes when filamins are exposed to forces within the cytoskeleton. When truncated at the ABD, homozygous *Flnb* mice also displayed stunted growth, delayed endochondral bone development and differentiation, and increased cell death before eventual demise (*56*), underscoring the importance of having filamin B protein.

Filamin C, encoded by the gene *FLNC*, is a filamin isoform important for cellular structure and function within heart and skeletal muscle. Unlike *FLNA* and *FLNB*, *FLNC* expression is enriched in skeletal and

cardiac muscle. The filamin C protein contains 2,725 amino acids and 24 Ig-like domains. One of the features of filamin C that distinguishes it from filamin A and filamin B is its longer Ig-like domain 20, caused by an insertion of 82 amino acids (*57*). Ig-like domain 20 is the site of interactions with muscle proteins like Xin-repeat protein and XIRP2, which is important for actin cytoskeleton remodeling and sarcomere assembly (*58, 59*). Filamin C is predominately found at the Z-disk, but the protein is also present at the plasma membrane, intercalated discs and costameres (*59*). Filamin C interacts with many cytoskeleton proteins. Specifically, filamin C interacts with the dystrophin-glycoprotein complex (DGC). The DGC is made up of dystrophin, dystroglycan, sarcoglycan and syntrophin, and this complex modulates signal transduction while also providing structural support to the muscle by its linking the extracellular matrix to the actin cytoskeleton (*60*). Genetic mutations in gene encoding DGC proteins cause disorders, such as Duchenne Muscular Dystrophy (DMD) and Limb Girdle Muscular Dystrophies (*61, 62*). Thus, filamin C contributes to the maintain structural support of the cytoskeleton and the sarcolemma of muscle, as it is present in heart and skeletal muscle.

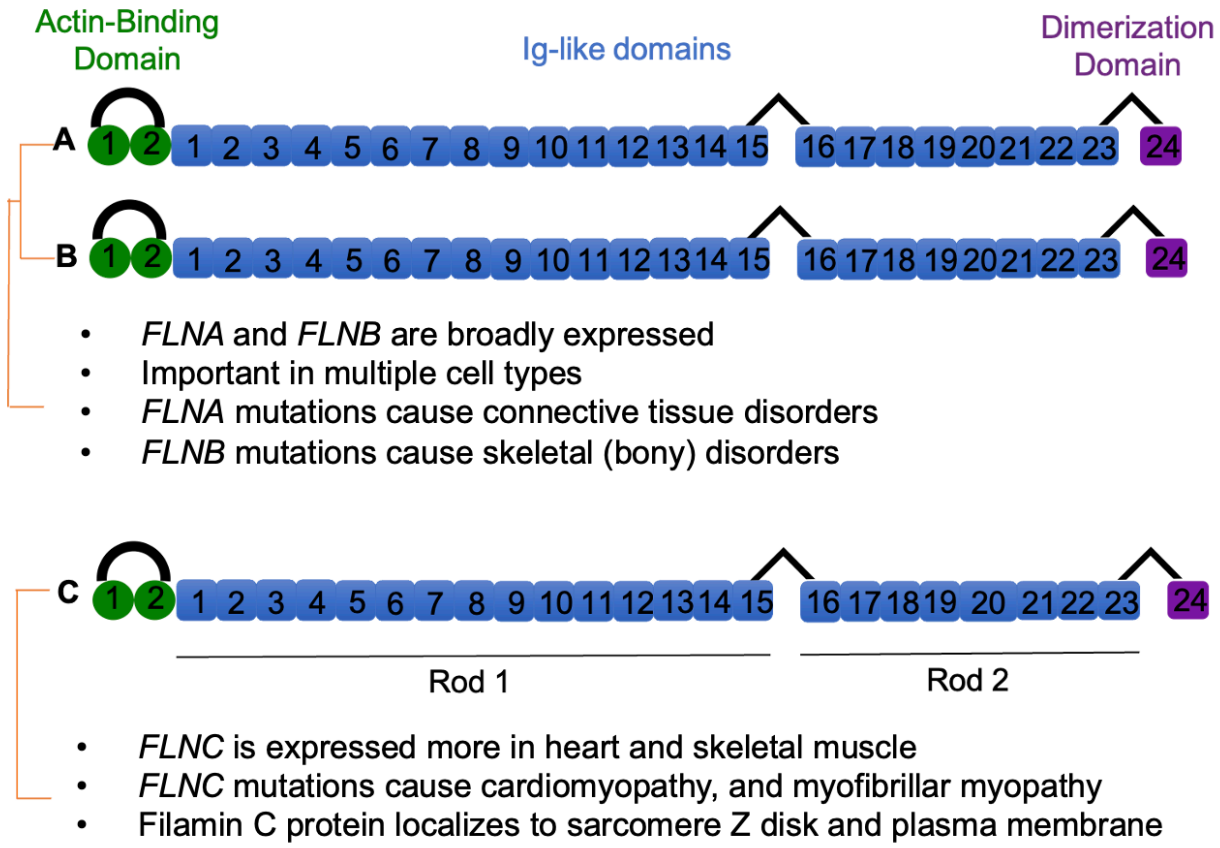

Figure 1.2. Structure of filamin isoforms. The filamin family of proteins consists of filamin A, B, and C, all of which are involved in dynamic shaping and maintaining the structure of the cytoskeleton. All of these isoforms contain an actin-binding domain at the N-terminus, a rod domain separated by two hinge regions, and a dimerization domain at the C-terminus. Filamins include 24 Ig-like domains encoded by 48 exons. Filamins A and B are broadly expressed but are highly expressed in smooth muscle. Filamin C expression is enriched in cardiac and skeletal muscle. Filamin C has a longer Ig-like domain 20, which is an important site for interactions with other proteins, such as Xin and XIRP2.

V. *FLNC* Mutations in Skeletal and Cardiac Muscle Disease

FLNC encodes the protein Filamin C and is located on chromosome 7q32.1, and mutations in *FLNC* were first described in patients with myofibrillar myopathy (MFM) (*63, 64*). MFM is characterized by progressive muscle weakness and intracellular protein aggregates. In normal striated muscle, filamin C protein is predominately located at the Z-disk of the sarcomere and is also found at the plasma membrane (*65, 66*). Filamin C also interacts with additional cytoskeletal proteins, such as desmin (DES) and BAG3 (*67, 68*). Filamin C helps maintain structural integrity and proper signaling within the skeletal muscle. The intracellular protein aggregates that develop in MFM include filamin C, as well as other interacting proteins like desmin (*68*). *FLNC* mutations have also been described linked to multiple forms of cardiomyopathy (*69, 70*). *FLNC* mutations account for 3-4% of cases of DCM (*71*). *FLNC* mutations have been described along the length of the *FLNC* transcript (*63, 72-74*). Missense and nonsense *FLNC* mutations may have different mechanisms of causing cardiomyopathy. Unlike nonsense mutations, missense mutations in *FLNC* more likely cause the formation sarcomeric aggregates, disrupt filamin C structure and functionality (*75, 76*). Aggregate formation, due to misfolding of many proteins including filamin C, can induce the autophagy response to remove these misfolded proteins. With FLNC missense mutations, the expression of proteins that regulate the autophagy process was increased, but with these missense mutation it is thought that the autophagy is inefficient causing MFM (*77*). Missense variants in *FLNC* associated with HCM are mainly located in the rod domain, which is important for regulating the dynamic structure of filamin C and its ability to respond to external forces within the cytoskeleton. However, aggregates have not been readily observed with *FLNC* mutations (*78*). The distinctive increase of aggregates in *FLNC* missense mutations as compared to *FLNC* nonsense mutations may highlight a distinctive mechanism of inducing cardiac dysfunction, and the approaches towards treating these aggregates may differ from the molecular consequences filamin C is heterozygously truncated or homozygously completely lost.

To date, *FLNC* mutations that affect the filamin C dimerization domain have been best studied. One of the first MFM *FLNC* mutations that was described was the *FLNC* mutation, p.Trp2710X, a nonsense mutation which truncates the terminal 16 exons in Ig-like domain 24 (*63*). This mutation was reported in a German

family including 17 men and women affected with MFM and an age of onset between 37-52 years old. These patients presented with progressive skeletal muscle weakness associated with limb-girdle muscular dystrophy (LGMD), moderately elevated levels of serine creatine kinase (CK), a marker for muscle damage, respiratory complications, and peripheral neuropathy (*63*). The position of this variant in the last two exons of *FLNC* is thought to explain why this variant escaped NMD. Histological examination of skeletal muscle biopsies from these patients showed abnormal and necrotic muscle fibers and also showed aggregates containing desmin and filamin C proteins. Z-disk streaming was also identified. Another study examined 31 patients ages 24-57 years old across four families, including the family previously mentioned (*63*). These patients displayed LGMD-related progressive muscle weakness, respiratory muscle weakness and impaired myofibrillar alignment (*64*). A subset of these patients showed cardiac findings with cardiac conduction defects, tachycardia, diastolic dysfunction, and left ventricular hypertrophy. Additionally, immunofluorescence microscopy detected protein aggregates containing other cytoskeleton proteins, such as desmin, myotilin, Xin, dystrophin, and sarcoglycans (*64*).

A 37-year-old male was described with the *FLNC* p.Val2375Ile missense variant in Ig-like domain 21 in the rod domain, and this individual had MFM with atrophied muscles in upper and lower extremities, progressive muscle weakness of his hands and reduced grip strength (*79*). He also had chronic denervation, impaired motility, and signs of lower motor neuron syndrome, which results in damaged motor neurons and muscle weakness. The etiology of the neuropathy symptoms is not known.

FLNC variants have been described in HCM patients. One of the first reports was a 53-year-old woman with *FLNC* p.Ala1539Thr missense mutation and a history of HCM and SCD. She presented after developing atrial fibrillation, and cardiac magnetic resonance imaging showed fibrosis in the apex, septum, and anterior wall, seen as late gadolinium enhancement (*75*). Histology of skeletal muscle biopsies from HCM patients and additional samples with the *FLNC* p.Ala1539Thr variant revealed sarcomeric aggregates, myofibrillar disarray, structural irregularities in the Z-band, and fibrosis. Additionally, 34% (n=26) of the affected patients with *FLNC* mutations p.Val123Ala, p.His2315Asp,

p.Ala2430Val showed an increase in serum CK as compared to healthy controls (*75*). Other members of her family who carried the p.Ala1539Thr variant also developed heart failure and died.

FLNC mutations have also been described in the filamin C rod domain (*77, 80*). A 23-year-old male with HCM was shown to have the *FLNC* p.Ala2430Val missense variant which maps to the rod domain of the filamin C protein. This patient had a systolic heart murmur at the 1 month age of diagnosis and displayed obstruction in his left ventricular tract, limiting blood flow out of the left ventricle, and increased levels of brain natriuretic peptide (BNP), a biomarker for heart failure (*80*).

Although most *FLNC* pathogenic variants have been described in autosomal dominant myopathy and/or cardiomyopathy, two brothers with hypotonia and DCM were described with likely recessive inheritance. When the second brother was diagnosed with similar findings to the first, whole genome sequencing was used to identify biallelic variants in *FLNC* (*81*). The *FLNC* p.Phe106Leu variant was maternally inherited, and this missense variant falls in the actin-binding domain (ABD) of the N-terminus. The second *FLNC* allele, Arg991X mutation, was paternally inherited and this truncating variant leading was predicted to lead to nonsense-mediated decay (NMD) of the mRNA (*81*). Histology on the explanted heart revealed myofibrillar disarray, reduced and ruptured myofibrils, irregular morphology, protein aggregates and vacuoles.

ClinVar is a public database that includes information from clinical genetic testing labs along with literature reports on genetic variation. Shown below is a depiction of a subset of *FLNC* variants reported in ClinVar as of May 2023 **(Figure 1.3)**.

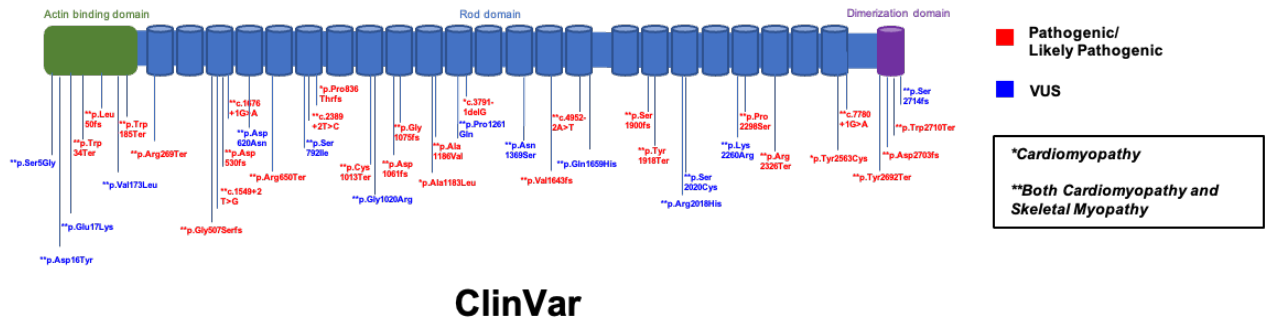

Figure 1.3. ClinVar reported *FLNC* mutations and clinical diagnoses. *FLNC* variants have been described in multiple cardiomyopathies. ClinVar is a public archive of reports of clinically important human variation, which derive from clinical genetic testing labs and literature aggregation. This ClinVar report was downloaded on May 1, 2023 [https://www.ncbi.nlm.nih.gov/clinvar/?term=FLNC%5Bgene%5D&redir=gene].

VI. Models of Filamin C

The role of filamin C in maintaining the structural integrity of the sarcomere has been evaluated using different models from animals to cells. The role of filamin C was tested in zebrafish using a knock down approach (*82*). Targeted antisense morpholino oligonucleotides were used to create a truncation in exon 30 of *flncb*, a FLNC ortholog. The *flncb* knocked-down fish had impaired slow muscle fibers and intracellular aggregates of myosin, both of which are physiologically relevant to human cases of MFM. The combined knockdown of *flnca* and *flncb* caused defects in both the slow and fast muscle fibers and created desmin aggregates. *Flnc* mutations representing DCM have also been generated in zebrafish. Morpholino oligonucleotides were used to knockdown *flncb* in exon 43, truncating the terminal 116 nucleotides (*83*). These *flncb* knockdown zebrafish models had reduced survival and a range of cardiac findings including abnormal contractility, ventricular collapse, enlarged atrium, abnormal blood flow, and/or reduced heart looping. Additionally, these truncating variants showed significantly elevated reserve flow fraction and decreased heart rate, and a slight decrease in stroke volume and cardiac output as compared to the uninjected control. These models show that reducing filamin C content is physiologically relevant to muscle and heart structure and development.

Mouse models have also been used to evaluate *FLNC* and its role in disease. The mouse *Flnc* variant p.W2711X (p.W2710X in humans) was generated to study MFM. This variant deletes the terminal 16 amino acids and was created by homologous recombination, resulting in a myopathic phenotype seen as increased fibrosis, centrally-placed myonuclei, and small and degenerating myofibers (*67, 84*). This *Flnc* variant also resulted in increased muscle damage accompanied by increased protein expression of Xin, a marker for muscle damage. Filamin C was mislocalized from the Z-disk to the lesions and myotendinous junctions compared to the wild-type control. Macrolesions with impaired sarcomeric structure were found in *Flnc* W2711X mice similar to the clinical pathology of MFM patients. A different *Flnc* mouse model was created by replacing the terminal eight exons of the mouse *Flnc* gene with a neomycin resistance gene, therefore terminating the terminal eight exons (*85*). These *Flnc* mice in the homozygous state showed reduced filamin C protein and early lethality with decreased muscle mass and abnormally low myofiber count resulting from deficient myofiber formation and differentiation. Additionally, immunofluorescence

microscopy showed disorganized sarcomeres in the homozygous *Flnc* muscle. This mouse model showed that complete reduction of filamin C protein impairs muscle development indicating that filamin C is an important factor for proper muscle development and sarcomere formation.

Because of the early lethality in the homozygous *Flnc* mice lacking the last 8 exons of the gene, a cardiac-specific inducible knockout (icKO) mouse model was created to delete exons 9-13 by crossing *Flnc*-floxed mice with αMHC-MerCreMer mice followed by tamoxifen exposure (TAM) at 2 months (*86*). Fibrosis was increased in *Flnc*-icKO hearts 6 weeks after TAM exposure along with increased expression of the profibrotic genes, *Col1a1* and *Col3a1*. Additionally, icKO *Flnc* mice had increased levels of cardiac stress makers such as *Nppa*, *Nppb*, and *Myh7*. The icKO mice developed reduced cardiac contractility although calcium signaling was unaffected (*87*). These icKO hearts also had misaligned Z-disks within their sarcomeres and reduced peak twitch tension. At the subcellular level, filamin C governs not only sarcomere structure but also its contractile force which determines its functionality. The icKO hearts demonstrate the importance of filamin C's role in the mature myocardium and provide evidence for the concept that reducing filamin C protein causes DCM.

Induced-pluripotent stem cell-derived cardiomyocytes (iPSC-CMs) or human embryonic stem cell- derived cardiomyocytes (hESC-CMs) also provide a cellular model for human cardiac diseases, including *FLNC* mutations. The *FLNC* variant p.V2297M was shown to heterozygously associate with restrictive cardiomyopathy (*88*). To evaluate this variant, gene editing was used to make *FLNC* p.V2297M homozygously using CRISPR-Cas9 and homology directed repair. A single guide RNA (sgRNA) was used to target exon 41 which encodes a portion of the filamin C rod domain in human embryonic stem cells that, once edited, were then differentiated into cardiomyocytes (*88*). Reduced fractional shortening was observed in the homozygous p.V2297M ESC-CMs consistent with impaired contractility. Other pathogenic *FLNC* variants were also generated using patient-derived iPSC-CMs as a model for DCM. iPSC-CMs from patients with *FLNC* p.Gly1891fs61X or *FLNC* p.Glu2189X were each generated and then differentiated into IPSC-CMs (*89*). DCM patients with the p.1891fs61X mutation presented with polymorphic sustained ventricular tachycardia, paroxysmal atrial fibrillation, and reduced left ventricular

systolic function while patients with arrhythmogenic right ventricular cardiomyopathy showed nonsustained ventricular tachycardia (NSVT) with left bundle branch block morphology and ventricular extrasystoles (*83, 90*). These iPSC-CMs had reduced contractility and increased variability in beating rate compared to the healthy control. *FLNC* p.Gly1891fs61X or *FLNC* p.Glu2189X iPSC-CMs each showed an increase in proarrhythmic cells, as shown by large variations in beat rate and abnormal action potential indicated by delayed afterdepolarizations, supporting a similar clinical phenotype in patients with arrhythmogenic cardiomyopathy. When treated with the platelet-derived growth factor receptor alpha (PDGFRA) inhibitor, crenolanib, contractility was improved, showing that inhibiting PDGFRA could be a mechanism for treating cardiomyopathies caused by *FLNC* mutations. The findings from *FLNC* truncating variants in iPSC-CMs are consistent with partial loss-of-function and reduction in filamin C protein. Modeling *FLNC* mutations in iPSC-CMs provides further insight on novel mechanisms that contribute to the cardiomyopathy process and potentially point to new therapeutic possibilities.

VII. Mechanical Injury and Chemical Stress in Striated Muscle

Within the actin cytoskeleton, proteins respond to mechanosensory signals and stressors in the sarcomere. Filamin C is a key protein related to the striated muscle injury and repair. Using neonatal mouse cardiomyocytes, which do not have the mature shape of adult cardiomyocytes, laser-induced microdamage was used to better understand to monitor filamin C dynamics during the injury process (*57*). In these studies, GFP-filamin C and RFP-α-actinin were overexpressed in mouse neonatal cardiomyocytes and then cells were subjected to laser injury. With cellular injury, filamin C was immediately recruited to the site of injury (*57*). This indicates that filamin C is an early mediator of myofibrillar remodeling. α-actinin was also recruited to the site of damage within 2-10 minutes. Thus, filamin C and α-actinin are both indicators for early myofibrillar damage repair, and they may potentially interact at these injured sites. Filamin C has also been shown to be a part of the repair signature in muscle (*91*). After mouse myofibers and human muscle fibers were subjected to eccentric exercise-induced injury, filamin C expression was enriched in damaged sites 5 and 24 hours within mouse myofibers and human muscle fibers post exercise, with aggregates formation present in at 24 hours (*91*). These data demonstrate that after injury, filamin C is recruited rapidly to injury sites where it participates

in sarcomere rebuilding. The interaction of filamin C with Xin and XIRP2 was measured in mice using fluorescence recovery after photobleaching, a technique used to quantify the kinetics of how proteins diffuse through cells. Xin and XIRP2- deficient cells showed longer filamin C half-lives at the Z-disk (*57*). Xin and XIRP2 colocalize with filamin C within protein aggregates and injured regions of *FLNC* p.W2710X human muscle fibers (*67*). The dynamic protein complex of filamin C and other cytoskeletal proteins contributes to the molecular machinery for muscle repair at injured areas.

Additional evidence for filamin C's role was seen in the myogenic C2C12 cell line. In C2C12 myotubes that transiently expressed filamin C fused to GFP, Z-disk streaming was seen after injury in a model where injury was induced with electrical pulse stimulation meant to simulate exercise *in vitro* (*92*). These damaged myotubes also showed evidence of lesion formation visualized by spinning disk confocal microscopy. Shorten sarcomeres were also seen in filamin C-EGFP transfected myotubes. This data suggests that filamin C is an important mediator of cellular damage and repair.

Mechanical force also drives the unfolding of filamin isoforms. Using purified protein, Filamin A was shown to gradually unfold between Ig-like domain pairs 20 and 21 in the rod domain in a force-dependent manner in a cell-free system (*93*). Using a single molecule competition assay, it was shows that increasing force also increased the affinity of the GPIbα peptide for its binding to FLNa20-21 and associated with conformational changes within this region of the rod domain. The binding probability of GPIbα increased with higher loads, causing filamin A to adopt an open conformation. Thus, force dictates the opening and closing of filamin A, and this interaction shifts the interaction between the filamin A and the cytoskeleton. The impact of mechanical force on filamin C is less well studied. The distinct and larger size of Ig-like domain 20 in filamin C, which is the region that facilitates interaction with other cytoskeleton proteins, may mean filamin C has a greater role in maintaining structure and stability within the sarcomere. One of the main proteins involved in muscle regeneration and autophagy is mammalian target of rapamycin complex 1 (mTORC1) (*94*). mTORC1 is a part of an mTOR family of proteins that regulate anabolism and catabolism within damaged skeletal muscle (*95, 96*). BAG3, a cytoskeletal protein and molecular co-chaperone, in tandem with mTORC1 is regulated by the TSC complex and binds to

mechanically unfolded filamin A (*97*). BAG3 is located at the Z-disk along with filamin C, and so this arrangement could point to a link of mTORC1 helping to modulate the unfolding of filamin isoform under mechanical stress as well.

VIII. Autophagy Mechanisms and Protein Quality Control in the heart

Proteostasis in the heart is critical for healthy functioning of the heart. Cardiac remodeling is an important adaptation to physiological and pathological changes in the heart, and proteostasis is an important aspect of cardiac remodeling. Specifically, hemodynamic stress can induce hypertrophic growth as an initial response but can transition to pathological growth with systolic and diastolic over time (*98*). During the remodeling process, proteins are turned over to maintain protein quality control (PQC). The perpetual synthesis and degradation of proteins is necessary as the body compensates adapts to growth stimuli. This process is controlled by the switch between the ubiquitin-proteasome system (UPS) and autophagy **(Figure 1.4)**. The autophagy response within cardiomyocytes, with a constricted proximal aorta as a model of heart failure, is heightened in response to pressure-overload hemodynamic stress (*99*). Protein misfolding leads to protein aggregation, which induces the autophagic response. In the pressure-overloaded heart, aggregates accumulate and induce autophagy to remove the misfolded proteins (*100*). Defects in UPS and autophagy both contribute to cardiomyopathy. Furthermore, inhibiting the proteasome activates the autophagy response (*100, 101*). When neonatal rat ventricular myocytes were treated with MG132, a proteasome inhibitor, ubiquitin-tagged protein accumulation in the insoluble fraction was increased, therefore marking these proteins for autophagic degradation (*100*). Proteasome inhibitors can also induce proteotoxic stress in the heart. Bortezomib, a proteasome inhibitor, can reduced contractility in the heart (*102*). Cardiomyopathy can be triggered by defects in this dynamic proteasome-autophagy switch in the heart. Understanding the effect of stress on the heart in the context of filamin C is important for elucidating its role in causing cardiomyopathy.

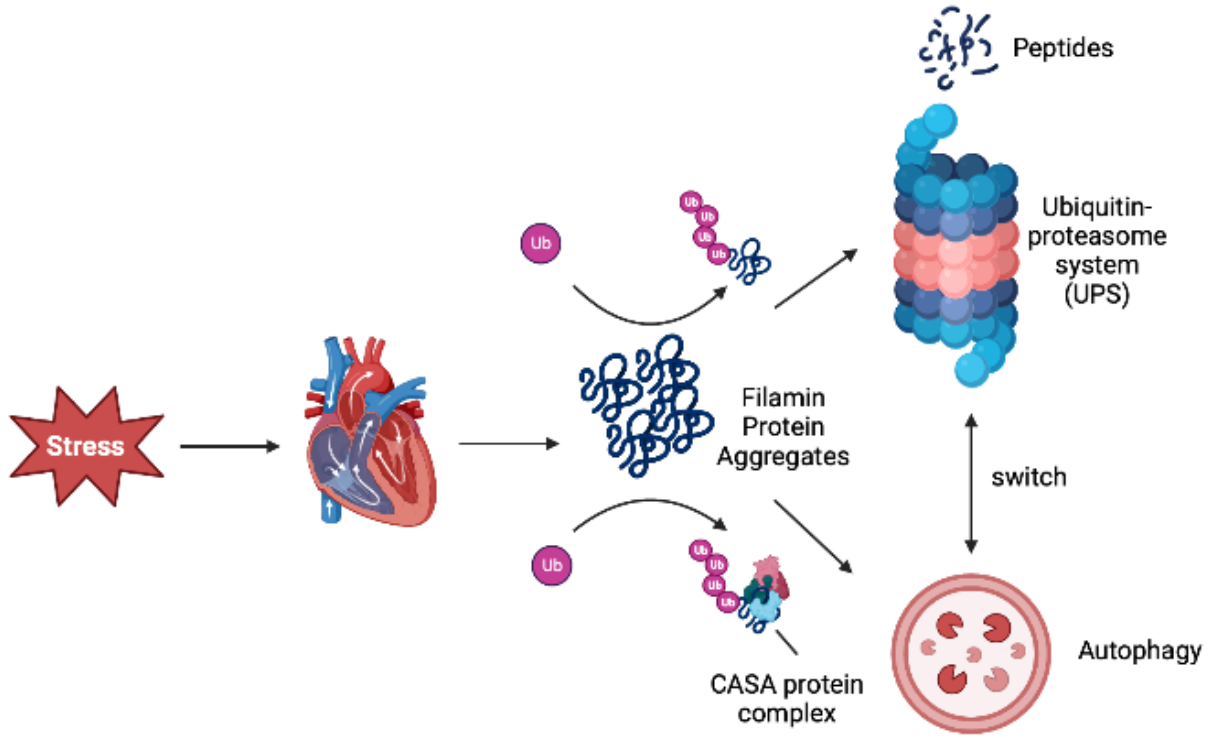

Figure 1.4. Ubiquitin proteasome system and autophagy degradation of filamin. The switch between the ubiquitin proteasome system (UPS) and autophagy is essential for maintaining protein quality control in the heart. During the remodeling process, cardiac proteostasis is necessary to control the degradation and regeneration of proteins, especially in the sarcomere. Autophagy in the heart is governed by the BAG3-mediated chaperone assisted selective autophagy pathway, which shuttles filamin C to the lysosome for degradation. Under stress, the heart will resort to either pathway to remove misfolded proteins. When either pathway is compromised, the proteins will switch between the two mechanisms. Figure created with BioRender.

The BAG3-mediated Chaperone-Assisted Selective Autophagy (CASA) pathway regulates autophagy in the heart. Z-disk streaming and formation of aggregates expressing filamin C and BAG3 were shown in human skeletal muscle following exercise-induced mechanical stress (*103*). This indicates BAG3's involvement in autophagy through its interaction with filamin C aggregates at the Z-disk. In the heart, the CASA pathway works through the close interaction of BAG3 to Filamin C at the Z-disk. Heat shock factor proteins (HSPs) are then recruited to form a complex with BAG3 around filamin C, which acts as a scaffold. p62 is then recruited and targets these filamentous aggregates for ubiquitin-tagged degradation at the lysosome. In BAG3 cardiomyocyte- deleted mice, the interaction of BAG3 with HSP70 was compromised and small SHPs, especially HSPB8, were destabilized and protein turnover was disabled (*104*). BAG3 is required for stabilizing its complex with HSPs that modulates proteostasis during cardiomyopathy (*104*). HSP70 has been shown to be important for autophagy through its C-terminus. Mice that were deficient for the C-terminal region of HSP70 displayed arrhythmia, increased myocardial injury, decreased survival, and impaired autophagic flux (*105*). HSPB8 (also known as HSP22) is another HSP that plays a role in maintaining cardiac function. The absence of HSPB8 in pressure-overloaded hearts of mice subjected to transverse aortic constriction results in decreased contractility and triggers ventricular remodeling under stress (*106*). HSPB8 directly interacts with BAG3 and is an important factor in the cardiac autophagy process (*107*). Acting as a link between UPS and autophagy, p62 is upregulated in cardiomyocytes and activates autophagy under proteotoxic stress (*108, 109*). Furthermore, increased levels of p62 prevented clearance of substrates for proteasomal degradation after autophagy was inhibited in Atg7 cells (*110*). The CASA pathway is essential for modulating protein quality control in the heart and acts as a cardioprotective force under stress.

IX. Summary

In order to generate cell models of cardiomyopathy, I focused on *FLNC* mutations since this gene was associated with multiple distinct forms of cardiomyopathy. In addition to cardiomyopathy, patients with *FLNC* mutations have high risk of arrhythmia and sudden cardiac death. Because filamin C is important for maintaining sarcomere structure and cell signaling, my studies were aimed at defining whether cellular models of *FLNC* mutations could reflect electrophysiological properties similar to what is seen in patients. Furthermore, my studies were aimed at assessing whether there

was a link between proteostasis and arrhythmia risk in *FLNC* mutations. However, the underlying mechanisms defining how disruption of *FLNC* impacts the autophagy response under stress, is not well known. Creating clinically relevant models of mutated *FLNC*-causing cardiomyopathy, especially under stress, will allow us to better understand the physiological role of filamin C. I hypothesize that reduction of filamin C disrupts normal protein turnover and impairs the electrophysiological properties of the cell through disrupted cell signaling, and further hinders the ability of the CASA pathway to maintain proteostasis in the heart while under stress.

X. Thesis Overview

This section will lay out a summary of the remaining chapters of my thesis.

Chapter 2. Creating Models of FLNC Cardiomyopathy

To model *FLNC* cardiomyopathy, I created induced pluripotent cell (iPSC) lines with heterozygous missense and nonsense variants of *FLNC*. I generated iPSC lines (Phe106Leu, Arg650X/c.970-4A>G, Glu2458SerfsX71, and Val2715fs87X) from patients clinically evaluated at Northwestern by isolating cells from either a urine or blood sample, reprogramming them into iPSCs using the four factor method, and then differentiating these iPSC into cardiomyocytes. To create isogenic *FLNC* cell lines, I used CRISPR/Cas9 to genetically engineer iPSCs using a guide directed to either exon 1 at the N-terminus or exon 47 at the C-terminus. This deletion created truncating variants at the actin-binding domain and dimerization domain. I validated the genotypes using Sanger sequencing and Amplicon sequencing and measuring gene and protein expression. Immunofluorescence microscopy was used to measure expression and display deficiencies in sarcomere structure when filamin C was mutated.

Chapter 3. Impact of FLNC Truncations Under Stress

Using the isogenic *FLNC* cell lines I created with CRISPR/Cas9, I measured the effect of protein expression of proteins involved in the CASA pathway while under proteotoxic stress. Bortezomib, a proteasome inhibitor, was used at various concentrations to provoke proteotoxic stress by overloading the proteasome. To measure how action potential was affected in these *FLNC* isogenic lines, I used the CardioExcyte96 system to measure extracellular field potential across a network of iPSC-CMs. These cells were treated with vehicle (0.01% DMSO) or 0.1 μM Bortezomib and these recordings were captured over 24 hours.

Chapter 4. Summary

While *FLNC* is known to play a major role in maintaining sarcomere structure at the Z-disk and cell signaling at the membrane, my thesis project has focused on the role of filamin C under cell stress with the hypothesis that cell stress may provide triggers for arrhythmias. I used proteotoxic stress to model a physiological response within iPSC-CMs, since these cells provide a model in which to study human cardiomyopathy. These data shed light on the clinical relevance of filamin C and why mutations in this

gene may be variable in penetrance and expressivity. Furthermore, my two-pronged approach in creating cell lines directly from patient samples and from CRISPR/Cas9 introduces a novel way to understand these mechanisms in a more clinically relevant and controlled manner.

Chapter 2.

Creating Models of *FLNC* mutation

I. Overview

FLNC mutations is one of the many genes associated with cardiomyopathy. Mutations in *FLNC* are distribute along the entire length of the gene including mutations that affect the protein's N-terminus to the C-terminus, and these mutations present with different phenotypic expression. In addition to cardiomyopathy, patients with missense and nonsense *FLNC* mutations have increased risks for arrhythmias and sudden cardiac death. While *FLNC* mutations have been documented in the context of cardiomyopathy, the mechanisms by which *FLNC* mutations cause specific phenotypes requires further study. To model *FLNC* mutations in cardiomyopathy, human skin fibroblasts, urine and blood samples were collected from *FLNC* patients, reprogrammed into iPSCs, and differentiated into iPSC-CMs. These cells serve as a direct translational model. CRISPR/Cas9 was used to genetically engineer iPSCs and then these engineered cells were differentiated into cardiomyocytes. These cells allowed us to understand downstream phenotypic effects in an isogenic background. Additionally, iPSC-CMs enabled studies to evaluate how these cells responded to physiological stress to better understand triggers for arrhythmias in *FLNC*-cardiomyopathy. The filamin C protein helps maintain sarcomere structure and mediates cell signaling processes within the cytoskeleton. By creating cell models of cardiomyopathy, we can use these innovative tools to uncover mechanisms that govern disease in the heart.

Respective Contributions

Joyce Ohiri helped collect urine samples, optimized the CRISPR/Cas9 system, generated patient and isogenic iPSCs, analyzed sequencing to validate genotypes, and performed quality control on all lines. Lisa Castillo coordinated the patient consenting process and retrieval for all patient samples, provided genetic information on patients, and produced patient pedigrees. Lisa Wilsbacher provided clinical information and advised on *FLNC* patients and their clinical details. Malorie Blancard generated the iPSC cell lines from the blood sample of the Arg650X/c.970-4A>G patient. Anthony Gacita significantly helped with implementing and optimizing CRISPR/Cas9 that was used to generate the isogenic cell lines. Elizabeth McNally conceived the study, was instrumental in write the manuscript and provided clinical information, resources, and direct access to *FLNC* patient materials.

II. Introduction

Mutations in *FLNC*, the gene encoding the actin binding protein filamin, lead to cardiomyopathy and myofibrillar myopathy (*78*). Multiple cardiomyopathy subtypes have been described in association with *FLNC* mutations, including dilated, hypertrophic, restrictive and arrhythmogenic (*71, 83, 111*). The myofibrillar myopathy associated with *FLNC* mutations affects distal or proximal skeletal muscles and features intracellular aggregates in myofibers (*112*). With *FLNC* mutations, cardiomyopathy can occur in the absence or presence of skeletal muscle myopathy.

The types of *FLNC* variants associated with myofibrillar myopathy include both missense and truncating mutations, and the inheritance pattern is primarily autosomal dominant with some cases of recessive inheritance (*78, 113*). Cardiomyopathy-associated *FLNC* variants are most commonly associated with dominant inheritance and the most readily interpretable cardiomyopathy-*FLNC* variants are premature truncations.

Here we describe multiple *FLNC* variants and a range of cardiomyopathy outcomes. We also describe a patient with biallelic *FLNC* variants in a woman who presented with peripartum cardiomyopathy and ventricular arrhythmias. The patient was found to have compound heterozygous *FLNC* variants (p.Arg650X and c.970-4A>G). Induced pluripotent stem cell- derived cardiomyocytes (iPSC-CMs) were generated from this patient. IPSC-CMs were also generated from individuals with truncating *FLNC* variants, which displayed reduced filamin C protein expression, or from a patient with a *FLNC* missense variant, which showed a normal level of filamin C protein. To better understand the effect of reducing filamin C protein, we used gene editing to reduce filamin C in iPSC-CMs.

Methods

Ethics and Approvals.

All participants provided informed consent for cell donation and access to medical record information under the Northwestern University Institutional Review Board.

Generation and differentiation of iPSC lines.

Human iPSCs were generated from human skin fibroblasts (Coriell, sample name GM03348, 10 year old male), urine-derived cells or peripheral blood mononuclear cells and reprogramed by electroporation with pCXLE-hOCT3/4-shp53-F (Addgene plasmid 27077), pCXLE-hSK (Addgene plasmid 27078), and pCXLE-hUL (Addgene plasmid 27080) as described previously (*113, 114*) **(Figure 2.1**). IPSCs were maintained on Matrigel^{TM}-coated 6-well plates in mTeSR-1 (Stem Cell technologies, Cat#85850) and passaged approximately every 5 days. IPSC-CMs were differentiated using Wnt modulation **(Figure 2.1)**. Differentiation was conducted in CDM3 (RPMI 1640 with L-glutamine, 213 µg/mL L- ascorbic acid 2-phosphate, 500µg/mL recombinant human albumin) (*115*). When reaching ~95% confluency, cells were treated with 6µM-10µM CHIR99021 for 24 hours and allowed to recover for 24 hours. Cells were then treated with 2µM Wnt-C59 for 48 hours, and the media was changed with CDM3 every two days. After differentiation (~day 6-12) when cells were visibly beating, cells were passed through a 100µm cell strainer and purified by MACS-based cardiomyocyte enrichment (Miltenyi, Cat#130-110-188), counted, and replated. iPSC-CMs were maintained by changing chemically defined cardiomyocyte differentiation media (RPMI, Cat#11875-119 supplemented with CDM3) every other day (*115*). Cells ($2X10^6$) were collected from each differentiation and tested for cardiomyocyte purity by staining for cardiac troponin T (BD, Cat#565744) and assessing by flow cytometry (BD, Acuri C6 Plus flow cytometer). Differentiations were >90% TNNT2-positive (**Figure 2.2)**.

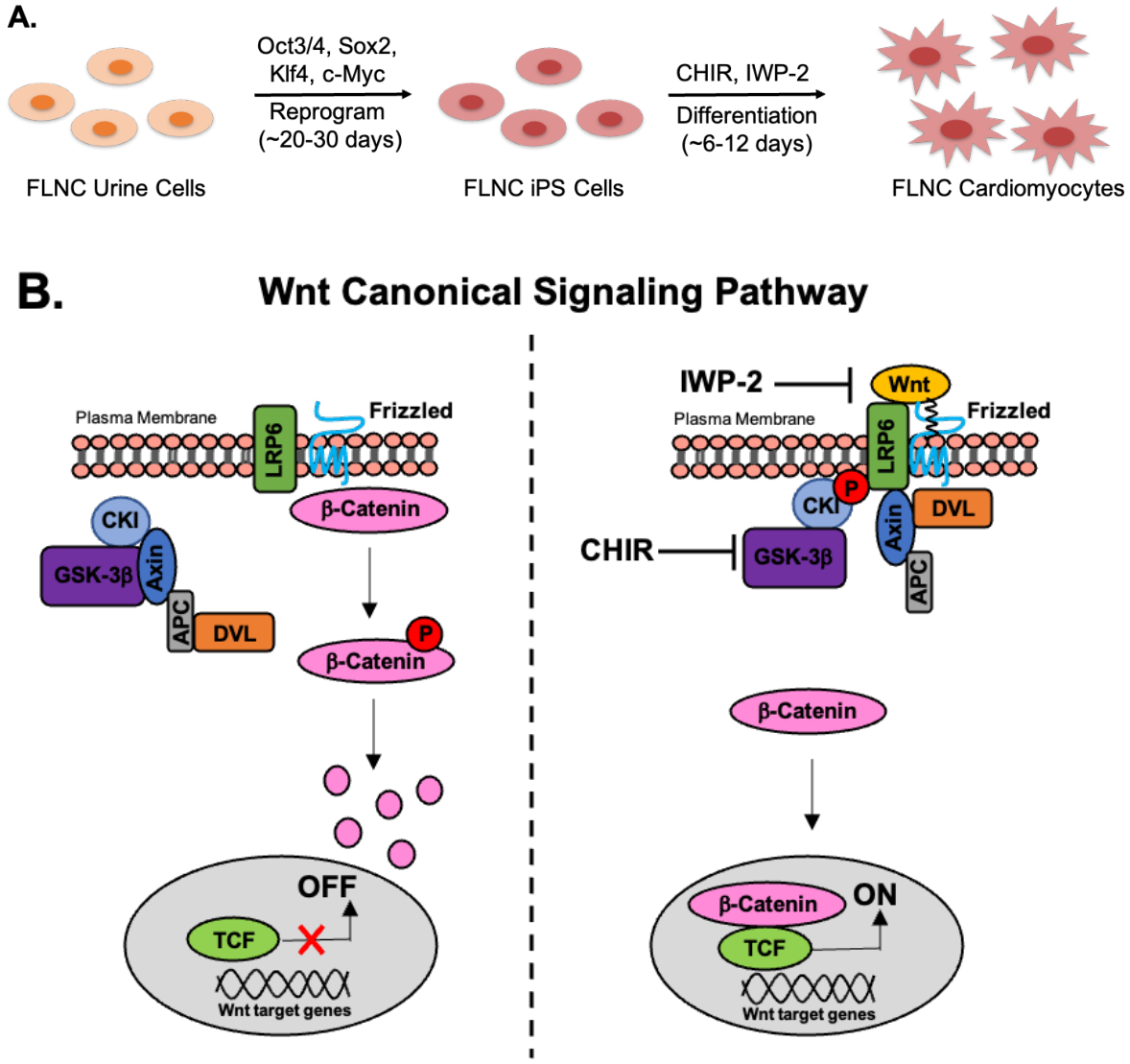

Figure 2.1. Reprogramming and Differentiation of *FLNC* patient iPSC-derived cardiomyocytes. A. Cells were collected from *FLNC* patients. Cells were reprogrammed into iPSCs using the Yamanaka factors, Oct3/4, Sox2, KLF4, and c-Myc, via electroporation over 21-30 days until colonies were visible. *FLNC* iPSCs were differentiated using 6-9 μm of CHIR and 2 μM IWP-2 over 6-12 days until iPSC-CMs were visibly beating. **B.** Differentiation is activated via the Wnt canonical signaling pathway. The inhibition of GSK-3β by CHIR and inhibition of Wnt by IWP-2 is necessary to turn on Wnt signaling. These inhibitory molecules allow β-catenin to translocate to the nucleus and induce transcription of Wnt genes. Unlike the calcium-dependent Wnt noncanonical signaling pathway, which acts late stages of cardiomyocyte differentiation, the Wnt canonical signaling pathway promotes early induction of the cardiac mesoderm while inhibiting differentiation of cardiac progenitor cells into cardiomyocytes (*116, 117*).

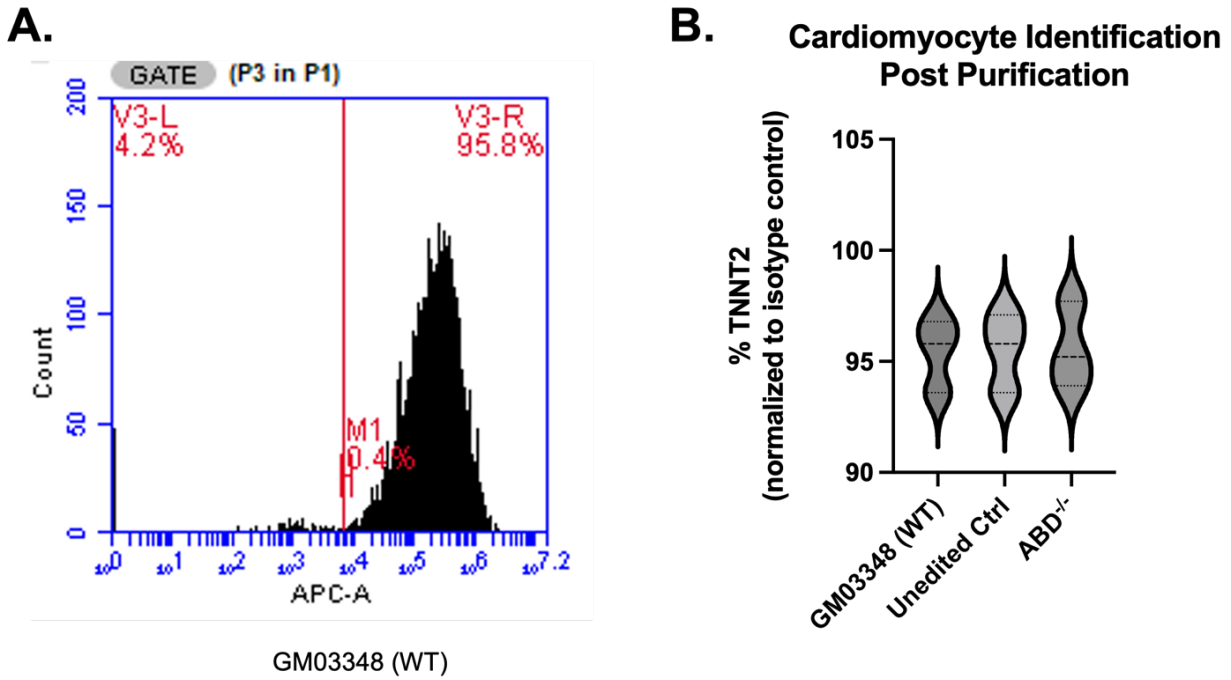

Figure 2.2. Validation of cardiomyocyte purity after human iPSC-CM differentiation protocol. Purity was assessed using flow cytometry for cardiac troponin T. **A.** Control and mutant iPSC-CMs were stained with isotype control IgG or IgG to cardiac troponin T (TNNT2, cTnT) at Day 30 post differentiation. iPSC-CMs were identified using the BD Acuri C6 flow cytometer. **B.** Differentiations of control and mutant iPSC-CMs with >90% cTnT-positive were used in studies.

Gene editing/off-target analysis, genotyping.

The guide RNA targeting *FLNC* exon 1 was designed using CRISPOR (26) (**Figure 2.7**). iPSCs at 70% confluency were trypsinized with TrypLE (Thermo, Cat#12563011), resuspended, and treated with 3µg of guide RNA with pSpCas9(BB)-2A-GFP (Addgene plasmid #48138) control, or no DNA control in Resuspension Buffer (Neon, Cat#MPK10096) and replated onto a 6-well Matrigel™-coated plate with 10% CloneR (Stem Cell, Cat#5888) and 2µM thiazovivin Rock Inhibitor (Sigma, Cat#SML1045) in mTESR. After 24 hours, cells were treated with 0.15µg/mL puromycin (Thermo, Cat#A1113803), and then switched to puromycin at 0.2µg/mL from 48-72 hrs after guide electroporation. After 14 days, colonies were isolated manually. Individual clones were genotyped by Sanger sequencing. Clones with Sanger sequencing suggestive of successful editing were further subjected to amplicon sequencing using the same primers to verify the purity of clones using Amplicon EZ sequencing, Azenta Life Sciences **(Figures 2.9-2.13)**. Analysis of potential off-target mutations was conducted using primers targeting regions identified by CRISPOR **(Table 2.1)**. These regions were amplified and subjected to Sanger sequencing to confirm the absence of inadvertent mutations (**Table 2.3 and 2.4)**. Chromosomal analysis was conducted using the hPSC Genetic Analysis kit (Stem Cell, Cat#07550).

IPSC-CM purification and flow cytometry

IPSC-CMs (day 6-12) were purified using the PSC-Derived Cardiomyocyte Isolation kit (Miltenyi, Cat#130-110-188) to deplete non-cardiomyocytes. After purification, $1x10^6$ iPSC-CMs were collected and stained with isotype control or cardiac troponin T (TNNT2, cTnT) antibody (BD biosciences, Cat#565744) to measure cTnT-positive cells using flow cytometer (BD Acuri C6). Samples that were >90% positive for cTnT were used in following experiments **(Figure 2.2) .**

Quantitative PCR

iPSC-CMs (day 30) were washed with cold 1X PBS and collected. RNA was isolated in TRIzol (Thermo, Cat#15596-018) following the manufacturer's instructions. Isopropanol was used to precipitate RNA, which was collected in ultrapure water. The NanoDrop 2000 (Thermo) was used to measure RNA concentration. One µg RNA was used to make complementary DNA (cDNA). Fifty ng of

cDNA, Amplitaq gold 360 Master Mix (Thermo, Cat#4398881), and primer sets amplifying the 5'UTR to exon 1 and exon 48 to the 3'UTR were used to conduct qPCR on the Thermocycler (Biorad). Gene expression was measured to calculate the $\Delta\Delta$Cq values by averaging Cq values of technical replicates, normalizing to *MYBPC3*, and normalizing the ΔCq value of each sample to the average ΔCq value for the unedited control.

Immunoblotting

iPSC-CMs (day 30) were washed with cold 1X PBS and collected in cell lysis buffer containing protease (Sigma, Cat#11836170001) and phosphatase inhibitor (Sigma, Cat# 4906837001) cocktails using a cell scraper. Samples were centrifuged at 7500 rpm for 5 min at 4°C and the supernatant was collected. Bradford assay was conducted by mixing sample with Bradford 1X Dye Reagent (Biorad, Cat#5000205) in a 1:50 ratio and monitored in a 96-well plate on a plate reader. Samples were aliquoted using cell lysis buffer with protease and phosphatase inhibitors and 4X Laemmli protein sample buffer (Biorad, Cat#1610747). Samples were warmed for 10 min at 75°C and separated using a 4-15% precast protein gel (Biorad, Cat#4561083) at 100V for 1 hr.

Gels were transferred onto PVDF membrane (Biorad, Cat#16201® 77) for 3 hr at 900 mA at 4°C. PVDF membranes were blocked with T20 blocking buffer (Thermo, Cat#37543) for 1 hr at RT and probed with primary antibodies to filamin C (Sigma, Cat#HPA006135, 1:1000), BAG3 (Proteintech, Cat#10599-1-AP, 1:1000), and α-sarcomeric actin (Sigma, Cat#A2172, 1:1000) in T20 blocking buffer o/n at 4°C. Immunoblots were washed with 1X TBS-Tween and secondary antibodies goat anti-mouse (Jackson ImmunoResearch, Cat#115-035-003), 1:2500) and goat anti-rabbit (Jackson ImmunoResearch, Cat#111-035-003, 1:2500) conjugated to horseradish peroxidase in T20 blocking buffer for 1 hr at RT. Immunoblots were imaged using PICO (Thermo, Cat#34580) and Femto (Thermo, Cat#34096) chemiluminescent substrates on the iBright 1500 (Invitrogen). Protein loading was measured using the Memcode reversible protein stain kit (Thermo, Cat#24585). The NIH Image J Fiji plug-in was used to quantify blots.

Statistical analyses.

Data were analyzed using GraphPad Prism and the specific statistical tests were selected based on data distribution and number of comparisons. T-test was used for direct pairwise comparison between the control and mutant cell lines with a significance factor of $p<0.05$.

Results

Cardiomyopathy and arrhythmias with FLNC mutations.

A 40-year-old woman presented with cough and shortness of breath eight weeks after giving birth to her fifth child. She was found to have a dilated left ventricle (LV) with severely globally reduced function (**Figure 2.3** and **Table 2.5**, individual A-1). Cardiac MRI reported a left ventricular end diastolic volume (LVEDV) index = 170 mL/m2 and left ventricular ejection fraction (LVEF) of 20%. There was a mid-myocardial stripe of late gadolinium enhancement in mid-basal interventricular septum extending into the mid-basal inferior wall. Laboratory values were significant for normal troponin and markedly elevated NT-pro-BNP (>4,000). She received intravenous diuretics with improvement of symptoms, and she was initiated on guideline directed medical therapy (GDMT) including carvedilol, spironolactone, ramipril, and oral furosemide. Cardiac telemetry showed ventricular tachycardia (VT) and (NSVT) (**Figure 2.3**), so she was discharged from the hospital with an external defibrillator vest while she recovered from presumed peripartum cardiomyopathy. Over the next several months, she had limited improvement in LVEF despite up titration of GDMT, and she continued to have NSVT.

Her past medical history included 5 successful pregnancies, including the most recent uneventful delivery. She had hypotonia at birth, delayed walking and motor milestones, scoliosis requiring surgery, internally rotated tibia and metatarus adductus of the feet. Because of these findings, she had a muscle biopsy at age 8, which was read as lipid storage myopathy (images unavailable). At the time of her adult presentation with heart failure, she was fully ambulatory and participated regularly in exercise activities with minimal to no weakness.

Table 2.1. Off target analysis of gene edited lines

#	Guide	#Mismatches	Location (hg19)	Annotation (Gene)	Results
1	FLNC_ABD_KO_G1	4	chr1_160165116	intron_CASQ1	Negative
2	FLNC_ABD_KO_G1	4	chr4_175444447	intergenic_HPGD|RP11-440I14.2	Negative
3	FLNC_DD_KO_G1	3	chr7_35435912	intergenic_AC009531.2|AC007652.1	Negative
4	FLNC_DD_KO_G1	4	chr2_227616872	intron_IRS1	Negative
5	FLNC_DD_KO_G1	4	chr4_11439010	intergenic_HS3ST1|RP11-281P23.1	Negative

Table 2.2. gRNA and primer sequences

Name	Sequence(s)	Experiments/Notes
FLNC_ABD_KO_G1	TCGAGTTCCTCGAGCGCGAG	Guide targeting exon 1
FLNC_DD_KO_G1	TCACGAAACATCCACGGTTC	Guide targeting exon 47
hsFLNC_5'UTR-ex1_qPCR	F: CCCCGATAGCCCAAACCG R: CGGCATCTCGTCTGTCTCAT	Gene expression in iPSC-CMs Efficiency= 2.00
hsFLNC_ex48-3'UTR_qPCR	F: GAGGAGGTGTACGTGAAGCA R: TGTAATGTGTGTGTGGCTGG	Gene expression in iPSC-CMs Efficiency= 2.02
hsMYBPC3_qPCR	F: CCCCATCTGAGTACGAGCG R: AGCCAGTTCCACGGTCAG	Gene expression in iPSC-CMs Efficiency= 2.02

Table 2.3. Genotypes of *FLNC* CRISPR isogenic cell lines

Target	Clone	Genotype	Allele 1	Allele 2
FLNC ABD	4	WT	WT	WT
FLNC ABD	17	Compound Heterozygous	Insertion +1 (A)	Deletion -7
FLNC DD	12	Compound Heterozygous	Deletion -2 (GG)	Insertion +1 (G)
FLNC DD	7	Heterozygous	Insertion +1 (T)	WT

Table 2.4. Chromosomal analysis of gene-edited iPSCs

A.

Unedited Ctrl		
Genes	**Copy Number**	**Status**
chr1q	1.78	Normal
chr4p_CTRL	1.91	Normal
chr8q	1.95	Normal
chr10p	1.83	Normal
chr12p	2.27	Normal
chr17q	2.19	Normal
chr18q	2.22	Normal
chr20q	1.96	Normal

B.

FLNC ABD -/-		
Genes	**Copy Number**	**Status**
chr1q	1.82	Normal
chr4p_CTRL	2.08	Normal
chr8q	2.21	Normal
chr10p	2.21	Normal
chr12p	2.05	Normal
chr17q	1.9	Normal
chr18q	2.05	Normal
chr20q	1.81	Normal

C.

FLNC DD -/-		
Genes	**Copy Number**	**Status**
chr1q	1.95	Normal
chr4p_CTRL	2.03	Normal
chr8q	2	Normal
chr10p	2.04	Normal
chr12p	1.99	Normal
chr17q	1.87	Normal
chr18q	2.1	Normal
chr20q	2.17	Normal

D.

FLNC DD2 C7 +/-		
Genes	**Copy Number**	**Status**
chr1q	1.94	Normal
chr4p_CTRL	2.10	Normal
chr8q	2.50	Possibly Abnormal
chr10p	2.12	Normal
chr12p	2.50	Possibly Abnormal
chr17q	2.16	Normal
chr18q	2.15	Normal
chr20q	2.15	Normal

Table 2.5. Summary of genetic and clinical finding

Pedigree (person) *=proband	Heterozygous *FLNC* variants	Interpretation	Clinical	AF
A-1* †	c.1948C>T, p.Arg650X/ c.970-4A>G	P LP	DCM, NSVT	NA 0.005%
A-2	c.970-4A>G	LP	NSVT	0.005%
B-1*	c.970-4A>G	LP	DCM, NSVT	0.005%
B-2	c.970-4A>G	LP	DCM, NSVT	0.005%
B-3	Inferred from proband		DCM, NSVT, cardiac transplant	0.005%
X-1*	c.8143_8144delGT, p. Val2715fs87X	LP		NA
X-2	Inferred from proband		SCD	NA
Y-1*	c.7371delT, p. Glu2458SerfsX71	LP		NA
Y-2	Inferred from proband		SCD	NA
Z-1*	c.318C>G, Phe106Leu	VUS	LGMD, AFib, hypertrophy	0.005%
Z-2	c.318C>G, Phe106Leu	VUS	LGMD	0.005%
Pedigree (person) *=proband	Heterozygous *FLNC* variants	Interpretation	Clinical	AF
A-1* †	c.1948C>T, p.Arg650X/ c.970-4A>G	P LP	DCM, NSVT	NA 0.005%
A-2	c.970-4A>G	LP	NSVT	0.005%
B-1*	c.970-4A>G	LP	DCM, NSVT	0.005%
B-2	c.970-4A>G	LP	DCM, NSVT	0.005%
B-3	Inferred from proband		DCM, NSVT, cardiac transplant	0.005%
X-1*	c.8143_8144delGT, p. Val2715fs87X	LP		NA
X-2	Inferred from proband		SCD	NA
Y-1*	c.7371delT, p. Glu2458SerfsX71	LP		NA
Y-2	Inferred from proband		SCD	NA
Z-1*	c.318C>G, Phe106Leu	VUS	LGMD, AFib, hypertrophy	0.005%
Z-2	c.318C>G, Phe106Leu	VUS	LGMD	0.005%

AF= allele frequency gnomAD; *proband; †The two genotypes for A-1 (compound heterozygote) are shown; P/LP, pathogenic, likely pathogenic; DCM, dilated cardiomyopathy; NSVT, nonsustained ventricular tachycardia; SCD, sudden cardiac death; LGMD, limb girdle muscular dystrophy; AFib, atrial fibrillation.

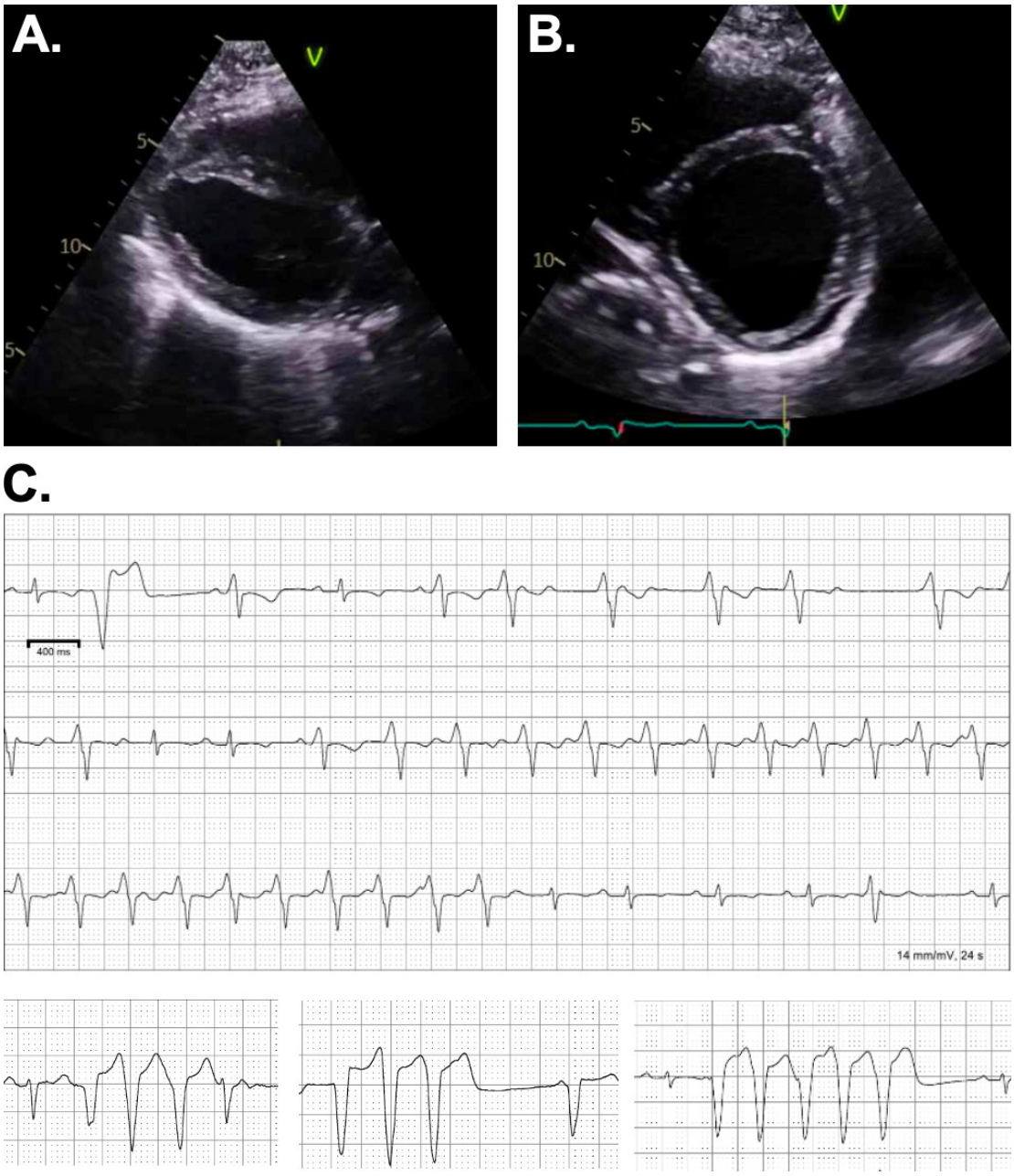

Figure 2.3. Clinical findings in a woman with dilated cardiomyopathy and mild, non- progressive skeletal myopathy. This individual presented 8 weeks postpartum with progressive heart failure symptoms and markedly reduced LV function. Her LV was markedly dilated (LV internal dimension in diastole, 6.1 cm with LVEF 30%). **A.** Parasternal long axis view. **B.** Short axis view. **C.** Nonsustained ventricular tachycardia (NSVT) was present on EKG monitor. Gene panel testing showed two different *FLNC* variants, p.Arg650X in exon 12 and c.970-4A>G in exon 5. Evaluation of her mother found only the single c.970-4A>G and confirmed these variants were in trans on two different alleles of *FLNC*.

Genetic testing with cardiomyopathy and arrhythmia gene panel (168 genes) identified two *FLNC* variants in exon 5 (c.970-4A>G) and exon 12 (c.1948C>T, p.Arg650X) (**Figure 2.4**). The premature truncation p.Arg650X is not found in population databases, and the exon 5 variant is present in 0.005% of the gnomAD cohort and is predicted to disrupt splicing. Her mother was found be heterozygous for c.970-4A>G but did not carry p.Arg650X, and at age 70, she had a long history of ventricular ectopy without syncope and normal LV function (**Figure 2.4** and **Table 2.5,** individual A-2). Her children were found to have either p.Arg650X or c.970-4A>G, confirming the compound heterozygous status. Her other relatives were unavailable for genetic testing.

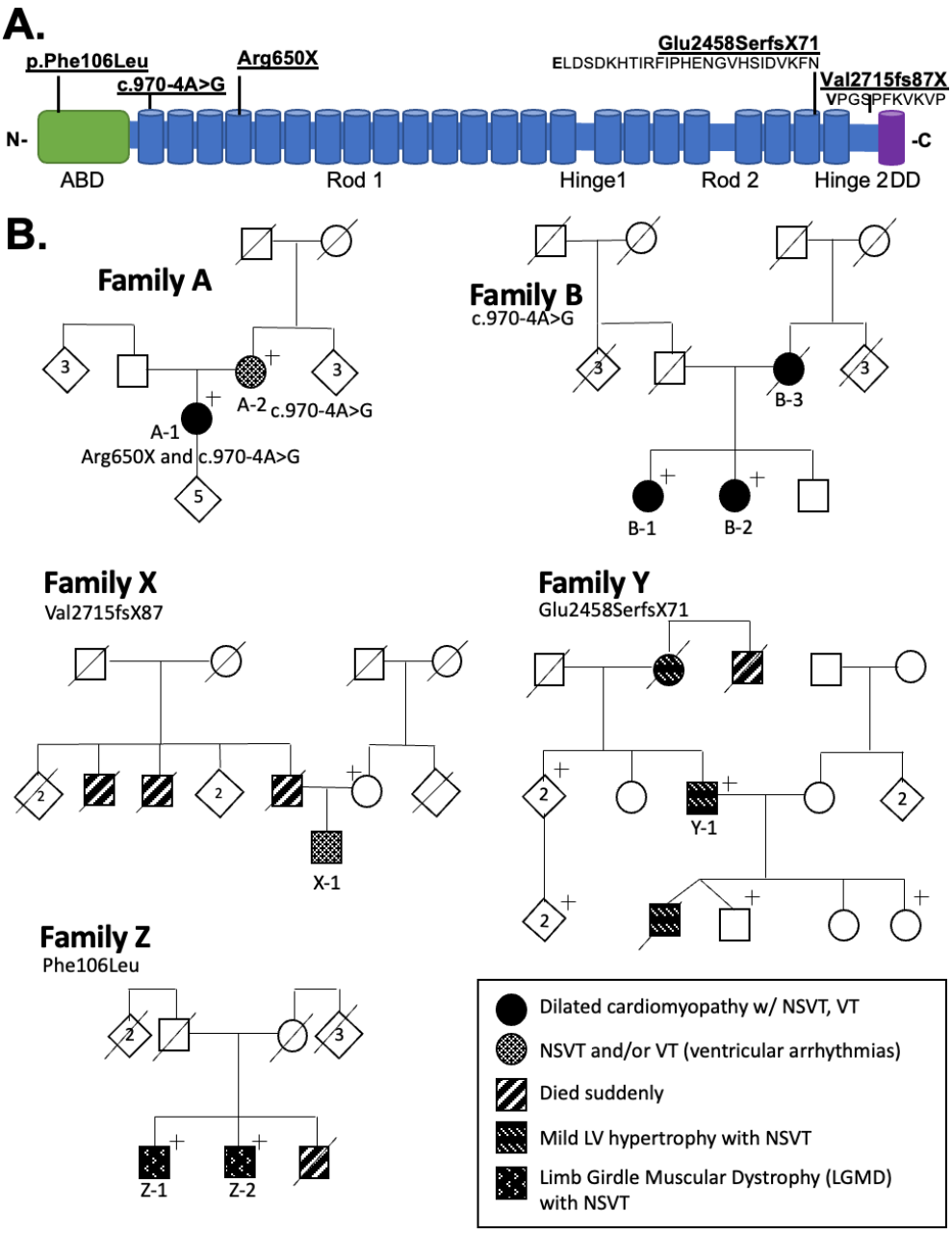

Figure 2.4. Summary of *FLNC* variants and pedigrees in this study. A. Schematic of the filamin C protein and the position of the *FLNC* variants in the pedigrees. **B.** Pedigrees of the families. The proband in family A carries two different *FLNC* variants in trans, Arg650X and c.970-4A>G, making her a compound heterozygote. The remaining families have a single *FLNC* variant in the heterozygous state. Family B has one of the two *FLNC* alleles (c.970- 4A>G) seen in the proband in Family A, but these two families are not related. Family X and Y have premature truncations in *FLNC (*Glu2458fsX71, Val2515fsX87), while family Z has a missense *FLNC* variant (Phe106Leu).

A second family (Family B) was found with heterozygous *FLNC* c.970-4A>G and DCM (**Figure 2.4** and **Table 2.5**, individual B-1). The proband in family B had DCM with a LVEF of 35%, left bundle branch block, and NSVT in her 50s. Her sister was diagnosed with DCM at age 47 (**Figure 2.4** and **Table 2.5**, individual B-2) with an LVEF of 8%; both sisters were confirmed to carry heterozygous *FLNC* c.970-4A>G. The proband's mother, prior to her death, was diagnosed with DCM and underwent cardiac transplant in her early 60's (**Figure 2.4** and **Table 2.5**, individual B-3). Family A and Family B both carry *FLNC* c.970-4A>G, but these two families derive from different parts of the United States and share no known relationship. This variant was reported as being associated with cardiomyopathy in independent reports (*78, 118*) and is interpreted as pathogenic in ClinVar (Accession Number SCV002587791.1). Based on the previous reports, we interpret this variant as likely pathogenic.

The proband in Family X was heterozygous for the *FLNC* frameshift variant (c.8143_8144delGT, p.Val2715fs87X) (**Figure 2.4** and **Table 2.5**, individual X-1). This patient was evaluated because of chest pain and intermittent episodes of dizziness at age 52. On telemetric monitoring he had NSVT, and treadmill stress testing identified runs of VT. Cardiac MRI showed normal LV cavity size and function with an LVEF of 66%, mild concentric hypertrophy, and evidence of mid myocardial enhancement highly suspicious of infiltrativecardiomyopathy. His father died suddenly at age 69, and two of the proband's uncles died suddenly in their 40s.

The proband in Family Y came to medical attention when his son suffered sudden cardiac death at age 17, and his autopsy identified HCM with a septum thickness of 2.0 cm. Whole genome sequencing on the surviving parent with mild HCM identified heterozygous *FLNC* c.7371delT, p.Glu2458Serfs71X. Site-specific testing of this same individual in a clinical genetic laboratory identified this same variant, which was interpreted as pathogenic. This proband was found to have mild hypertrophic cardiomyopathy and NSVT, and an ICD was implanted (**Figure 2.4** and **Table 2.5**, individual Y-1). The mother of this proband had a diagnosis of HCM at age 65 and died suddenly at age 93, and a maternal great uncle died suddenly at age 16 of an unknown etiology. One relative who was found to have the same pathogenic variant was found with extensive delayed enhancement on cardiac MRI.

Family Z had two brothers who developed muscle weakness in their 30s. The proband was heterozygous for a *FLNC* variant of uncertain significance (VUS) (c.318C>G, p.Phe106Leu). His brother had a similar presentation and carried the same *FLNC* VUS (**Figure 2.4** and **Table 2.5**, individuals Z-1 and Z-2). The proband had a history of atrial fibrillation, and cardiac MRI showed mild basal anterior wall hypertrophy with a maximal wall thickness of 1.5 cm with focal increased signal of delayed enhancement in the mid anteroseptal wall. A summary of the pedigrees is shown in **Figure 2.4** with genetic and clinical findings presented in **Table 2.5**. These findings underscore the association of *FLNC* with variable cardiomyopathy subtypes.

In iPSC-CMs derived from *FLNC* patients, the cardiomyocytes displayed morphologies distinct from healthy control iPSC-CMs. IPSC-CMs with *FLNC* heterozygous truncating mutations affecting the protein's C-terminus generally had delayed differentiation seen as taking longer to develop regular beating (~10-12 days of differentiation) as compared to healthy control lines (~6-8 days of differentiation). Patient-derived iPSC-CMs also showed irregular beating and cell death visible by human eye. Abnormal morphology in *FLNC* iPSC-CMs was also characterized by islands of differentiated cells and clumped cardiomyocyte networks in iPSC-CMs in contrast to healthy control iPSC-CMs had intact cardiomyocyte networks with minimal cell death **(Figure 2.5).** mRNA expression of the *FLNC* transcript was not decreased the patient-derived lines, including the lines with truncating *FLNC* mutations **(Figure 2.6)**. iPSC-CMs at day 30 were purified using the Miltenyi system, and flow cytometry was used to validate purity of iPSC-CMs by assessing percentage of cardiac troponin T (TNNT2, cTnT)- positive cells **(Figure 2.2.**

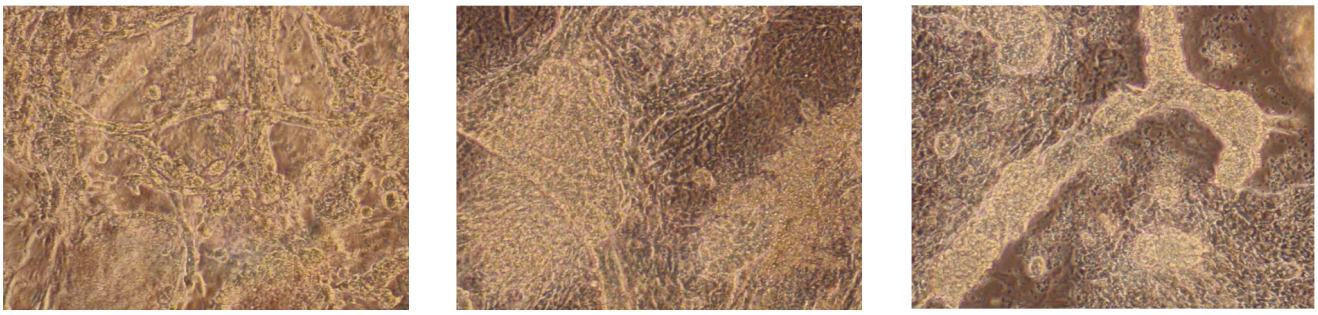

Figure 2.5. Morphology of *FLNC* patient-derived iPSC-CMs. Patient-derived iPSC-CMs with heterozygous *FLNC* truncations affecting the C-terminus showed clusters of cardiomyocytes and clumped cell networks compared to the healthy control line. Mutant iPSC-CMs showed delayed differentiation, irregular beating, and increased cell death as visible by human eye.

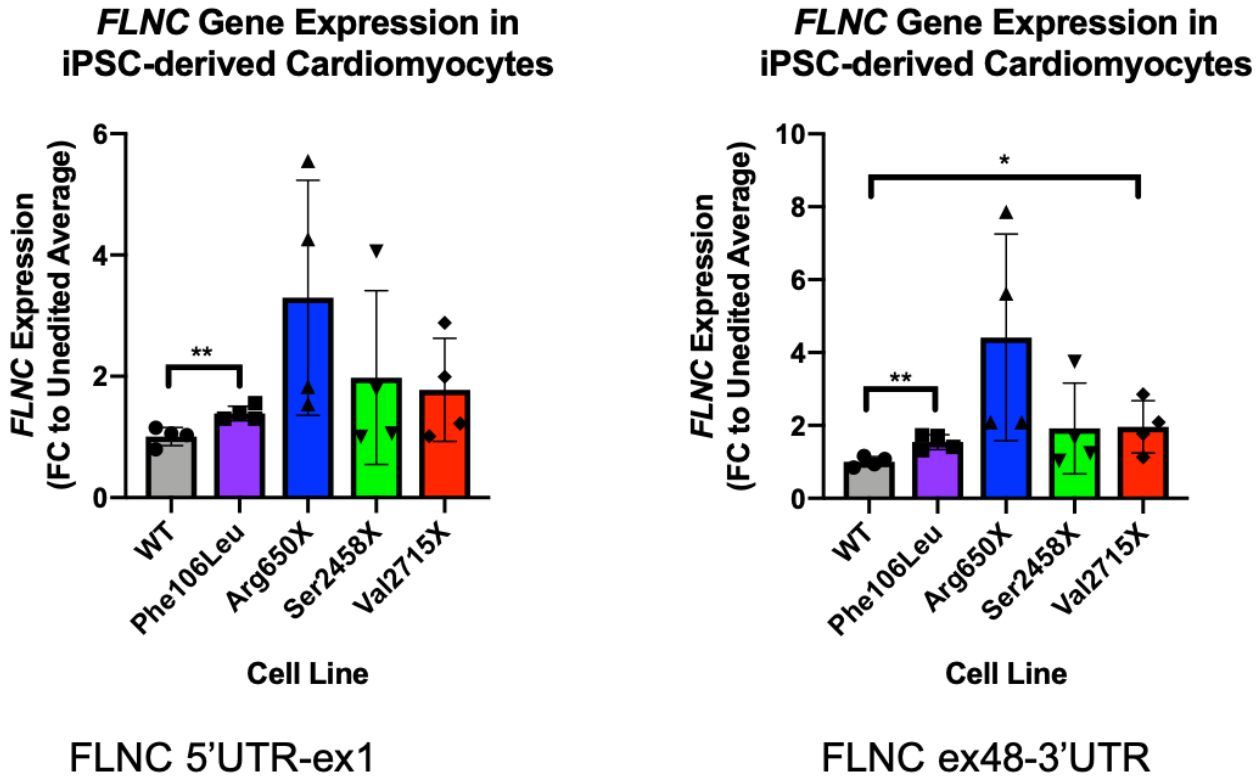

Figure 2.6. *FLNC* mRNA expression in iPSC-CMs was not reduced in *FLNC* patient lines. A. *FLNC* gene mRNA expression was evaluated using quantitative RT-PCR using primers to the 5' end (left panel) and the 3' end (right panel). mRNA expression was relatively unchanged to increased, consistent with no clear evidence for nonsense-mediated decay. Expression level was normalized to *MYBPC3* gene expression, as determined by qPCR. All data shown as mean ± SD. **, $p<0.05$ by unpaired t-test.

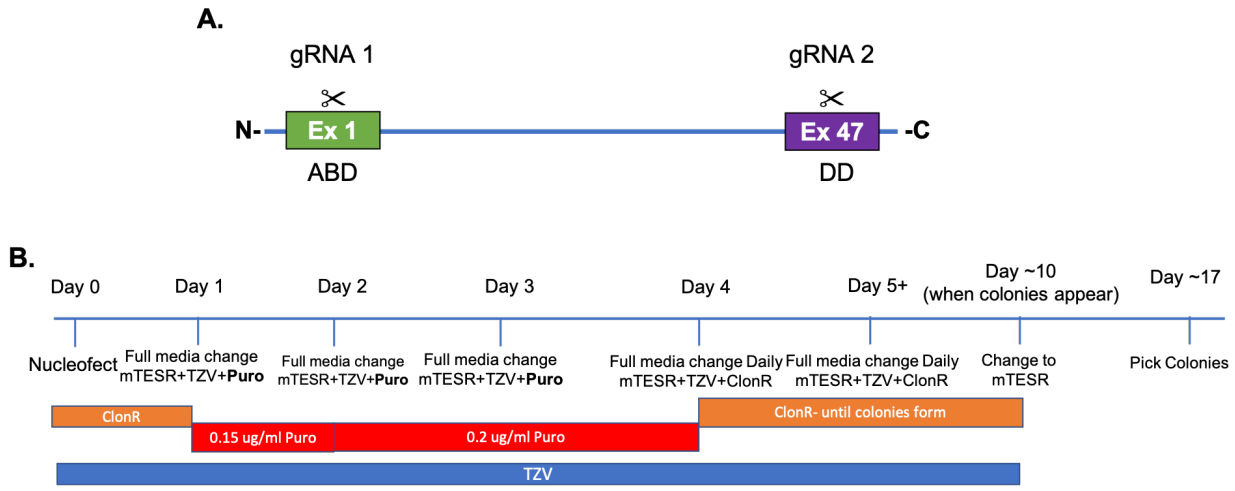

Figure 2.7. Strategy for generation of isogenic iPSC cell line using gene editing. A. Target sites for guide RNA (gRNA) to generate a homozygous deletion in *FLNC* were directed at exon 1. Exon 1 encodes the actin binding domain. **B.** Schematic for generating iPSCs and gene editing. Cells from a human healthy control individual (Coriell GM03348) were converted to iPSCs. IPSCs were transfected with 3µg of plasmid encoding Cas9 protein and the guide RNA. iPSCs were treated with 0.15µg/mL puromycin 24 hours post nucleofection and 0.2µg/mL puromycin 48-72 hours post nucleofection. Colonies were manually isolated. Sequence changes were verified by Sanger and next generation amplicon sequencing.

FLNC CRISPR isogenic cell lines

Abnormal morphology was also seen in iPSC-CMs generated to homozygously lack *FLNC* expression. CRISPr-Cas9 was used to generate mutations on both alleles of *FLNC* at either the 5' end or 3' end. When *FLNC* was mutated on both alleles in exon 1 encoding the ABD at the N-terminus, filamin C protein production was ablated. The cardiomyocyte network of *FLNC* ABD$^{-/-}$ iPSC-CMs was disrupted ~15 days post differentiation and 7 days after the cells were replated **(Figure 2.8).** Slower beat rate and increased cell death were visible by eye. In these lines, the biallelic nature of the *FLNC* mutations was validated in IPSCs using Sanger sequencing (NU Sequencing Core) and Amplicon EZ sequencing (Azenta). The parent line (GM03348) and unedited control line, which went through the gene editing process, showed no insertions or deletions within the target regions of the two alleles in exon 1 in the ABD or exon 47 in DD **(Figure 2.9 and Figure 2.10)**. The *FLNC* ABD$^{-/-}$ line had a 1 bp insertion on one allele and 7 bp deletion on the second allele in exon 1, truncating 2,595 amino acids following the miscoding of 25 amino acids and 2,611 amino acids following the miscoding of 11 amino acids, respectively. Amplicon EZ sequencing confirmed that this cell line was 99.88% certain to be a compound heterozygous variant for *FLNC* **(Figure 2.11).** *FLNC* DD$^{-/-}$ contained a 2 bp deletion on one allele which miscoded 70 amino acids leading to the truncation of terminal 46 amino acids, and a 1 bp deletion on the second allele in exon 47 of the DD, resulting in 71 miscoded amino acids resulting in the truncation of terminal 45 amino acids. This cell line was proven to be a compound heterozygote with 99.90% certainty **(Figure 2.12).** One *FLNC* DD$^{+/-}$ line was heterozygous, confirmed as having a 1 bp deletion on one allele, resulting in 97 miscoded amino acids causing a deletion of terminal 19 amino acids. and no indels in the second allele at exon 47 in the DD with >98% certainty **(Figure 2.13).** *FLNC* mRNA was measured in gene edited and isogenic iPSC-CMs at day 30 and demonstrated a reduction of *FLNC* mRNA in homozygous mutant cell lines in comparison to the control. *FLNC* gene expression was reduced in FLNC ABD$^{-/-}$ and FLNC DD$^{-/-}$ iPSC-CMs in using primer sets amplifying the 5'UTR to exon 1 and exon 48 to 3'UTR target regions before and after the sites of mutation, respectively **(Figure 2.14)**. The *FLNC* DD$^{+/-}$ line did not show a reduction of mRNA, suggesting that mRNA reduction is a feature of homozygous lines. Immunoblotting was used to measure the reduction in filamin C protein expression the *FLNC* gene edited and isogenic iPSC-CMs. Filamin C protein expression was significantly reduced in *FLNC* ABD$^{-/-}$ and *FLNC* DD$^{-/-}$ iPSC-CMs and

was also partially reduced in *FLNC* DD$^{+/-}$ iPSC-CMs **(Figure 2.15)**. Thus, in the homozygous FLNC gene edited lines, the mRNA may be subjected to nonsense mediated decay, which could also contribute to the reduction in filamin C protein. BAG3 protein levels were unchanged. All values were normalized to alpha-sarcomere actin.

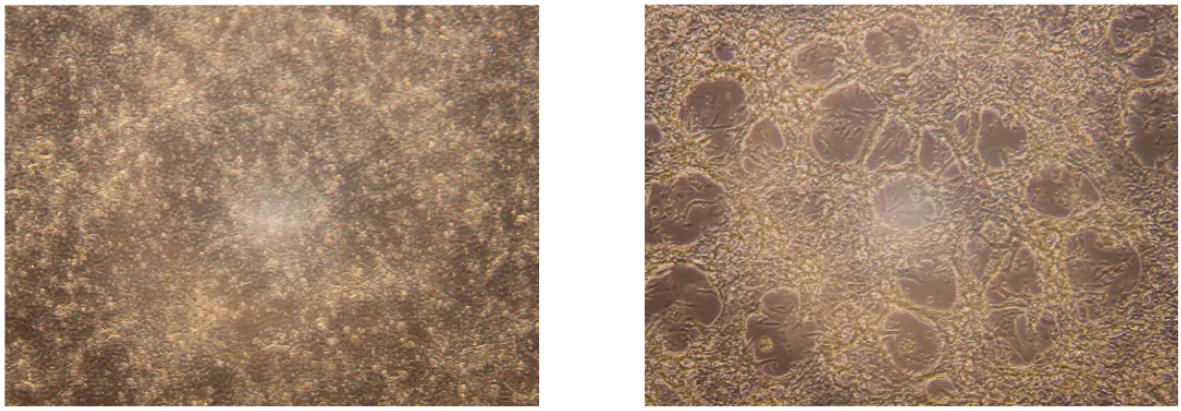

Unedited
Control

FLNCABD -/-

Figure 2.8. Morphology of *FLNC* CRISPR isogenic iPSC-CMs. Gene-edited iPSC-CMs with heterozygous *FLNC* mutations which affect the protein's N-terminus show disrupted network of cardiomyocytes as compared to the healthy isogenic control. Mutant iPSC-CMs showed slower beating and increased cell death as visible by human eye.

=

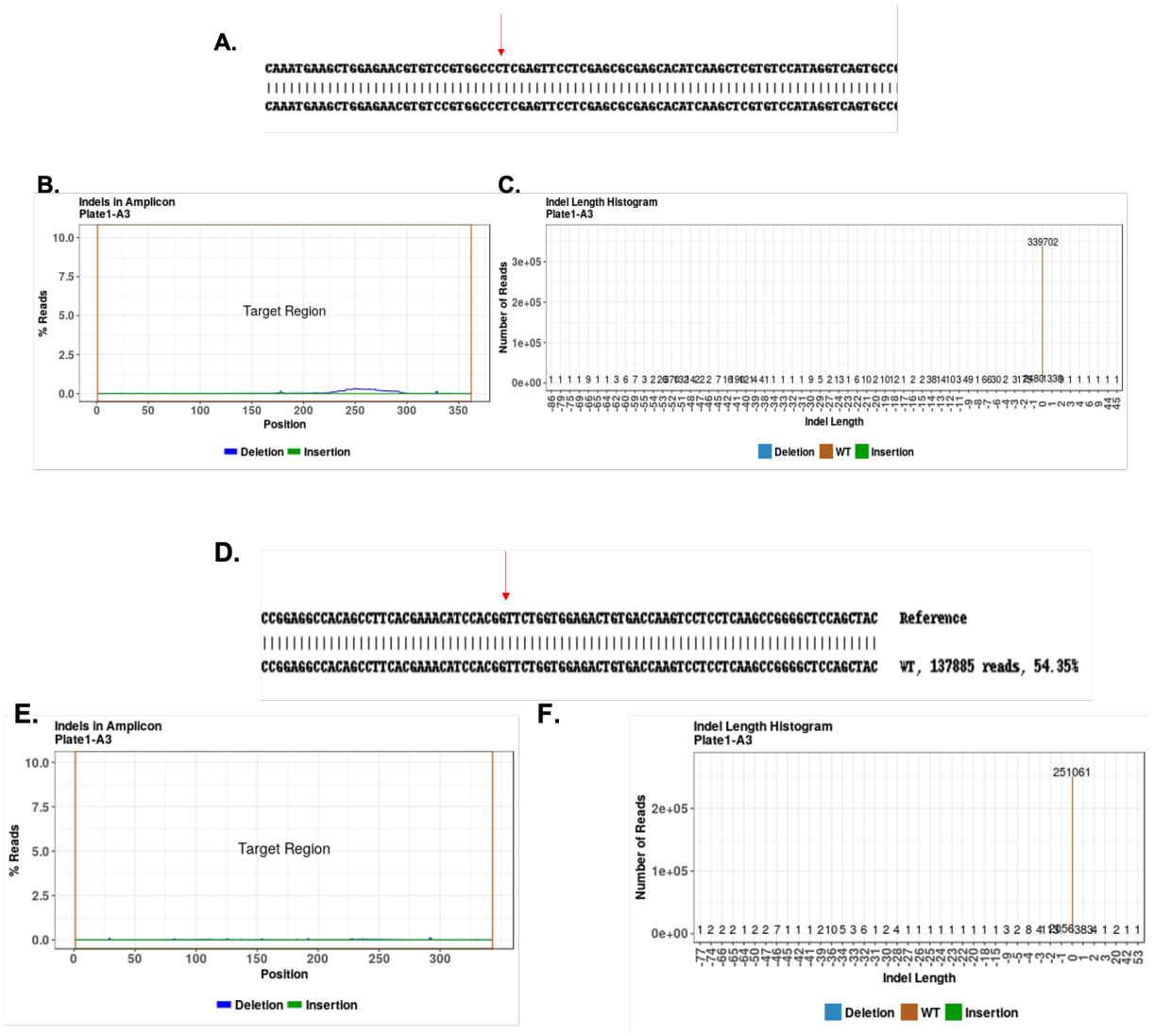

Figure 2.9. Confirmation of GM03348 parent iPS cell line as normal as determined by Amplicon EZ sequencing. A. Target site of guide RNA in exon 1 in the actin binding domain. **B-C.** GM03348 iPS cell line was identified as a homozygous normal as no deletions or insertions were detected in either of two alleles within the target region of exon 1. **D.** Target site of guide RNA in exon 47 in the dimerization domain. **D-E.** GM03348 iPS cell line was identified as a homozygous normal as no deletions or insertions were detected in either of two alleles within the target region of exon 47.

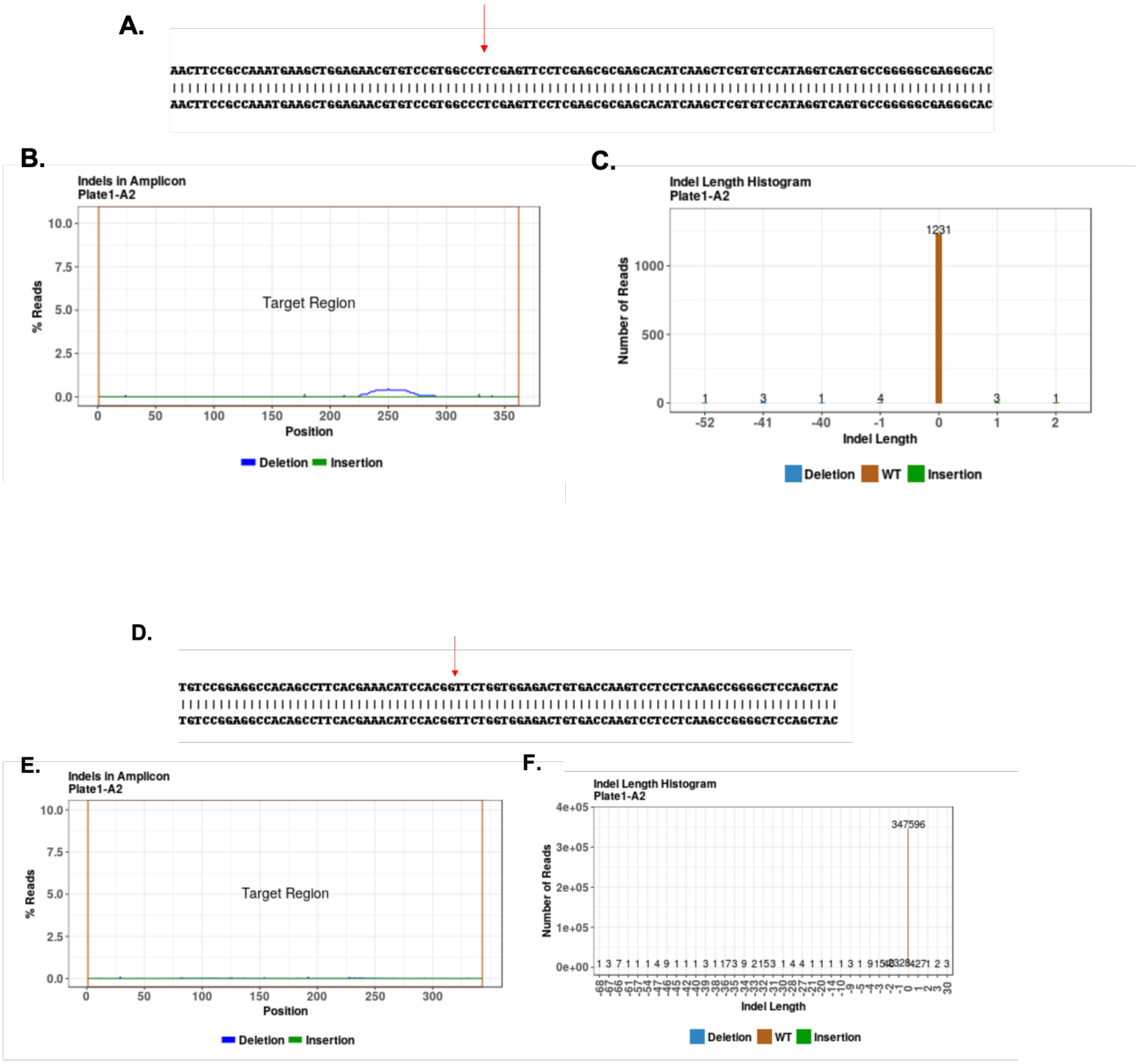

Figure 2.10. Confirmation of unedited control iPS cell lines as normal as determined by Amplicon EZ sequencing. A. Target site of guide RNA in exon 1 in the actin binding domain. **B-C.** Unedited control iPS cell line was identified as a homozygous normal as no deletions or insertions were detected in either of two alleles within the target region of exon 1. **D.** Target site of guide RNA in exon 47 in the dimerization domain. **D-E.** Unedited control iPS cell line was identified as a homozygous normal as no deletions or insertions were detected in either of two alleles within the target region of exon 47.

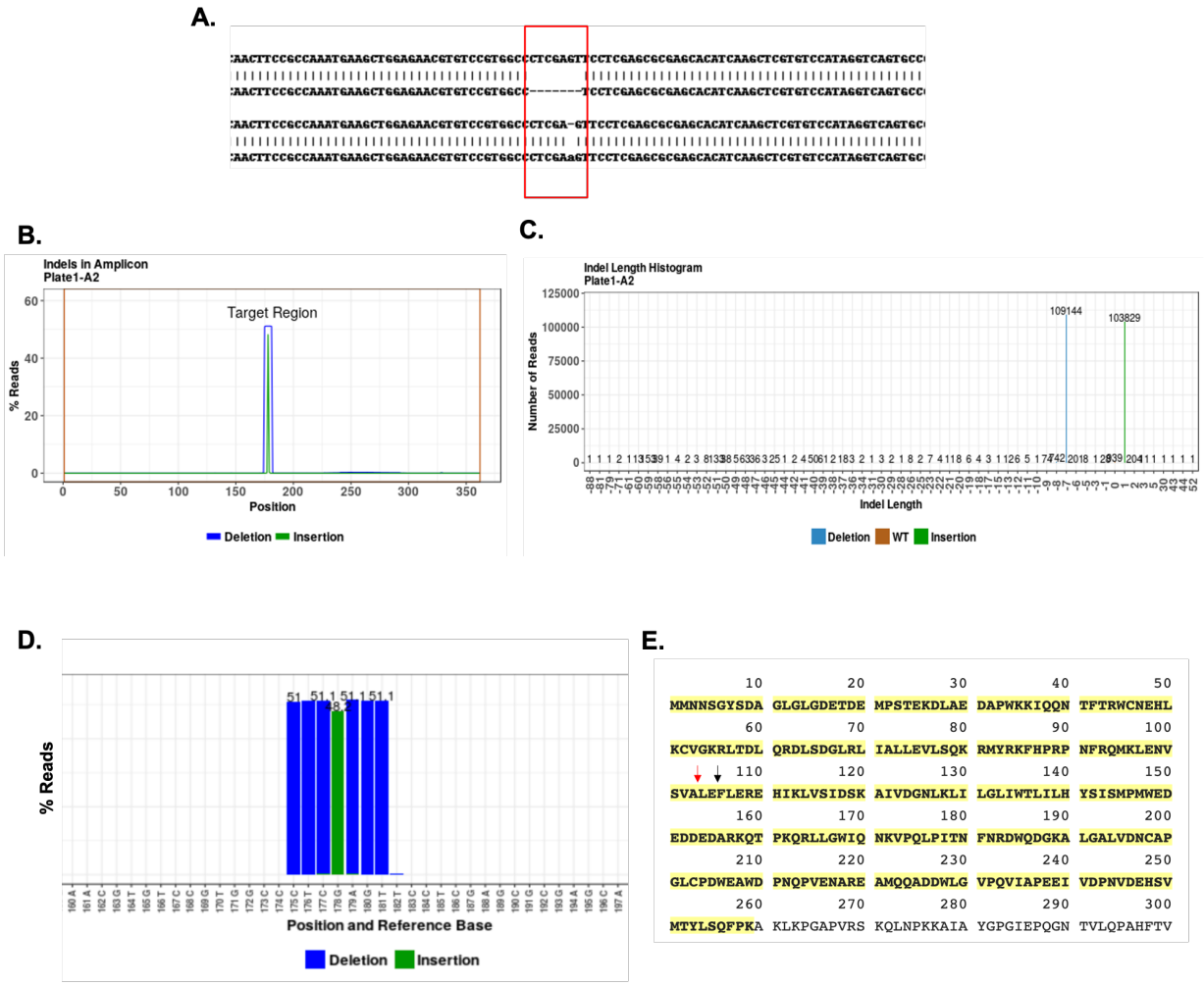

Figure 2.11. Confirmation of *FLNC* ABD Clone 17 iPS cell line as compound heterozygote as determined by Amplicon EZ sequencing. A. Target site of guide RNA in exon 1 in the actin binding domain. **B-D.** *FLNC* ABD Clone 17 was identified as a compound heterozygous with a 1 bp insertion on one allele and a 7 bp deletion on the second allele at exon 1 with 99.88% certainty that this cell line is a mutant. **E.** Filamin C protein sequence indicating target site of mutation. This mutation causes 25 miscoded amino acids until premature stop coding resulting to 2,595 amino acid truncation on one allele and 11 miscoded amino acids until premature stop codon resulting in 2,611 amino acid truncation on the second allele.

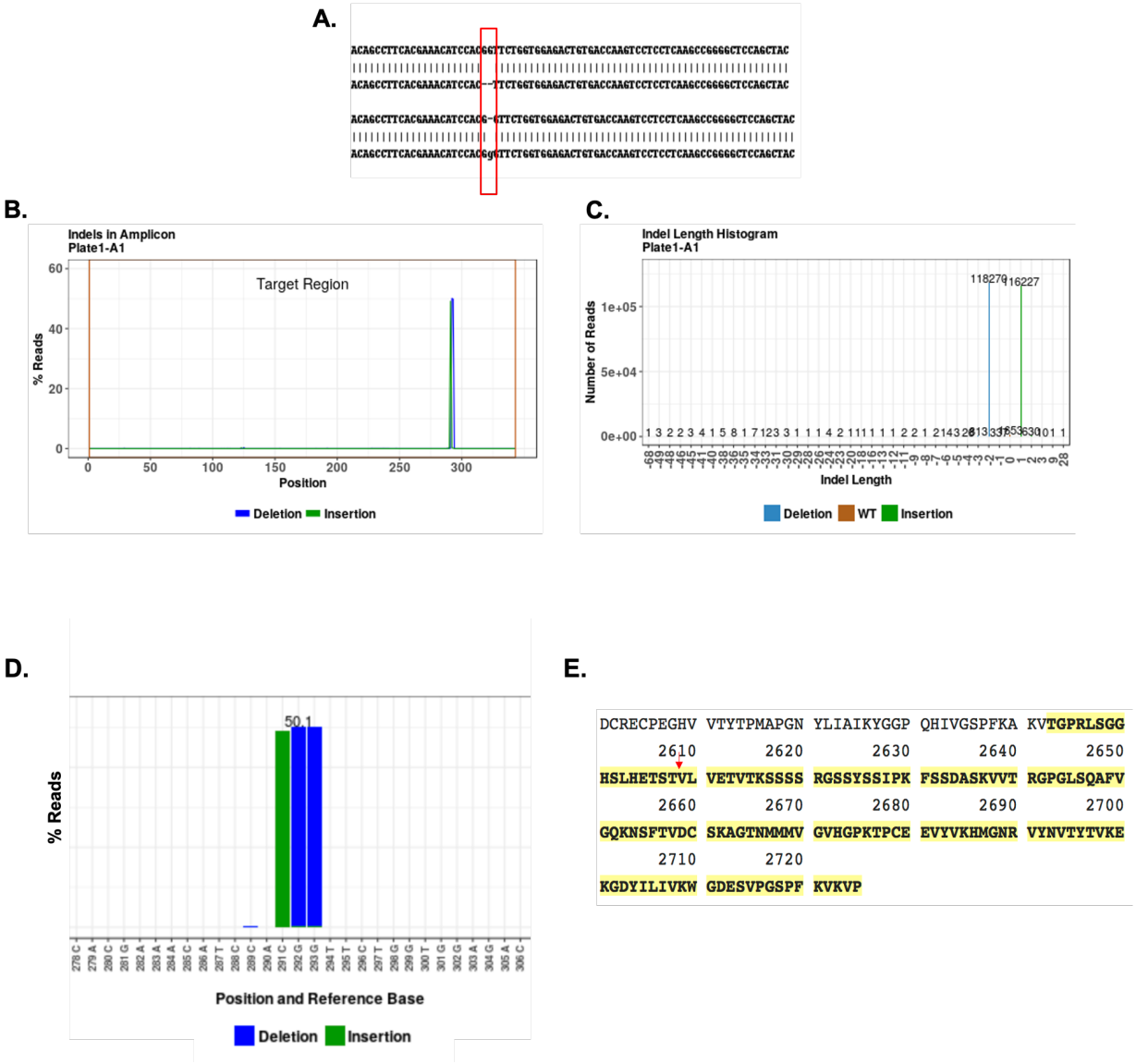

Figure 2.12. Confirmation of *FLNC* DD Clone 12 iPS cell line as compound heterozygote as determined by Amplicon EZ sequencing. A. Target site of guide RNA in exon 47, which encodes the dimerization domain. **B-D.** *FLNC* DD clone 12 was identified as a compound heterozygous with a 2 bp deletion on one allele and a 1 bp insertion on the second allele at exon 47 with 99.90% certainty that this cell line is a mutant. **E.** Filamin C protein sequence indicating target site of mutation. This mutation causes 70 miscoded amino acids until premature stop coding resulting to 46 amino acid truncation on one allele, and 71 miscoded amino acids until premature stop codon resulting in 45 amino acid truncation on the second allele.

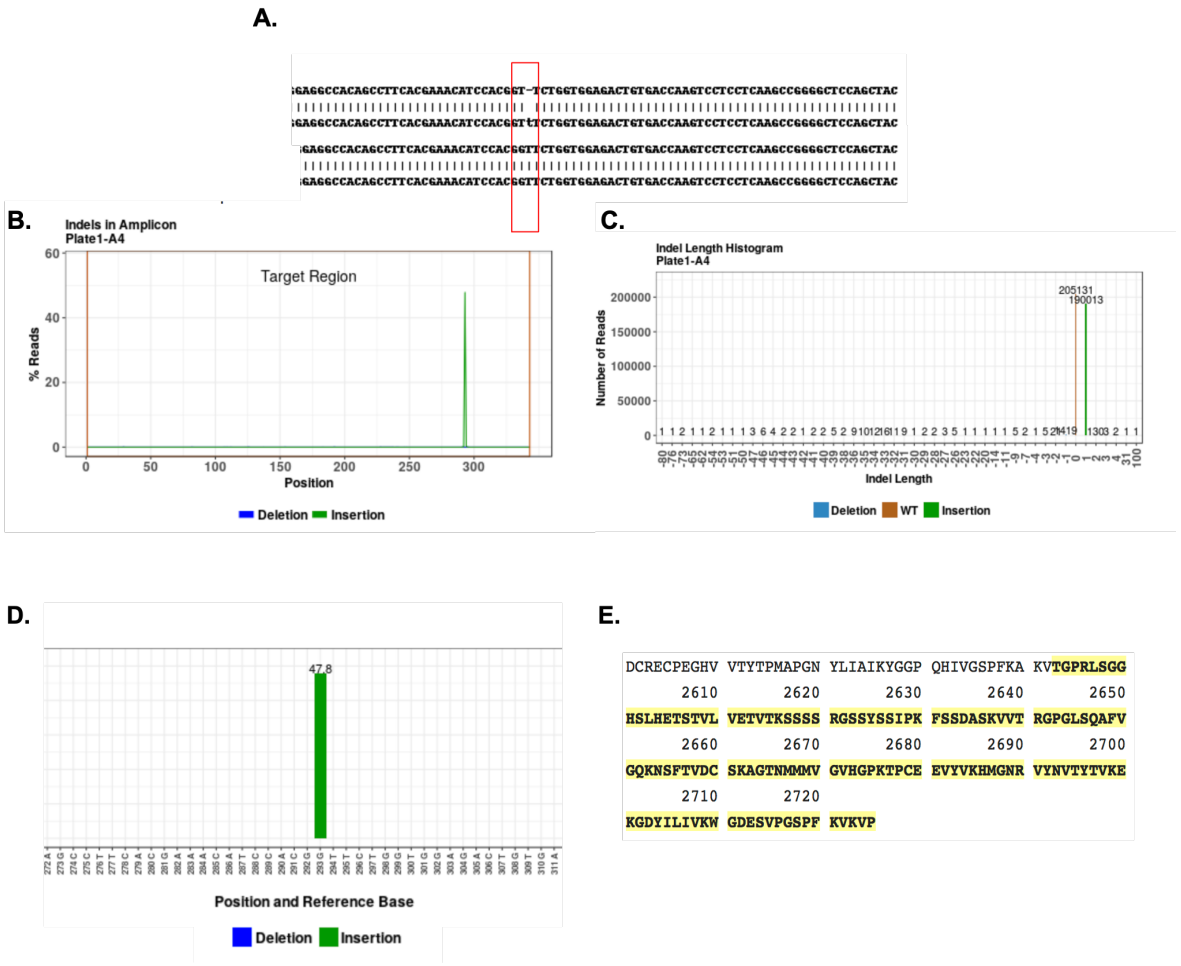

Figure 2.13. Confirmation of *FLNC* DD Clone 7 iPS cell line as heterozygote as determined by Amplicon EZ sequencing. A. Target site of guide RNA in exon 47 encoding the dimerization domain. **B-D.** *FLNC* DD Clone 7 was identified as a heterozygous with a normal allele and a 1 bp insertion on the other allele at exon 47 with >98% certainty that this cell line is a mutant. **E.** Filamin C protein sequence indicating target site of mutation. This mutation causes 97 miscoded amino acids until premature stop coding resulting to 19 amino acid truncation on one allele.

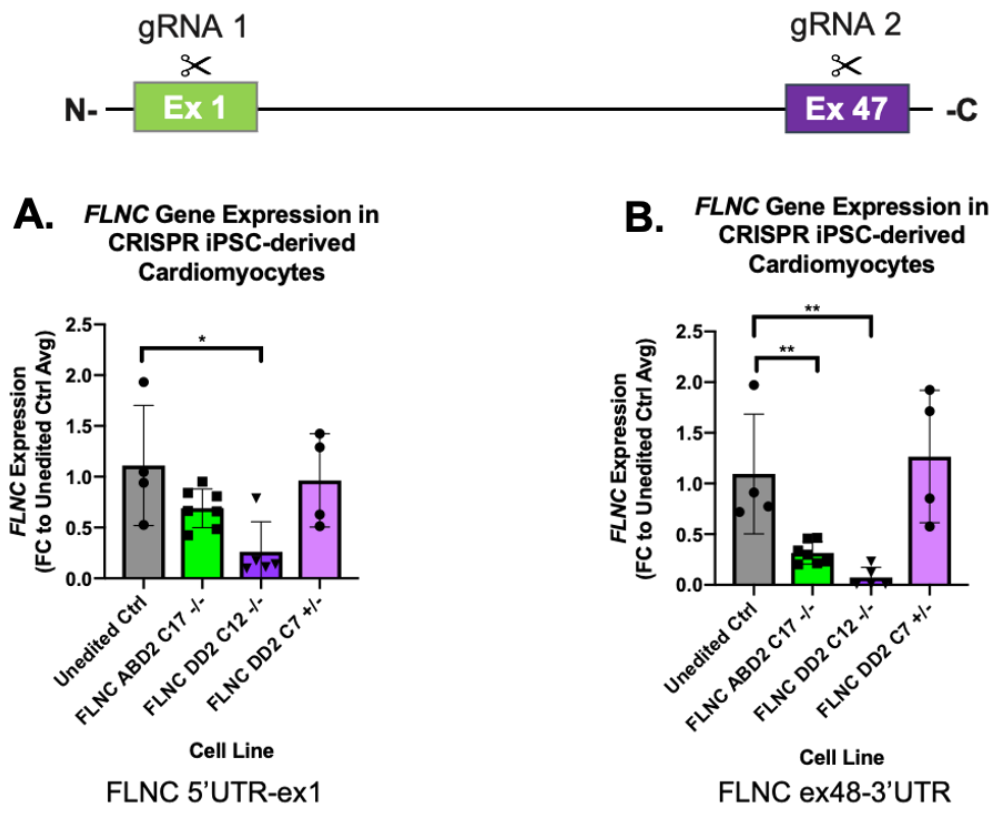

Figure 2.14. *FLNC* mRNA expression in iPSC-CMs comparing unedited control and *FLNC* ABD$^{-/-}$. *FLNC* gene expression was reduced in *FLNC* ABD$^{-/-}$ and *FLNC* DD$^{-/-}$. Expression level was normalized to *MYBPC3* gene expression, as determined by qPCR using primers amplifying the region between the 5'UTR and exon 1 before the mutation sites (left) or using primers directed at exon 48 and the 3'UTR (right). All data shown as mean ± SD. **, $p<0.05$ by unpaired t-test.

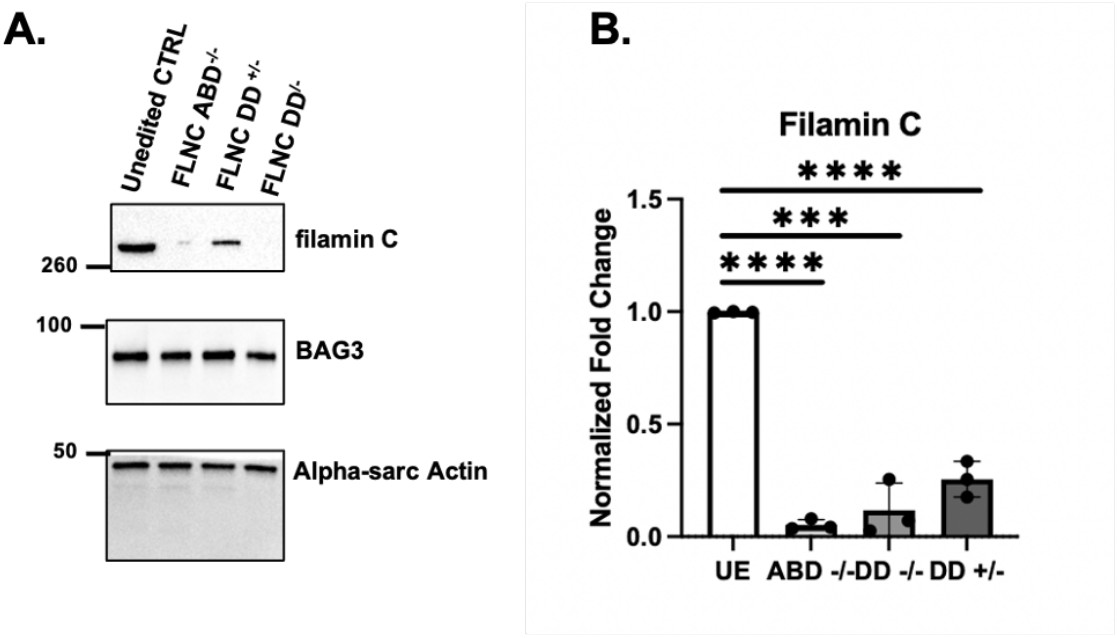

Figure 2.15. *FLNC* protein expression in iPSC-CMs comparing unedited control and *FLNC* ABD$^{-/-}$.A. Filamin C protein expression was reduced in *FLNC* ABD$^{-/-}$, *FLNC* DD$^{-/-}$, and *FLNC* DD$^{+/-}$ iPSC- CMs as determined by immunoblot using an antibody to the carboxy-terminus of filamin C (Sigma, Cat#HPA006135). **B.** Quantification of filamin C protein expression in unedited control iPSC-CMs and *FLNC* ABD$^{-/-}$, *FLNC* DD$^{-/-}$, and *FLNC* DD$^{+/-}$ iPSC-CMs. All data shown as mean ± SD. ****, $p<0.0001$ by unpaired t-test.

Discussion

Variable cardiomyopathy expression with FLNC mutations.

Heterozygous truncating *FLNC* mutations have been associated with hypertrophic, dilated, and arrhythmogenic cardiomyopathy (*78, 111*). Among the families and cases reported here, we also observed a range of cardiomyopathies including DCM and HCM and risk for ventricular arrhythmias for the truncating *FLNC* variants. The index case present herein manifested in the peripartum interval with biallelic *FLNC* variants, both of which disrupted filamin C expression. Through family studies involving her offspring, we confirmed these two *FLNC* truncations were in *trans* on two separate alleles. We previously reported one of the first cases of sudden cardiac death linked to *FLNC* in a young woman carrying c.3791-1 G>C, which was subsequently identified in the Ashkenazi population (*119, 120*). The *FLNC* c.3791-1 G>C variant disrupts a splicing acceptor at the end of intron 21 and was associated with reduced filamin C transcript expression in fibroblasts. *FLNC* truncation mutations have been described in peripartum cardiomyopathy (*121*). Although *TTN* truncations are the most common genetic variants contributing to peripartum cardiomyopathy, the next most common genetic mutations are *FLNC* and *DSP* truncating mutations (*121*). Cardiac demand increases during pregnancy with cardiac adaptations in all trimesters and distinct shifts in the postpartum interval. Titin, filamin C and desmoplakin are key proteins that regulate sarcomere formation and formation of intercalated disks, which may be especially subject to turnover with the cardiac adaptations during late pregnancy (*122, 123*).

Genetic assessment of targeted populations enriched for arrhythmias and cardiomyopathies has identified an enrichment of *FLNC* mutations, especially truncating variants (*3, 18, 71, 111, 118*). Conversely a genotype “first” approach, where genetic findings are then correlated with electronic health record reports, also confirmed that *FLNC* truncations increase risk of cardiac disease. In this recent survey of 171,948 subjects in a medical biobank with exome sequencing, *FLNC* loss of function (truncation) variants associated with an increased risk of ventricular arrhythmia and dysfunction. Biobank participants with *FLNC* truncation variants had significantly increased odds of dilated cardiomyopathy, left ventricular dysfunction, supraventricular tachycardia, and arrhythmia (*124*). Because of findings like these and other reports (*125*), the American College of Medical Genetics and

Genomics (ACMG) recently recommended reporting pathogenic *FLNC* variants incidentally identified through genome sequencing citing the high penetrance and elevated risk for cardiomyopathy and sudden death. In these studies, the penetrance of *FLNC* variants was relatively low, supporting the idea that additional stressors or second “hits” likely contribute to disease manifestation. Our studies identify cell stimuli that further stress protein turnover as contributing to that risk.

Study Limitations

FLNC patients were consented during appointment visits. Thus, we had to coordinate sample collection around the time when they would be coming into the clinic. Certain urine samples were difficult to isolate cells from and required additional or alternative attempts, including collecting samples from family members who also had the same variant or collecting a blood sample since this process has a higher yield for cell isolation. A significant amount of time was spent on building accurate and sustainable cell models, including a wide array of control, *FLNC* patient, and *FLNC* CRISPR isogenic cell lines, performing quality control to ensure integrity, reliability, and reproducibility, and implementing technologies and systems. These efforts limited the breadth of functional experiments on these cell lines that were initially planned. Differentiation of mutated cardiomyocytes was often delayed and yielded fewer cardiomyocytes due to the reduction or loss of filamin C, since this protein is an essential component in maintaining sarcomere structure. Due to the COVID-19 pandemic, experiments were delayed as a result of reduced working hours in the lab in accordance with university guidelines, vendor supply chain issues that made it difficult to obtain lab materials and reagents in a timely manner, and reduced lab personnel, who are essential for exchanging ideas, helping with experimental troubleshooting, and allowing the lab to operate efficiently overall.

Chapter 3.

Impact of *FLNC* Truncations Under Stress

Overview

Mutations in *FLNC*, which encode the actin binding protein filamin C, lead to myofibrillar myopathy as well as cardiomyopathy. Heterozygous premature truncations in *FLNC* are enriched in cohorts with cardiomyopathy with ventricular arrhythmias playing a prominent role in *FLNC*-related cardiomyopathies. Filamin C is highly expressed in heart and skeletal muscle, and animal models with disrupted *Flnc* display a range of outcomes from early lethality to a mild, exercise-induced skeletal muscle myopathic phenotype characterized by protein aggregates, depending on the position of the *Flnc* mutation and the result on filamin C protein production.

Although similar protein aggregates have not been well described in hearts carrying *FLNC* truncations, a shared pathology between skeletal and cardiac myopathies is likely. Here we describe multiple families with *FLNC* mutations and a range of cardiomyopathic phenotypes, including an individual with postpartum cardiomyopathy and NSVT who had *FLNC* p.Arg650X on one allele and c.970-4A>G on the other *FLNC* allele. Induced pluripotent stem cell-derived cardiomyocytes (iPSC-CMs) were generated from patients and also by gene editing of a human healthy control line. We identified a reduction in filamin C protein in patient-derived iPSC-CMs harboring truncation *FLNC* alleles but filamin C reduction was not seen with a missense *FLNC* allele. After exposure to the proteasome inhibitor bortezomib, *FLNC* iPSC-CMs showed an increase of filamin C protein, BAG3, HSP70 and HSPB8, compared to unedited control, consistent with a role for filamin C in mediating protein turnover. *FLNC* null and patient-derived *FLNC* iPSC-CMs showed prolonged electric field potential, providing a cellular surrogate for the predisposition to arrhythmias in *FLNC*-cardiomyopathy patients. Proteasome inhibition further elongated field potential duration, consistent with a model where additional stressors, especially proteotoxic stressors, exacerbate arrhythmia potential in *FLNC* cardiomyopathy.

Respective Contributions

Joyce Ohiri conducted all experiments and analysis of data. Dr. David Barefield helped guide the projects in its initial phase and helped with optimizing immunofluorescence microscopy. Dr. Dominic Fullenkamp implemented the differentiation technique and tools to measure mechanical stress in the lab and helped tremendously with providing expertise, guidance, and feedback throughout the course of my experiments. Dr. Tanner Monroe provided ideas to help steer the course of my experiments and data collection. Drs. Alexis Demonbreun and Megan Puckelwartz significantly helped with data analysis. Dr. Malorie Blancard helped with use of the CardioExcyte system and helped with data analysis. Drs. Al George and Lisa Wilsbacher provided expertise and strong ideas that helped me better navigate my data. Dr. Elizabeth McNally was a pivotal person in the inception of this project, provided the clinical data, helped considerably with drafting the manuscript and making this story come to life.

Introduction

Ventricular arrhythmias (VA) are associated frequently with *FLNC*-cardiomyopathy and include nonsustained and sustained ventricular tachycardia. Notably, VA occur even with mildly reduced left ventricular dysfunction or in minimally hypertrophied left ventricles, indicating that risk assessment strategies should take into consideration *FLNC* genotype (*18, 70, 118*). In the myofibrillar myopathies, intracellular aggregates are a characteristic finding in skeletal muscle; however, these aggregates have not readily apparent in cardiomyopathic hearts (*111*). The presence of intracellular aggregates in skeletal muscle and the lack of finding aggregates in the heart might reflect the limited sampling of the heart. Alternatively, the lack of detectable aggregates could derive from intrinsic differences between heart and skeletal muscle, and/or more likely the nature of specific *FLNC* variants.

In heart and skeletal muscle, filamin C is enriched near Z discs, and there is a concentration of filamin C protein at the plasma membrane. In the heart, filamin C is also found at intercalated discs (*65, 111*). Filamin C has an actin binding domain at its amino terminus, followed by 24 immunoglobulin (Ig)-like repeat domains. Between the 15th and 16th repeat domains is a region that is variably spliced with inclusion or exclusion of exon 31 (*126*). This splicing event encodes an additional flexible hinge into the filamin C protein. Exon 31-containing transcripts are increased in failed hearts (*18*). The final Ig-like repeat domain mediates dimerization of filamin C, and a premature truncation in this domain, W2710X, was first identified in German families with myofibrillar myopathy and associated cardiomyopathy (*63, 77*).

Mice engineered with the equivalent of human W2710X, called W2711X in mice, express both the truncated filamin C protein and the full-length form in skeletal muscle, indicating that the truncated filamin C, under some circumstance, may be expressed (*67*). Heterozygous W2711X mice develop an exercise-induced myopathic process characterized by intracellular aggregates in skeletal myofibers (*67*). Mice with homozygous W2711X similarly develop skeletal muscle myopathy with a faster time course to disease. In contrast to the W2711X mice, homozygous deletion of the last eight exons of *Flnc* (*D*41-48), which removes the last five Ig domains, results in early postnatal lethality from

respiratory muscle weakness (*85*). Unlike the W2711X mice, there is little expression of filamin C protein in the *D*41-48 muscle, supporting the idea that some *FLNC* truncations may produce mRNA subject to nonsense-mediated decay and/or proteins that are unstable.

Multiple lines of evidence support a role for filamin C in proteostasis, and this process is especially important in striated muscle that undergoes hypertrophy and atrophy in response to different stimuli (*127*). Filamins, including filamin C, can undergo unfolding of specific Ig domains under mechanical and other stressors (*57*). BAG3 and small heat shock proteins interact with filamin C to mediate the chaperone-assisted selective autophagy (CASA) pathway to remove damage and misfolded proteins (*128-130*). BAG3 is essential to stabilize the interaction with heat shock factor proteins and to maintain proteostasis (*104*).

We found that *FLNC*-null iPSC-CMs displayed increased sensitivity to proteotoxic stress with impaired response to heat shock proteins and components of the autophagy pathway. To model clinically relevant arrhythmias associated with *FLNC* mutations, we assessed extracellular field potential as a reflection of action potential, and we identified prolonged field potential duration in *FLNC* null iPSC-CMs. Furthermore, when subjected to proteotoxic stress with bortezomib, field potential prolonged even more, providing a link between proteostasis and arrhythmia susceptibility. Together, these findings identify filamin C as a critical regulator of stress pathways in cardiomyocytes, which creates a substrate that promotes arrhythmogenesis.

Methods

Immunofluorescence Microscopy

iPSC-CMs (3 x 10^5 cells) were replated on Matrigel™-coated 12mm Micro coverglass slips (Electron Microscopy Sciences, Cat#72231-01) in a 24-well plate. At days 19-25, coverglass slips were washed with 1X PBS and fixed with 2% paraformaldehyde. Glass coverslips were washed with 1X PBS, permeabilized with 0.2% Triton and blocked with 5% BSA for 1 hr at RT. Coverslips were incubated with primary antibodies to filamin C (ABClonal, Cat#A13018, 1:200) and alpha-actinin (Sigma, Cat#A7811, 1:1000) in 5% BSA overnight at 4°C. Coverslips were washed with 0.1% Tween and secondary antibodies Goat anti-Rabbit IgG (Invitrogen, Cat#A11012, 1:1000) and Donkey anti-Mouse IgG (Invitrogen, Cat#A21202, 1) were added at 1:1000 in 5% BSA for 1 hr at RT. Coverslips were washed and mounted onto glass slides with Prolong Gold (Thermo, Cat#P36930) and imaged (Zeiss, Axio Imager M2).

Proteotoxic stress with bortezomib.

iPSC-CMs were replated onto 12-well plates at 2x10^6 cells/well and treated at day 30 with proteasome inhibitor, bortezomib (Cell Signaling, 2204S) at varying concentrations or 0.01% DMSO for 24 hrs. Cells were collected and protein was isolated and aliquoted as described above. Protein expression was measured using immunoblotting.

Mechanical stress with FlexCell system.

Rubber membranes of BioFlex 6-well plates were activated with 3-Aminopropyltriethoxysilane, washed with 1X PBS and ultrapure water, and coated with Matrigel. iPSC-CMs were replated onto BioFlex 6-well plates at 1.5x10^6 cells/well. Unflexed control cells were collected before flexing and the flexed cells were flexed day 20 at 10% strain for 20 hours in the FlexCell chamber. Cells were collected and protein was isolated and aliquoted as described above. Protein expressing was measured using immunoblotting.

Multielectrode array (MEA) measurements.

iPSC-CMs were replated onto a 96-well MEA plate (Nanion Technologies, Cat#201003). Media change was completed 1 hr before the treatment plate was read on the CardioExcyte 96 platform (Nanion

Technologies). iPSC-CMs were paced at 1 Hz, 20 ms burst length and 10% intensity at a sweep duration of 30 sec with a repetition interval of 10 min. iPSC-CMs were treated with bortezomib or DMSO when stabilized after ~10 sweeps by adding to existing media in a 1:4 dilution for final concentration of 0.1uM or 0.01%, respectively. Quality control and data analysis was performed using DataControl software for the CardioExcyte Nanion.

Statistical analyses.

Data were analyzed using GraphPad Prism and the specific statistical tests were selected based on data distribution and number of comparisons.

Results

Filamin C is reduced in iPSC-CMs with FLNC mutations.

Induced pluripotent stem cells (iPSCs) were established from several of the above individuals and used to generate cardiomyocytes (iPSC-CMs). Using immunoblotting with an antibody to the filamin C carboxy-terminus, we evaluated filamin C protein production in iPSC-CMs from healthy control lines and lines carrying *FLNC* variants p.Arg650X,c.970-4A>G, p. Glu2458SerfsX71 (referred to as p.Glu2458fs), p.Val2715fs87X (referred to p.Val2715fs) and p.Phe106Leu (**Figure 3.1A)**. Compared to healthy control iPSC-CMs, the amount of filamin C protein was reduced in the three lines with *FLNC* truncation variants (p.Arg650X, p.Glu2458fs, p.Val2715fs), but not in the missense line p.Phe106Leu (**Figure 3.1B**). Filamin C protein was most reduced in p.Arg650X iPSC-CMs, consistent with this line having a second *FLNC* variant as a compound heterozygote (c.970-4A>G) (*118*).

iPSC-CMs were evaluated for protein localization using immunofluorescence microscopy (IFM) with a focus on the iPSC-CM lines that produced reduced but detectable filamin C protein content (Glu2458fs and Val2751fs). Localization of α-actinin was used to evaluate sarcomere content (green imaging in **Figure 3.1C**), and α-actinin staining demonstrated sarcomeres in the two lines with heterozygous *FLNC* frameshifting alleles, Glu2458fs and Val2751fs as well as in the Phe106Leu iPSC-CMs. As expected in healthy control human iPSC-CMs, filamin C co-localized with α-actinin (merged images in **Figure 3.1C**).

Qualitatively, there were more areas where filamin C protein was reduced in sarcomeres in the mutant cardiomyocytes with truncated filamin C (compare filamin C staining in red boxes in **Figure 3.1C**). The iPSC-CM line with Phe106Leu showed scattered areas of filamin C protein aggregates (white arrows), and similar findings were not readily evident in the healthy control iPSC-CMs nor in the *FLNC* truncating iPSC-CMs. In addition, Z-line streaming was observed in all three *FLNC* mutant iPSC-CM lines (compare green boxes in Glu2458fs, Val2715fs and Phe106Leu demonstrating disruption of Z line integrity). These data support a reduction in total filamin C protein and Z line streaming as potential mechanisms that contribute to cardiomyopathy.

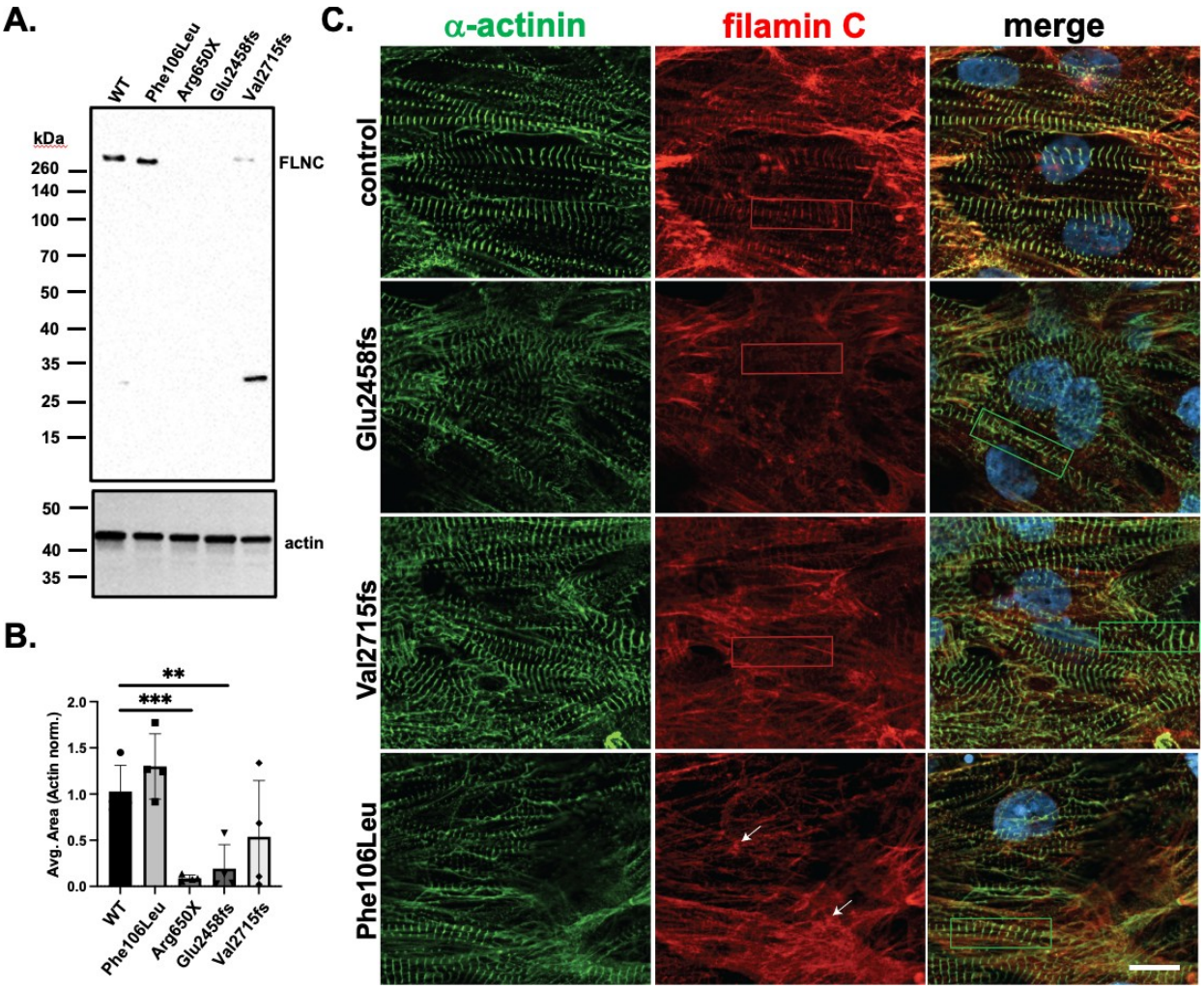

Figure 3.1. Filamin C protein is reduced in iPSC-CMs from patients carrying protein truncating variants. A. Immunoblotting of iPSC-CMs from the truncating mutants, Arg650X, Glu2458fs, and Val2715fs and the missense Phe106Leu iPSC-CM line. **B.** Quantification of immunoblots from multiple different differentiations is shown. Data is shown as mean ±SD with significance determined using an unpaired t-test. ** p=0.0049, ***p=0.0006,. **C.** Immunofluorescence microscopy showed reduced filamin C in patient-derived IPSC-CMs with truncating *FLNC* variants compared to a *FLNC* missense variant. An antibody to α-actinin (green) was used to evaluate sarcomere formation in the left column. The appearance of the sarcomeres was similar between the truncation variants and the missense line, with all *FLNC* variants demonstrating some degree of Z band streaming (examples in green boxes in merged image). The middle column shows filamin C staining highlighting sarcomere-associated filamin C was reduced in the two *FLNC* truncating lines (compare red box areas in middle two panels, which show intact sarcomeres in green channel but little filamin C protein incorporation in the red channel), but reduction in filamin C expression was not evident in the missense Phe106Leu line. Filamin C protein aggregates were visible in the Phe106Leu iPSC-CMs (white arrows). Scale bar, 20μm.

Defective response to proteotoxic stress in the absence of filamin C.

As an actin crosslinking protein, filamin C is a regulator of cellular stress and injury. After exercise or experimentally-induced cell injury, filamin C is enriched at sites of injury in skeletal myofibers and in cardiomyocytes, where it is positioned to participate in the repair response including sarcomere rebuilding (*57, 91*). Under conditions of mechanical stress, filamin C is upregulated to manage injury and repair responses in skeletal muscle and cardiomyocytes (*68, 103*). In skeletal muscle, unfolded or misfolded filamin C is disposed of by chaperone-assisted selective autophagy, which engages BAG3 and heat shock proteins to target unfolded proteins to lysosomes for degradation (*127, 128*). We generated *FLNC* null iPSCs from a healthy control cell line using CRISPR-Cas9 using guide RNAs targeting an exon encoding the actin binding domain of filamin C, referred to as *FLNC* ABD$^{-/-}$ (ABD, **Figure 3.2 and Figure 2.2**). The *FLNC* ABD$^{-/-}$ iPSCs carried two different alleles that disrupted the reading frame, and the cells had no off-target mutations (**Figure 2.9 and Figure 2.10**). *FLNC* ABD$^{-/-}$ iPSC-CMs had reduced mRNA expression when assessing exon 48, and filamin C protein expression was undetectable (**Figure 2.13 and Figure 2.14**).

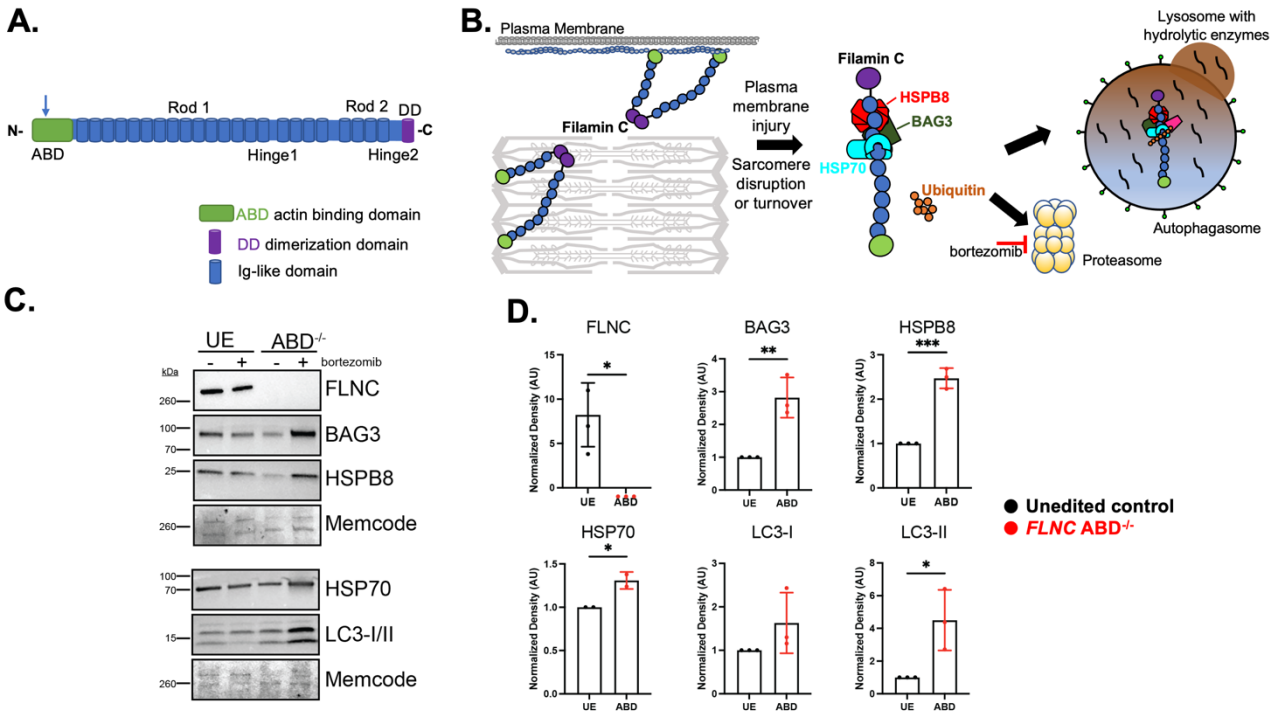

Figure 3.2. Human iPSC-CMs lacking filamin C (*FLNC* ABD$^{-/-}$) have impaired response to proteotoxic stress. **A.** A healthy control human iPSC line was gene edited in the actin binding domain (ABD) to generate *FLNC* ABD$^{-/-}$ cells (blue arrow marks position of deletion). **B.** Filamin C is found at the Z disk and plasma membrane. Misfolded or unfolded filamin C protein is bound by chaperones like BAG3 and heat shock proteins and then disposed through proteasomal degradation or autophagy (17). **C.** Unedited control (UE) and isogenic *FLNC* ABD$^{-/-}$ iPSCs (ABD) were differentiated to cardiomyocytes and then treated with the proteasome inhibitor bortezomib (0.1µm) for 24 hours. In the absence of filamin C, bortezomib exposure results in an increase in chaperone proteins and autophagy markers in iPSC-CMs. **D.** Compared to the unedited control, *FLNC* ABD$^{-/-}$ iPSC-CMs displayed an increase in the chaperone proteins BAG3, HSP70 and HSPB8 when exposed to bortezomib. *FLNC* ABD$^{-/-}$ iPSC-CMs also had an increase in LC3-1 and LC3-II after bortezomib compared to unedited control iPSC-CMs. Expression levels for each protein are shown as fold change relative to the unedited control. *p = 0.02 FLNC, 0.0067 BAG3, 0.04 HSP70, 0.0004 HSPB8, and p = 0.03 LC3-II. The normalized data was analyzed with an unpaired t test and is shown as mean ±SD.

BAG3 and heat shock proteins are critical to mediating proteostasis, which is an important function for mechanically-stressed cardiomyocytes and skeletal myofibers (17, 22, 30, 31) (**Figure 3.2B**). Additionally, abnormal lysosomal accumulation was previously described as a feature of *FLNC* disruption in iPSC-CMs (32). Therefore, we assessed baseline expression and expression of proteins after proteasome inhibition using bortezomib, an inhibitor of the 26S proteasome. Unedited control and FLNC ABD -/- iPSC-CMs tolerated low dose bortezomib (0.1μm) for 24 hours of treatment. Under these conditions, this low dose of bortezomib is expected to partially perturb the proteasome while the higher doses appeared to cause toxicity, as evidenced by loss of contractility. When exposed to bortezomib, *FLNC* ABD$^{-/-}$ iPSC-CMs displayed an increase in BAG3, HSP70, and HSPB8, relative to unedited control iPSC-CMs, indicating that this excessive response to proteasome stress supports a role for filamin C in mediating chaperone activity. Additionally, *FLNC* ABD$^{-/-}$ iPSC-CMs showed enhanced autophagy markers, LC3-1 and LC3-II, consistent with an increase in autophagy. We interpret these findings to indicate that reducing filamin C renders cardiomyocytes less able to tolerate perturbations in protein turnover, such as those that occur during cell stress states.

Filamin C provides structural support to the sarcomere while under physiological stress. In the injured heart, filamin C is present at the site of injury, showing its involvement in muscle repair (*57, 91*). Physiological force can promote the unfolding of filamin C and trigger the formation of the CASA complex, which binds to misfolded filamin C to later target to the lysosome for degradation **(Figure 3.3A)**. This process was modeled by applying mechanical stress to iPSC-CMs. Using the FlexCell system, cells were stressed by inducing 10% equibiaxial strain on iPSC-CMs plated on a BioFlex 6-well plate for 20 hours **(Figure 3.3B**). CASA protein expression did not consistently shift in *FLNC* unedited or mutant iPSC-CMs under mechanical stress **(Figure 3.3C,D).** The fold change in CASA protein expression (BAG3, HSP70, HSPB8, and p62) also did not reliably shift in Arg650X/c.970-4A>G iPSC-CMs after mechanical stress **(Figure 3.3E,F)**. We interpret these findings to mean that mechanical stress under these conditions was not sufficient to elicit a consistent change in filamin C or the CASA pathway proteins. It is possible that greater mechanical stress is needed to elicit this response.

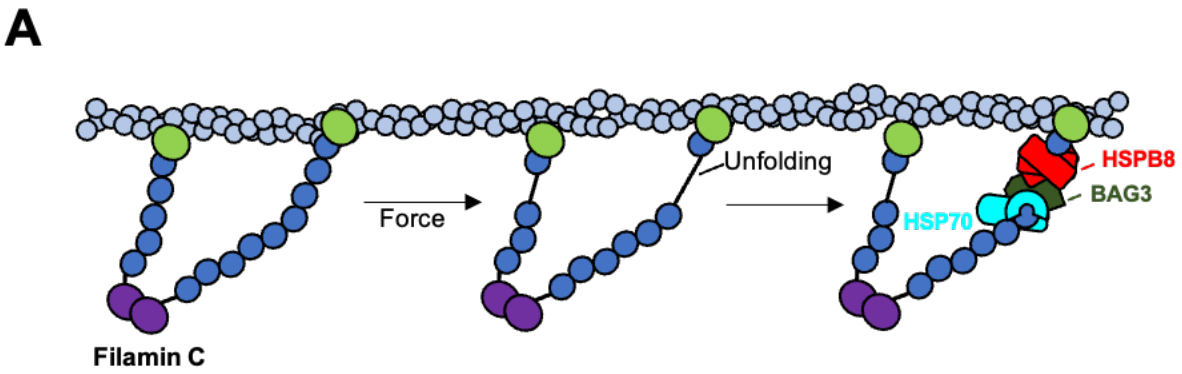
A
Force
Unfolding
HSPB8
BAG3
HSP70
Filamin C

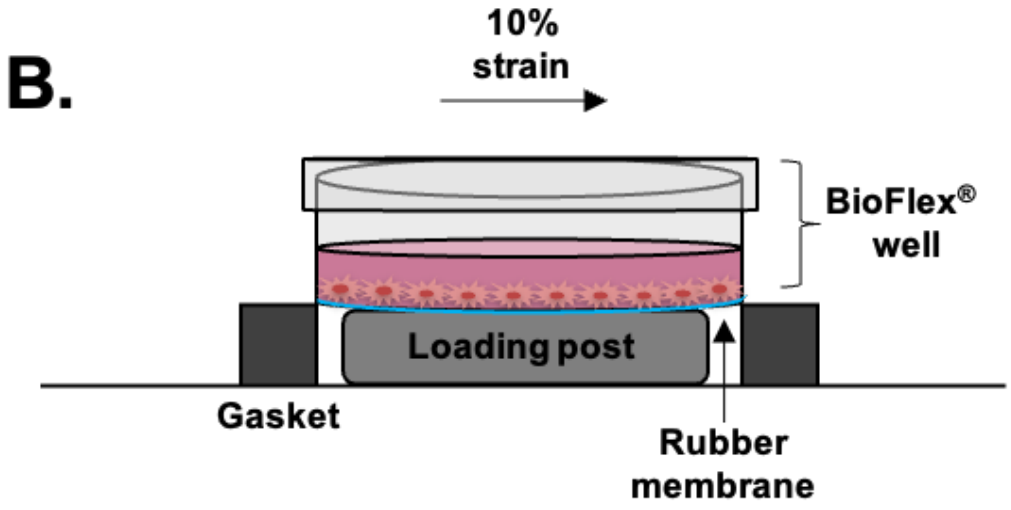
B.
10%
strain
BioFlex®
well
Loading post
Gasket
Rubber
membrane

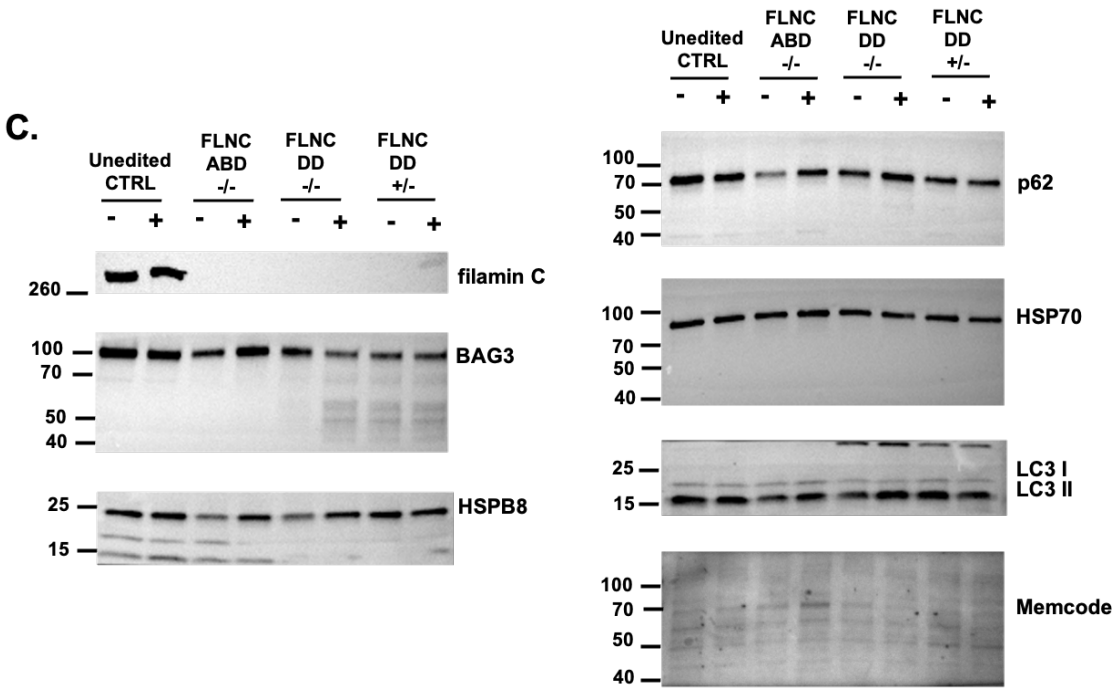
C.
Unedited CTRL
FLNC ABD -/-
FLNC DD -/-
FLNC DD +/-
- + - + - + - +
260
filamin C
100
70
50
40
BAG3
25
15
HSPB8
p62
HSP70
LC3 I
LC3 II
Memcode

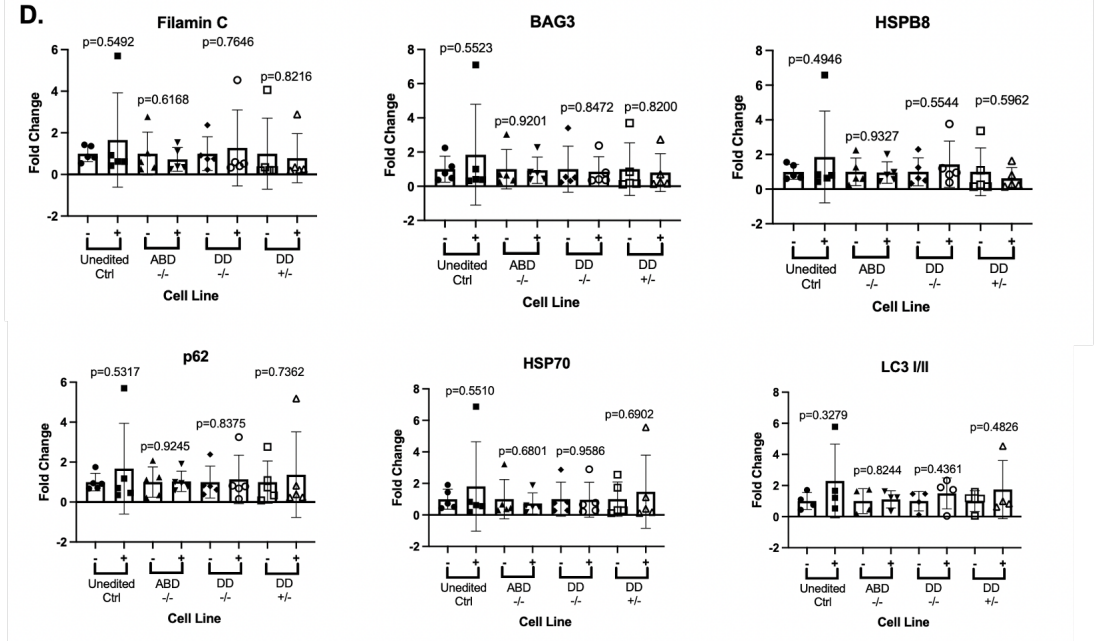
D.
Filamin C
BAG3
HSPB8
p62
HSP70
LC3 I/II
Fold Change
Unedited Ctrl
ABD -/-
DD -/-
DD +/-
Cell Line

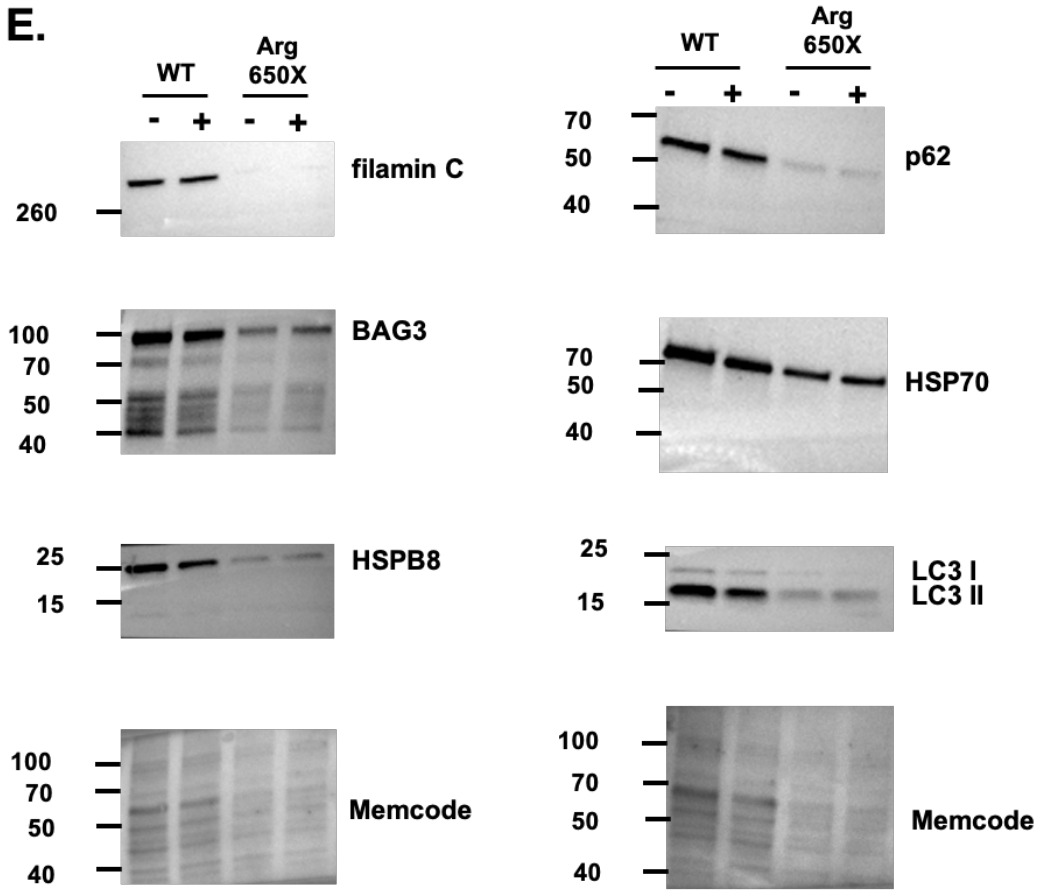
E.
WT
Arg 650X
- + - +
filamin C
260
BAG3
100
70
50
40
HSPB8
25
15
Memcode
100
70
50
40
WT
Arg 650X
- + - +
p62
70
50
40
HSP70
70
50
40
LC3 I
LC3 II
25
15
Memcode
100
70
50
40

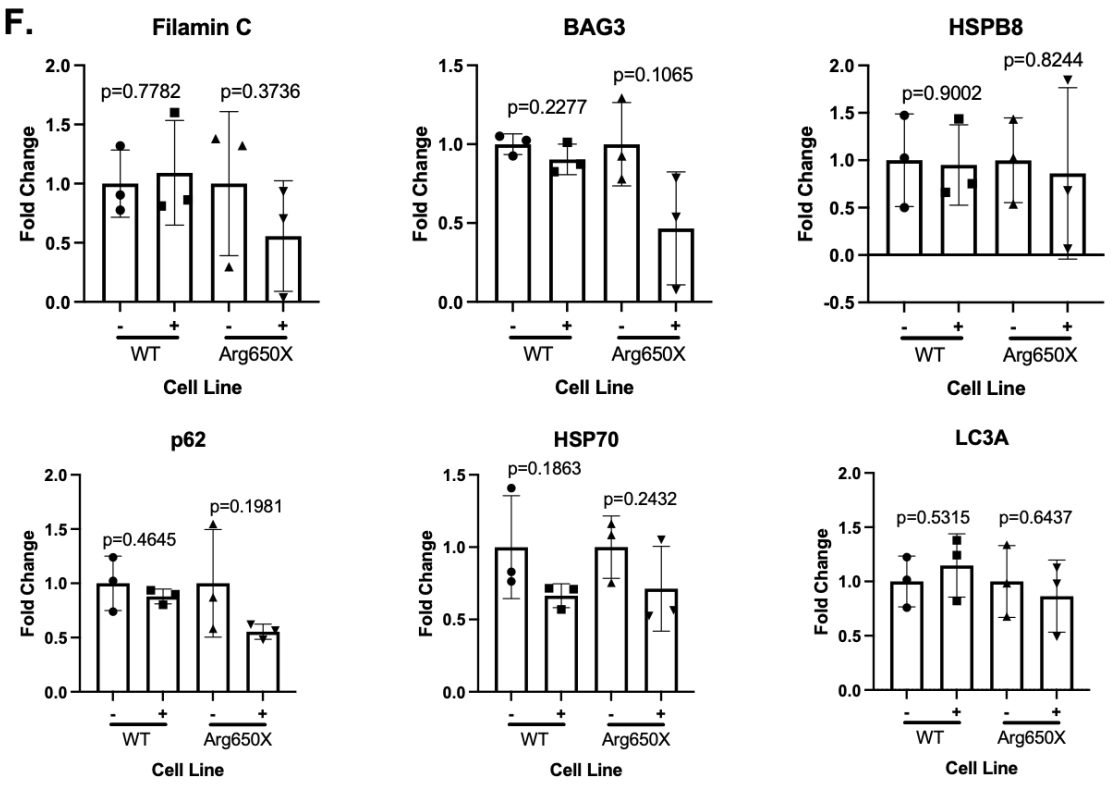

Figure 3.3. Protein Expression of CASA pathway under mechanical stress in iPSC-CMs. **A.** Filamin C unfolds under mechanical stress and acts as a scaffold for the BAG3-HSP70-HSPB8 CASA complex to direct it for ubiquitination and degradation at the lysosome in autophagy. **B.** Flex Cell system induces 10% strain on cardiomyocyte network plated onto Matrigel-coated rubber membrane in BioFlex® well. **C-D.** *FLNC* isogenic and mutant iPSC-CMs were subjected to 10% strain for 20 hours using the FlexCell system. Fold change in protein expression of BAG3, HSPB8, p62, HSP70, and LC3 1/II was not consistently altered after flexing in *FLNC* ABD$^{-/-}$, *FLNC* DD$^{-/-}$, and *FLNC* DD$^{+/-}$ iPSC-CMs as compared to the unedited control **E-F** Arg650X/ c.970-4A>G iPSC-CMs were subjected to 10% strain for 20 hours using the FlexCell system. The difference in fold change in protein expression of BAG3, HSPB8, p62, HSP70, and LC3 1/II in Arg650X/ c.970-4A>G iPSC-CMs was not consistently changed under mechanical stress. We conclude this degree of mechanical stress, both amount and time, may be insufficient to elicit consistent shifts in the CASA pathway proteins.

Prolonged extracellular field potential in FLNC mutant iPSC-CMs is enhanced under proteasomal inhibition.

Although the cardiomyopathic expression of *FLNC* truncation variants is variable, a major clinical complication in *FLNC* cardiomyopathic mutations is ventricular arrhythmia, which can be unpredictable in its timing (2, 8, 9). To assess arrhythmic potential of iPSC-CMs, we measured extracellular field potential as a proxy for action potential duration in paced iPSC-CMs. Field potential duration is measured from the start of depolarization to the end of repolarization back to baseline and may reflect conduction and repolarization. For these studies, we tested unedited control iPSC-CMs, *FLNC* ABD$^{-/-}$ iPSC-CMs, and the p.Arg650X/c.970-4A>G compound heterozygous patient-derived iPSC-CMs (referred to as p.Arg650X for simplicity). At baseline, extracellular field potential was prolonged in both *FLNC* ABD$^{-/-}$ and p.Arg650X iPSC- CMs compared to the unedited control iPSC-CM line (compare y axes in **Figure 3.4A**). These findings are consistent with prolonged action potential duration. Further, when treated with 0.1μm bortezomib, which was sufficient to elicit a boost in filamin C and chaperones proteins in healthy control iPSC-CMs, extracellular field potential remained normal in the unedited healthy control cells. However with this dose of bortezomib, the extracellular field potential remained prolonged in the *FLNC* ABD$^{-/-}$ iPSC-CMs and further prolonged in p.Arg650X iPSC-CMs, consistent with a stress-induced substrate for arrhythmia risk (**Figure 3.4B,C**). These findings highlight defective proteostasis in cardiomyocytes with disrupted filamin C and identify stressors associated with greater protein turnover as proarrhythmic in the setting of filamin C deficiency. Electric field potential was also measured in FLNC patient iPSC-CMs. At baseline, *FLNC* Val2715fs87X iPSC-CMs have prolonged field potential as compared to the unaffected control. Yet, the field potential in Glu2458SerfsX71 was reduced, suggesting that other parameters may be important influences on field potential duration **(Figure 3.5)**.

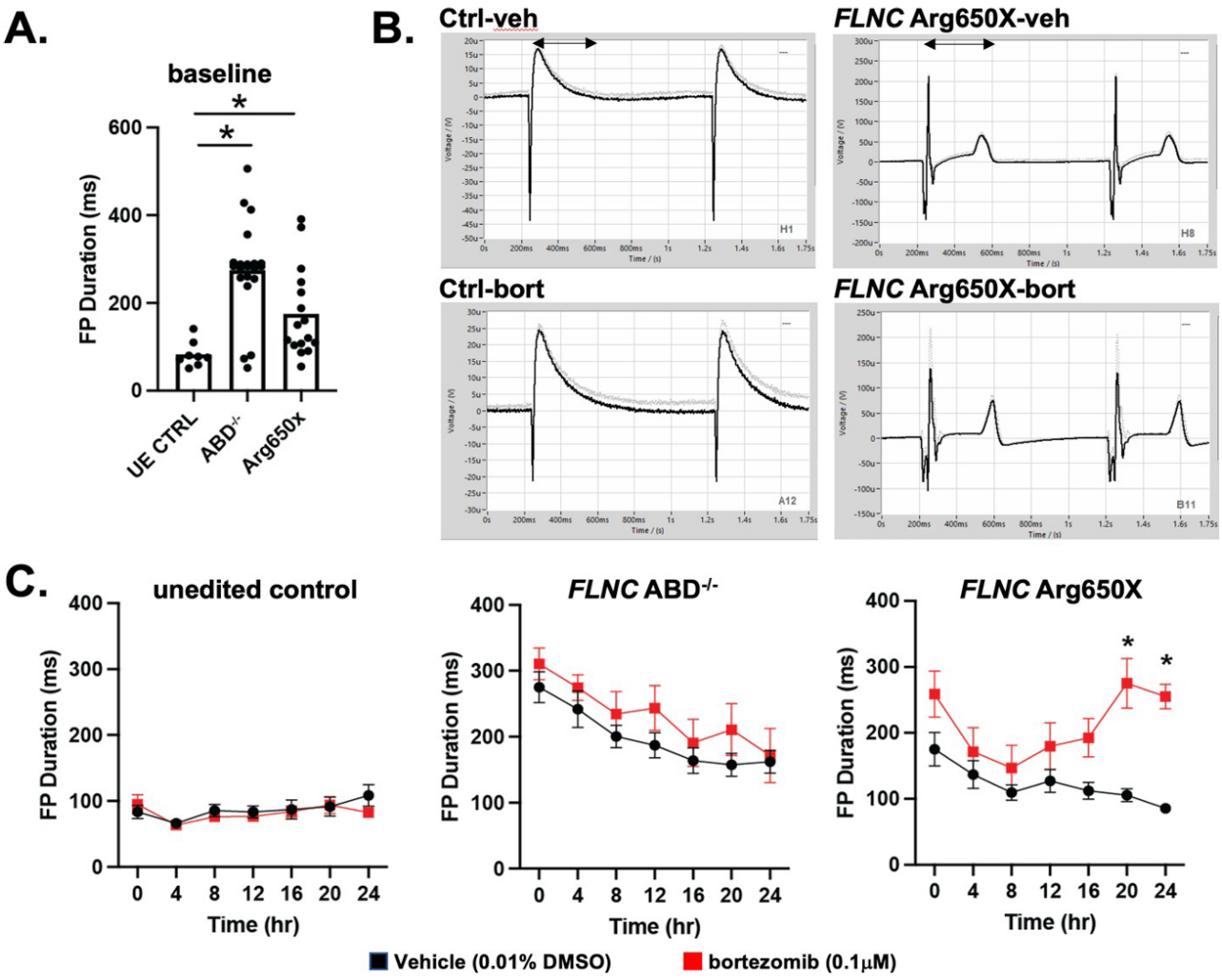

Figure 3.4. Prolonged extracellular field potential of *FLNC* ABD$^{-/-}$ iPSC-CMs and Arg650X iPSC-CMs at baseline and after bortezomib-induced proteotoxic stress. iPSC-CMs were transferred to microelectrode array (MEA) plates for electrical field potential measurements. Extracellular field potential duration was monitored on the Nanion CardioExcyte-96 platform. **A.** The baseline field potential duration was significantly prolonged in *FLNC* ABD$^{-/-}$ iPSC-CMs compared to the unedited control. Similarly the patient-derived *FLNC* p.Arg650X cells, which carry the second pathogenic *FLNC* allele in trans, showed a similar prolonged field potential duration at baseline (*p<0.001 for ABD$^{-/-}$, p=0.02 Arg650X, t-test). **B.** When subjected to low dose (0.1μm) bortezomib, the same dose that stimulated an increase in BAG3, HSP70 and HSPB8 in control cells, control cells did not shift field potential duration. In contrast, field potential duration remained prolonged in *FLNC* ABD$^{-/-}$, and field potential prolonged further in the *FLNC* Arg650X. **C.** Time course of field potential duration with low dose bortezomib exposure (p<0.001 at 20hr, and p<0.001 at 24hr) (red lines). iPSC-CMs were paced at 1 Hz. These data demonstrate that proteotoxic stress creates a substrate for arrhythmia that can be monitored in iPSC-CMs. Data are shown as ±SEM.

Discussion

Role of filamin C in cellular repair of skeletal myofibers and cardiomyocytes.

In skeletal muscle, resistance exercise is associated with an increase in chaperone-assisted selective autophagy components including filamin C (28). When mouse hearts are subjected to transaortic construction or isoproterenol stress, filamin C is upregulated (29). Acute injury to myotubes is associated with recruitment of *Flnc* mRNA and filamin C protein to the site of injury where it plays an essential role in injury repair (27, 41). Similarly, injury to iPSC-CMs is also associated with recruitment of filamin C to the injury site (18). Filamin C may serve as a scaffold onto which small and larger heat shock proteins assemble to manage excess or misfolded proteins at the sites of injury (42).

Recent work using human iPSC-CMs with *FLNC* truncations identified an accumulation of lysosomal proteins. Agarwal and colleagues generated heterozygous and homozygous *FLNC* mutant iPSC-CMs (32). Homozygous *FLNC* null lines showed reduced Z band and select sarcomere proteins, while heterozygous loss of *FLNC* resulted in an accumulation of lysosomal proteins. The heterozygous *FLNC* iPSC-CMs not only had increased lysosomal content but also displayed increased autophagic flux and depletion of autophagy proteins, which could reflect a compensation for impaired proteasomal degradation and disposal of proteins through the proteasome pathways. Our findings are consistent with the increase in autophagic flux based on the observed increase in LC3 under proteasome inhibition. In a separate line of experiments, gene expression profiling identified excess platelet derived growth factor A (PDGFRA) signaling in *FLNC* null iPSC-CMs, and the authors demonstrated that crenolanib, a receptor tyrosine kinase inhibitor with preference for mutant receptor tyrosine kinases was effective at improved contractile dysfunction in *FLNC* mutant iPSC-CMs (43). How these signaling pathways may intersect with enhanced proteasomal sensitivity and autophagy is not known.

In summary, we identified a series of *FLNC* variants associated with diverse cardiomyopathies and significant arrhythmia risk, including one individual with compound heterozygous *FLNC* mutations that significantly reduce filamin C protein expression. Using iPSC-CMs, we identified that low dose bortezomib, a proteasome inhibitor, results in an increase in chaperone proteins and autophagy

markers in *FLNC* deficient iPSC-CMs. This response to proteasomal inhibition as a stressor was excessive in the absence of filamin C. *FLNC* iPSC-CMs had an electrical signature of prolonged field potential duration, which identifies an arrhythmogenic substrate. These findings support a model where filamin C reduction impairs the ability for myofibers and cardiomyocytes to undergo repair and makes them susceptible to injury and cell stress, which increases arrhythmia risk.

Chapter 4.

Summary and Conclusions

Summary and Conclusions

The filamin family of proteins is encoded by three genes *FLNA*, *FLNB*, and *FLNC* that have different tissue distribution and level of expression. *FLNA* and *FLNB* are important modulators in vascular development; *FLNA* is expressed enriched in smooth muscle containing structures, including vasculature, while *FLNB* is predominately expressed in endothelial and other cells **(Figure 4.1)**. However, *FLNC's* expression is much more enriched in skeletal and cardiac muscle. *FLNA* and *FLNB* are important modulators in vascular development. Filamin A mediates protein interactions of cytoskeletal proteins and human mutations in FLNC cause a wide range of connective tissue disorders (*131*). Within endothelial cells, filamin B plays a role in VEGF signaling to induce angiogenesis and stimulates cell migration by acting as a scaffolding protein for different cytoskeletal proteins, including mediating the interaction of Rac-1 and Vav-2 (*131*). Filamin B is an important factor in coordinating protein interactions and vessel formation in space and time within the cytoskeleton during muscle development. On the contrary, *FLNC*'s higher expression in heart and skeletal muscle and its role in mechano-transduction and cellular signaling explain why human mutations in *FLNC* lead to heart and muscle disorders (*132*). Filamin C differs from filamins A and B due to an 82 amino acid insertion in Ig-like domain 20 in the rod domain, a site that is important for proteins interactions that regulate striated muscle development and function. Filamin C's rod domain undergoes conformational changes when force is induced within the cytoskeleton, and this attribute may be critical for filamin C's role in helping the sarcomere withstand mechanical strain.

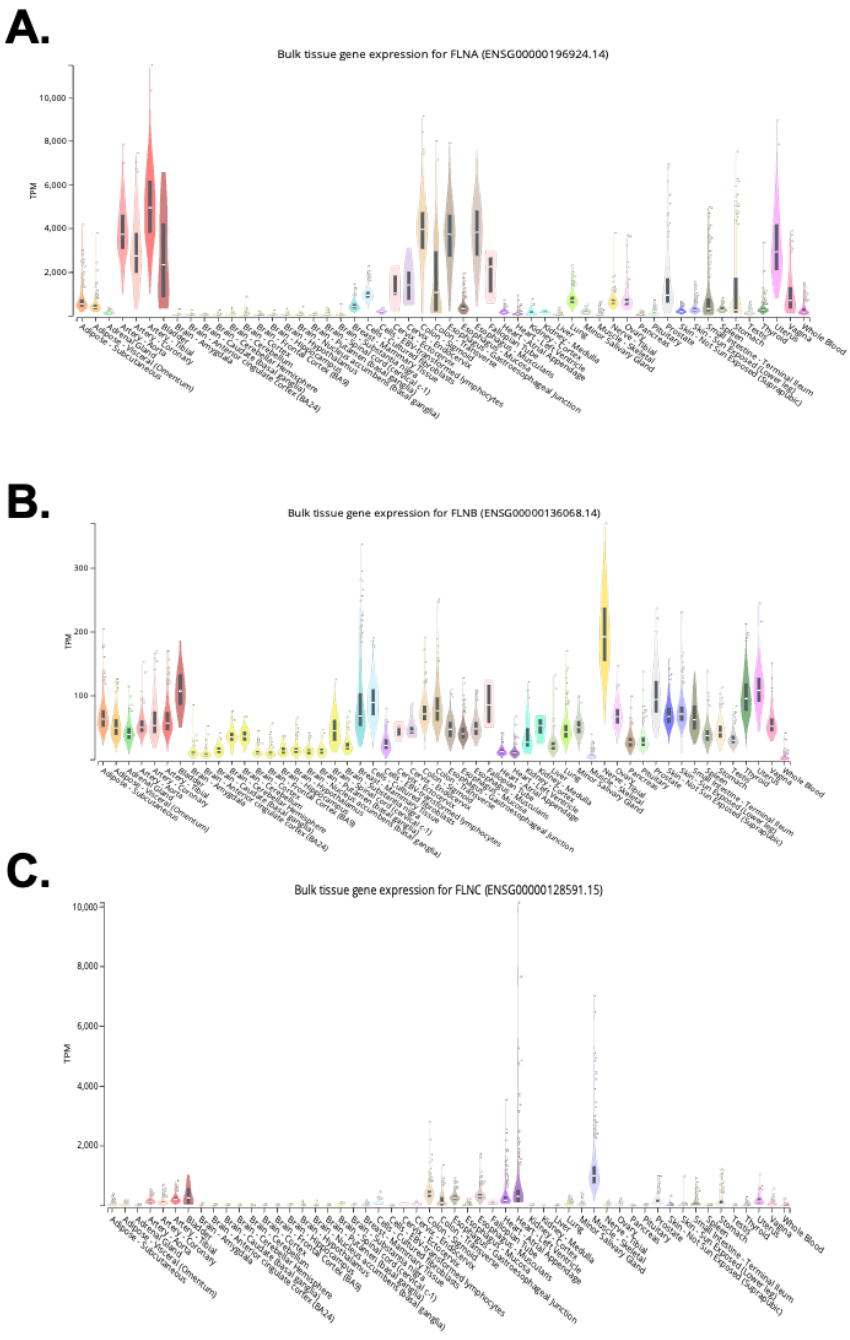

Figure 4.1. Gene expression of *FLNA*, *FLNB*, and *FLNC* in multiple human tissues as reported in GTEx. A-B. *FLNA* is expressed in many tissues with smooth muscle while *FLNB* is expressed at lower levels and in more tissues. **C.** *FLNC* is expressed highest in cardiac and skeletal muscle and plays a major role in muscle development such as Z-disk formation, mechantransduction and facilitates interactions of proteins that are essential for sarcomere assembly and function. (GTEx, https://gtexportal.org/home/ accessed May 15, 2023).

Filamin C has been associated with multiple subtypes of cardiomyopathy but each of these forms has variable penetrance and expressivity. Initial studies identified filamin C as a cause of myofibrillar myopathy by providing structural support and modulating cell signaling within the cytoskeleton (*63, 64*). Filamin C consists of three distinct domains: ABD, RD and DD. Mutations within these domains have been shown to cause muscle and heart disease in patients that present with variations in phenotypic expressivity. Yet, the impact of the location of filamin C mutations on clinical outcomes is not well understood.

In *FLNC* patients with the p.Phe1720LeufsX63 and myofibrillar myopathy, there was evidence for nonsense mediated decay, and the reduction in *FLNC* mRNA expression and resulting loss of filamin C protein expression in muscle were linked to the patients' phenotypes (*133*). iPSC-CMs from an ACM patient with *FLNC* c.970-4A>G variant, the same variant we described in a family and as the second allele in a patient with p.Arg650X, were treated with cycloheximide and showed increased transcript levels and recovery of the spliced transcript (*134*). This *FLNC* patient had NSVT and a family history of SCD. Prolonged action potential duration and abnormal action potentials, including early after depolarizations, were also seen with this *FLNC* variant. NMD associated with specific *FLNC* mutations may contribute to cardiomyopathy. Additionally, NMD regulates stress responses, such as autophagy, to contribute to proteostasis and protein quality control (PQC) in the cell (*135*). NMD has been described as downregulating the unfolded protein response, leading to reduced autophagy and impaired PQC (*136*). Thus, multiple factors, including NMD, haploinsufficiency, CASA and its role in PQC, all contribute to *FLNC*-related cardiomyopathy and its risks for arrhythmia. These additional factors may explain the variable penetrance and expressivity seen with *FLNC* cardiomyopathy.

Using a two-pronged approach, I created *FLNC* mutated iPSC-CMs to model cardiomyopathy and better understand the dynamics of the loss of filamin C on phenotypic expression. Samples were collected from *FLNC* patient and, additionally, gene editing was used to create *FLNC* isogenic cell lines. In **Chapter 2,** I described the clinical findings of these patients and how these cell lines (Phe106Leu, Arg650X/c.970-4A>G, Glu2458SerfsX71, and Val2715fs87X) were created. These

patients had *FLNC* mutations distributed along the transcript and had a history of arrhythmia and sudden cardiac death. One patient, who had both *FLNC* Arg650X and c.970-4A>G, presented with non-progressive muscle disease, NSVT, and DCM. Interestingly, the c.970-4A>G variant was also present in another family with cases of DCM, confirming its role on its own as contributing to cardiomyopathy. Phe106Leu, Arg650X/c.970-4A>G, Glu2458SerfsX71, and Val2715fs87X iPSC-CMs each had irregular morphology, as shown by the presence of Z-disk streaming in cardiomyocytes and, in the cultured cells, abnormal cardiomyocyte networks were seen.

Interestingly, the patient with the *FLNC* Arg650X/c.970-4A>G developed heart failure symptoms in the postpartum interval, indicating she carried the pregnancy successful but did not tolerate postpartum cardiac remodeling. During pregnancy, the heart increases mass and function to accommodate the needs of supporting the growing fetus (*137*). The loss of filamin C, an important modulator for mechanical stress in the sarcomere, further impairs the sarcomere and the heart's ability to withstand these external forces, and this may account for the observation of *FLNC* mutations in pregnancy related cardiomyopathy, since this also includes the peripartum interval. Given the need for increased heart mass and the accompanying cardiac regression that occurs in the postpartum interval, it is reasonable to expect that FLNC mutations might impair this normal process (*138*). We expect that additionally stressors like postpartum remodeling may create the substrate where filamin C deficiency increases risk for arrhythmias.

The *FLNC* p.Phe106Leu variant has been reported as likely pathogenic in DCM (*78*), and patients with *FLNC* missense mutations have been shown to have protein aggregates as compared to those with nonsense mutations (*75*). Histology of heart explants from a *FLNC* patient with biallelic *FLNC* mutations including the p.Phe106Leu variant showed protein aggregates (*81*) . *FLNC* p.Phe106Leu most likely contributes to reduced function of filamin C through its formation of intracellular aggregates. Gene-edited *FLNC* iPSC-CMs also showed abnormal morphology and increased cell death over time compared to the unedited control as visible by eye.

In **Chapter 3**, I investigated the effect of proteotoxic and mechanical stress on the *FLNC* mutant iPSC-CMs. Proteostasis is important for maintaining PQC in muscle and heart since there are many physiological conditions that support hypertrophy and atrophy. The misfolding of filamin C triggers protein aggregate formation at the Z-disk. Filamin C was also identified in protein aggregates in the muscle (*68*). In order to properly dispose of protein aggregates, the CASA pathway responds by complexing of BAG3 with heat shock proteins, including HSP70 and HSPB8, and filamin C provides a substrate for this assembly. Filamin C is also present at the sites of muscle injury, showing that this protein is important for the repair in muscle (*57, 91*). The repair process in the heart is likely to use similar processes to skeletal muscle. Bortezomib, a proteasome inhibitor, was used to induce proteotoxic stress in *FLNC* mutant iPSC-CMs. *FLNC* ABD$^{-/-}$ cells displayed increased CASA protein expression, as compared to the unedited control under bortezomib stress. The Flex Cell system was also used to induce mechanical stress in *FLNC* mutant iPSC-CMs. The mechanical stress protocol tested did not produce significant shifts in CASA protein expression, and it is possible that these stress conditions were insufficient in amount and duration to instigate the necessary CASA pathway shifts. Furthermore, bortezomib was used to measure the effect of proteotoxic stress on action potential in iPSC-CMs. *FLNC* ABD$^{-/-}$ and Arg650X/c.970-4A>G iPSC-CMs displayed prolonged field potential at baseline and in the p.Arg650X cell line, this extended further under bortezomib-induced stress, showing that *FLNC* deficiency perturbs cell signaling and prolongs the repolarization phase within the action potential.

Under physiological stress, the injured heart used filamin C as a key factor that modulates support and signaling by responding to biochemical and mechanical forces within the cell. Proteostasis is an important process for maintaining PQC in the heart for proper muscle function. It has been shown that truncating *FLNC* mutations including p.Gln1662X, p.Tyr2704X, and p.Trp2710X variants causing MFM are associated with *FLNC* haploinsufficiency and defects in protein quality systems required for maintaining functional proteins (*139*). These truncating *FLNC* mutations showed differential expression in CASA pathway proteins and activation of protein quality systems. Understanding how *FLNC* mutations alter proteostasis and whether the position of the FLNC

mutation impact proteostasis may uncover mechanisms of PQC and stress responses in the heart. In my thesis, I have shed light on how different *FLNC* mutations respond to these stressors. These data highlight that filamin C is an essential component that impacts the proteostasis and arrhythmia potential in iPSC-CMs.

Future Directions

Understanding the underlying mechanisms of the loss of filamin C on the proteostasis is important to better understand how CASA pathway proteins interact when the scaffold is no longer present. Future studies will examine the interaction and localization of CASA pathway proteins under stress to determine where these proteins may travel to the sites of sarcomere rebuilding and/or disassembly. Additionally, we will aim to further explore the impact of proteotoxic stress and its dependency on the filamin C scaffold.

References

1. B. J. Maron, J. A. Towbin, G. Thiene, C. Antzelevitch, D. Corrado, D. Arnett, A. J. Moss, C. E. Seidman, J. B. Young, Contemporary definitions and classification of the cardiomyopathies: an American Heart Association Scientific Statement from the Council on Clinical Cardiology, Heart Failure and Transplantation Committee; Quality of Care and Outcomes Research and Functional Genomics and Translational Biology Interdisciplinary Working Groups; and Council on Epidemiology and Prevention. *Circulation* **113**, 1807-1816 (2006).
2. T. Ciarambino, G. Menna, G. Sansone, M. Giordano, Cardiomyopathies: An Overview. *Int J Mol Sci* **22**, (2021).
3. A. Paldino, M. Dal Ferro, D. Stolfo, I. Gandin, K. Medo, S. Graw, M. Gigli, G. Gagno, D. Zaffalon, M. Castrichini, M. Masè, A. Cannatà, F. Brun, G. Storm, G. M. Severini, S. Lenarduzzi, G. Girotto, P. Gasparini, F. Bortolotti, M. Giacca, S. Zacchigna, M. Merlo, M. R. G. Taylor, L. Mestroni, G. Sinagra, Prognostic Prediction of Genotype vs Phenotype in Genetic Cardiomyopathies. *J Am Coll Cardiol* **80**, 1981-1994 (2022).
4. J. Lukas Laws, M. C. Lancaster, M. Ben Shoemaker, W. G. Stevenson, R. R. Hung, Q. Wells, D. Marshall Brinkley, S. Hughes, K. Anderson, D. Roden, L. W. Stevenson, Arrhythmias as Presentation of Genetic Cardiomyopathy. *Circ Res* **130**, 1698-1722 (2022).
5. H. Sisakian, Cardiomyopathies: Evolution of pathogenesis concepts and potential for new therapies. *World J Cardiol* **6**, 478-494 (2014).
6. J. Brieler, M. A. Breeden, J. Tucker, Cardiomyopathy: An Overview. *Am Fam Physician* **96**, 640-646 (2017).
7. E. M. McNally, L. Mestroni, Dilated Cardiomyopathy: Genetic Determinants and Mechanisms. *Circ Res* **121**, 731-748 (2017).
8. R. A. Shah, B. Asatryan, G. Sharaf Dabbagh, N. Aung, M. Y. Khanji, L. R. Lopes, S. van Duijvenboden, A. Holmes, D. Muser, A. P. Landstrom, A. M. Lee, P. Arora, C. Semsarian, V. K. Somers, A. T. Owens, P. B. Munroe, S. E. Petersen, C. A. A. Chahal, Frequency, Penetrance, and Variable Expressivity of Dilated Cardiomyopathy-Associated Putative Pathogenic Gene Variants in UK Biobank Participants. *Circulation* **146**, 110-124 (2022).
9. B. J. Maron, M. S. Maron, Hypertrophic cardiomyopathy. *Lancet* **381**, 242-255 (2013).
10. S. C. Greaves, A. H. Roche, J. M. Neutze, R. M. Whitlock, A. M. Veale, Inheritance of hypertrophic cardiomyopathy: a cross sectional and M mode echocardiographic study of 50 families. *Br Heart J* **58**, 259-266 (1987).
11. Q. Li, C. Gruner, R. H. Chan, M. Care, K. Siminovitch, L. Williams, A. Woo, H. Rakowski, Genotype-positive status in patients with hypertrophic cardiomyopathy is associated with higher rates of heart failure events. *Circ Cardiovasc Genet* **7**, 416-422 (2014).
12. B. J. Maron, M. S. Maron, The 25-year genetic era in hypertrophic cardiomyopathy: revisited. *Circ Cardiovasc Genet* **7**, 401-404 (2014).
13. E. J. Rowin, M. S. Maron, The Role of Cardiac MRI in the Diagnosis and Risk Stratification of Hypertrophic Cardiomyopathy. *Arrhythm Electrophysiol Rev* **5**, 197-202 (2016).
14. C. Y. Ho, S. M. Day, E. A. Ashley, M. Michels, A. C. Pereira, D. Jacoby, A. L. Cirino, J. C. Fox, N. K. Lakdawala, J. S. Ware, C. A. Caleshu, A. S. Helms, S. D. Colan, F. Girolami, F. Cecchi, C. E. Seidman, G. Sajeev, J. Signorovitch, E. M. Green, I. Olivotto, Genotype and Lifetime Burden of Disease in Hypertrophic Cardiomyopathy: Insights from the Sarcomeric Human Cardiomyopathy Registry (SHaRe). *Circulation* **138**, 1387-1398 (2018).
15. E. Jordan, L. Peterson, T. Ai, B. Asatryan, L. Bronicki, E. Brown, R. Celeghin, M. Edwards, J. Fan, J. Ingles, C. A. James, O. Jarinova, R. Johnson, D. P. Judge, N. Lahrouchi, R. H. Lekanne Deprez, R. T. Lumbers, F. Mazzarotto, A. Medeiros Domingo, R. L. Miller, A. Morales, B. Murray, S. Peters, K. Pilichou, A. Protonotarios, C. Semsarian, P. Shah, P. Syrris, C. Thaxton, J. P. van Tintelen, R. Walsh, J. Wang, J. Ware, R. E. Hershberger, Evidence-Based Assessment of Genes in Dilated Cardiomyopathy. *Circulation* **144**, 7-19 (2021).
16. H. L. Granzier, S. Labeit, The giant protein titin: a major player in myocardial mechanics, signaling, and disease. *Circ Res* **94**, 284-295 (2004).

17. D. S. Herman, L. Lam, M. R. Taylor, L. Wang, P. Teekakirikul, D. Christodoulou, L. Conner, S. R. DePalma, B. McDonough, E. Sparks, D. L. Teodorescu, A. L. Cirino, N. R. Banner, D. J. Pennell, S. Graw, M. Merlo, A. Di Lenarda, G. Sinagra, J. M. Bos, M. J. Ackerman, R. N. Mitchell, C. E. Murry, N. K. Lakdawala, C. Y. Ho, P. J. Barton, S. A. Cook, L. Mestroni, J. G. Seidman, C. E. Seidman, Truncations of titin causing dilated cardiomyopathy. *N Engl J Med* **366**, 619-628 (2012).
18. M. M. Akhtar, M. Lorenzini, M. Cicerchia, J. P. Ochoa, T. M. Hey, M. Sabater Molina, M. A. Restrepo-Cordoba, M. Dal Ferro, D. Stolfo, R. Johnson, J. M. Larrañaga-Moreira, A. Robles-Mezcua, J. F. Rodriguez-Palomares, G. Casas, M. L. Peña-Peña, L. R. Lopes, M. Gallego-Delgado, M. Franaszczyk, G. Laucey, D. Rangel-Sousa, M. Basurte, J. Palomino-Doza, E. Villacorta, Z. Bilinska, J. Limeres Freire, J. M. Garcia Pinilla, R. Barriales-Villa, D. Fatkin, G. Sinagra, P. Garcia-Pavia, J. R. Gimeno, J. Mogensen, L. Monserrat, P. M. Elliott, Clinical Phenotypes and Prognosis of Dilated Cardiomyopathy Caused by Truncating Variants in the TTN Gene. *Circ Heart Fail* **13**, e006832 (2020).
19. M. M. Refaat, S. A. Lubitz, S. Makino, Z. Islam, J. M. Frangiskakis, H. Mehdi, R. Gutmann, M. L. Zhang, H. L. Bloom, C. A. MacRae, S. C. Dudley, A. A. Shalaby, R. Weiss, D. M. McNamara, B. London, P. T. Ellinor, Genetic variation in the alternative splicing regulator RBM20 is associated with dilated cardiomyopathy. *Heart Rhythm* **9**, 390-396 (2012).
20. A. M. Fenix, Y. Miyaoka, A. Bertero, S. M. Blue, M. J. Spindler, K. K. B. Tan, J. A. Perez-Bermejo, A. H. Chan, S. J. Mayerl, T. D. Nguyen, C. R. Russell, P. P. Lizarraga, A. Truong, P. L. So, A. Kulkarni, K. Chetal, S. Sathe, N. J. Sniadecki, G. W. Yeo, C. E. Murry, B. R. Conklin, N. Salomonis, Gain-of-function cardiomyopathic mutations in RBM20 rewire splicing regulation and re-distribute ribonucleoprotein granules within processing bodies. *Nat Commun* **12**, 6324 (2021).
21. M. Methawasin, K. R. Hutchinson, E. J. Lee, J. E. Smith, 3rd, C. Saripalli, C. G. Hidalgo, C. A. Ottenheijm, H. Granzier, Experimentally increasing titin compliance in a novel mouse model attenuates the Frank-Starling mechanism but has a beneficial effect on diastole. *Circulation* **129**, 1924-1936 (2014).
22. L. Ollila, K. Nikus, M. Holmström, M. Jalanko, R. Jurkko, M. Kaartinen, J. Koskenvuo, J. Kuusisto, S. Kärkkäinen, E. Palojoki, E. Reissell, P. Piirilä, T. Heliö, Clinical disease presentation and ECG characteristics of LMNA mutation carriers. *Open Heart* **4**, e000474 (2017).
23. J. Lee, V. Termglinchan, S. Diecke, I. Itzhaki, C. K. Lam, P. Garg, E. Lau, M. Greenhaw, T. Seeger, H. Wu, J. Z. Zhang, X. Chen, I. P. Gil, M. Ameen, K. Sallam, J. W. Rhee, J. M. Churko, R. Chaudhary, T. Chour, P. J. Wang, M. P. Snyder, H. Y. Chang, I. Karakikes, J. C. Wu, Activation of PDGF pathway links LMNA mutation to dilated cardiomyopathy. *Nature* **572**, 335-340 (2019).
24. J. Coste Pradas, G. Auguste, S. J. Matkovich, R. Lombardi, S. N. Chen, T. Garnett, K. Chamberlain, J. M. Riyad, T. Weber, S. K. Singh, M. J. Robertson, C. Coarfa, A. J. Marian, P. Gurha, Identification of Genes and Pathways Regulated by Lamin A in Heart. *J Am Heart Assoc* **9**, e015690 (2020).
25. F. J. Ramos, S. C. Chen, M. G. Garelick, D. F. Dai, C. Y. Liao, K. H. Schreiber, V. L. MacKay, E. H. An, R. Strong, W. C. Ladiges, P. S. Rabinovitch, M. Kaeberlein, B. K. Kennedy, Rapamycin reverses elevated mTORC1 signaling in lamin A/C-deficient mice, rescues cardiac and skeletal muscle function, and extends survival. *Sci Transl Med* **4**, 144ra103 (2012).
26. A. Muchir, P. Pavlidis, V. Decostre, A. J. Herron, T. Arimura, G. Bonne, H. J. Worman, Activation of MAPK pathways links LMNA mutations to cardiomyopathy in Emery-Dreifuss muscular dystrophy. *J Clin Invest* **117**, 1282-1293 (2007).
27. T. Hamid, Y. Xu, M. A. Ismahil, G. Rokosh, M. Jinno, G. Zhou, Q. Wang, S. D. Prabhu, Cardiac Mesenchymal Stem Cells Promote Fibrosis and Remodeling in Heart Failure: Role of PDGF Signaling. *JACC Basic Transl Sci* **7**, 465-483 (2022).
28. A. J. Marian, E. Braunwald, Hypertrophic Cardiomyopathy: Genetics, Pathogenesis, Clinical Manifestations, Diagnosis, and Therapy. *Circ Res* **121**, 749-770 (2017).
29. S. M. Day, J. C. Tardiff, E. M. Ostap, Myosin modulators: emerging approaches for the treatment of cardiomyopathies and heart failure. *J Clin Invest* **132**, (2022).

30. A. Snoberger, B. Barua, J. L. Atherton, H. Shuman, E. Forgacs, Y. E. Goldman, D. A. Winkelmann, E. M. Ostap, Myosin with hypertrophic cardiac mutation R712L has a decreased working stroke which is rescued by omecamtiv mecarbil. *Elife* **10**, (2021).
31. J. R. Teerlink, R. Diaz, G. M. Felker, J. J. V. McMurray, M. Metra, S. D. Solomon, K. F. Adams, I. Anand, A. Arias-Mendoza, T. Biering-Sørensen, M. Böhm, D. Bonderman, J. G. F. Cleland, R. Corbalan, M. G. Crespo-Leiro, U. Dahlström, L. E. Echeverria, J. C. Fang, G. Filippatos, C. Fonseca, E. Goncalvesova, A. R. Goudev, J. G. Howlett, D. E. Lanfear, J. Li, M. Lund, P. Macdonald, V. Mareev, S. I. Momomura, E. O'Meara, A. Parkhomenko, P. Ponikowski, F. J. A. Ramires, P. Serpytis, K. Sliwa, J. Spinar, T. M. Suter, J. Tomcsanyi, H. Vandekerckhove, D. Vinereanu, A. A. Voors, M. B. Yilmaz, F. Zannad, L. Sharpsten, J. C. Legg, C. Varin, N. Honarpour, S. A. Abbasi, F. I. Malik, C. E. Kurtz, Cardiac Myosin Activation with Omecamtiv Mecarbil in Systolic Heart Failure. *N Engl J Med* **384**, 105-116 (2021).
32. E. M. Green, H. Wakimoto, R. L. Anderson, M. J. Evanchik, J. M. Gorham, B. C. Harrison, M. Henze, R. Kawas, J. D. Oslob, H. M. Rodriguez, Y. Song, W. Wan, L. A. Leinwand, J. A. Spudich, R. S. McDowell, J. G. Seidman, C. E. Seidman, A small-molecule inhibitor of sarcomere contractility suppresses hypertrophic cardiomyopathy in mice. *Science* **351**, 617-621 (2016).
33. L. M. R. Abella, C. Höhm, B. Hofmann, U. Gergs, J. Neumann, Effects of omecamtiv mecarbil and mavacamten in isolated human atrium. *Naunyn Schmiedebergs Arch Pharmacol* **396**, 499-511 (2023).
34. H. Watkins, D. Conner, L. Thierfelder, J. A. Jarcho, C. MacRae, W. J. McKenna, B. J. Maron, J. G. Seidman, C. E. Seidman, Mutations in the cardiac myosin binding protein-C gene on chromosome 11 cause familial hypertrophic cardiomyopathy. *Nat Genet* **11**, 434-437 (1995).
35. D. Barefield, M. Kumar, J. Gorham, J. G. Seidman, C. E. Seidman, P. P. de Tombe, S. Sadayappan, Haploinsufficiency of MYBPC3 exacerbates the development of hypertrophic cardiomyopathy in heterozygous mice. *J Mol Cell Cardiol* **79**, 234-243 (2015).
36. E. M. McNally, D. Y. Barefield, M. J. Puckelwartz, The genetic landscape of cardiomyopathy and its role in heart failure. *Cell Metab* **21**, 174-182 (2015).
37. J. M. Lind, C. Chiu, J. Ingles, L. Yeates, S. E. Humphries, A. K. Heather, C. Semsarian, Sex hormone receptor gene variation associated with phenotype in male hypertrophic cardiomyopathy patients. *J Mol Cell Cardiol* **45**, 217-222 (2008).
38. K. S. Kolahi, M. R. Mofrad, Molecular mechanics of filamin's rod domain. *Biophys J* **94**, 1075-1083 (2008).
39. J. B. Gorlin, R. Yamin, S. Egan, M. Stewart, T. P. Stossel, D. J. Kwiatkowski, J. H. Hartwig, Human endothelial actin-binding protein (ABP-280, nonmuscle filamin): a molecular leaf spring. *J Cell Biol* **111**, 1089-1105 (1990).
40. R. W. Washington, D. A. Knecht, Actin binding domains direct actin-binding proteins to different cytoskeletal locations. *BMC Cell Biol* **9**, 10 (2008).
41. R. Pudas, T. R. Kiema, P. J. Butler, M. Stewart, J. Ylänne, Structural basis for vertebrate filamin dimerization. *Structure* **13**, 111-119 (2005).
42. E. M. Wade, B. J. Halliday, Z. A. Jenkins, A. C. O'Neill, S. P. Robertson, The X-linked filaminopathies: Synergistic insights from clinical and molecular analysis. *Hum Mutat* **41**, 865-883 (2020).
43. H. Kim, C. A. McCulloch, Filamin A mediates interactions between cytoskeletal proteins that control cell adhesion. *FEBS Lett* **585**, 18-22 (2011).
44. I. D. Campbell, Studies of focal adhesion assembly. *Biochem Soc Trans* **36**, 263-266 (2008).
45. A. Kumar, M. S. Shutova, K. Tanaka, D. V. Iwamoto, D. A. Calderwood, T. M. Svitkina, M. A. Schwartz, Filamin A mediates isotropic distribution of applied force across the actin network. *J Cell Biol* **218**, 2481-2491 (2019).
46. S. Bandaru, J. Grönros, B. Redfors, Ç. Çil, D. Pazooki, R. Salimi, E. Larsson, A. X. Zhou, E. Ömerovic, L. M. Akyürek, Deficiency of filamin A in endothelial cells impairs left ventricular remodelling after myocardial infarction. *Cardiovasc Res* **105**, 151-159 (2015).
47. E. Reinstein, S. Frentz, T. Morgan, S. García-Miñaúr, R. J. Leventer, G. McGillivray, M. Pariani, A. van der Steen, M. Pope, M. Holder-Espinasse, R. Scott, E. M. Thompson, T. Robertson, B. Coppin, R. Siegel, M. Bret Zurita, J. I. Rodríguez, C. Morales, Y. Rodrigues, J. Arcas, A. Saggar,

M. Horton, E. Zackai, J. M. Graham, D. L. Rimoin, S. P. Robertson, Vascular and connective tissue anomalies associated with X-linked periventricular heterotopia due to mutations in Filamin A. *Eur J Hum Genet* **21**, 494-502 (2013).
48. A. W. Hart, J. E. Morgan, J. Schneider, K. West, L. McKie, S. Bhattacharya, I. J. Jackson, S. H. Cross, Cardiac malformations and midline skeletal defects in mice lacking filamin A. *Hum Mol Genet* **15**, 2457-2467 (2006).
49. F. Nakamura, T. P. Stossel, J. H. Hartwig, The filamins: organizers of cell structure and function. *Cell Adh Migr* **5**, 160-169 (2011).
50. J. Zhou, X. Kang, H. An, Y. Lv, X. Liu, The function and pathogenic mechanism of filamin A. *Gene* **784**, 145575 (2021).
51. S. Bandaru, C. Ala, A. X. Zhou, L. M. Akyürek, Filamin A Regulates Cardiovascular Remodeling. *Int J Mol Sci* **22**, (2021).
52. Q. Xu, N. Wu, L. Cui, Z. Wu, G. Qiu, Filamin B: The next hotspot in skeletal research? *J Genet Genomics* **44**, 335-342 (2017).
53. A. van der Flier, I. Kuikman, D. Kramer, D. Geerts, M. Kreft, T. Takafuta, S. S. Shapiro, A. Sonnenberg, Different splice variants of filamin-B affect myogenesis, subcellular distribution, and determine binding to integrin [beta] subunits. *J Cell Biol* **156**, 361-376 (2002).
54. H. Wu, Y. Wang, X. Chen, Y. Yao, W. Zhao, L. Fang, X. Sun, N. Wang, J. Jiang, L. Gao, J. Zhao, C. Xu, Cell-Dependent Pathogenic Roles of Filamin B in Different Skeletal Malformations. *Oxid Med Cell Longev* **2022**, 8956636 (2022).
55. X. Zhou, F. Tian, J. Sandzén, R. Cao, E. Flaberg, L. Szekely, Y. Cao, C. Ohlsson, M. O. Bergo, J. Borén, L. M. Akyürek, Filamin B deficiency in mice results in skeletal malformations and impaired microvascular development. *Proc Natl Acad Sci U S A* **104**, 3919-3924 (2007).
56. J. Lu, G. Lian, R. Lenkinski, A. De Grand, R. R. Vaid, T. Bryce, M. Stasenko, A. Boskey, C. Walsh, V. Sheen, Filamin B mutations cause chondrocyte defects in skeletal development. *Hum Mol Genet* **16**, 1661-1675 (2007).
57. Y. Leber, A. A. Ruparelia, G. Kirfel, P. F. van der Ven, B. Hoffmann, R. Merkel, R. J. Bryson-Richardson, D. O. Fürst, Filamin C is a highly dynamic protein associated with fast repair of myofibrillar microdamage. *Hum Mol Genet* **25**, 2776-2788 (2016).
58. D. O. Fürst, L. G. Goldfarb, R. A. Kley, M. Vorgerd, M. Olivé, P. F. van der Ven, Filamin C-related myopathies: pathology and mechanisms. *Acta Neuropathol* **125**, 33-46 (2013).
59. P. F. van der Ven, E. Ehler, P. Vakeel, S. Eulitz, J. A. Schenk, H. Milting, B. Micheel, D. O. Fürst, Unusual splicing events result in distinct Xin isoforms that associate differentially with filamin c and Mena/VASP. *Exp Cell Res* **312**, 2154-2167 (2006).
60. K. P. Campbell, S. D. Kahl, Association of dystrophin and an integral membrane glycoprotein. *Nature* **338**, 259-262 (1989).
61. E. M. McNally, E. de Sá Moreira, D. J. Duggan, C. G. Bönnemann, M. P. Lisanti, H. G. Lidov, M. Vainzof, M. R. Passos-Bueno, E. P. Hoffman, M. Zatz, L. M. Kunkel, Caveolin-3 in muscular dystrophy. *Hum Mol Genet* **7**, 871-877 (1998).
62. L. E. Lim, F. Duclos, O. Broux, N. Bourg, Y. Sunada, V. Allamand, J. Meyer, I. Richard, C. Moomaw, C. Slaughter, et al., Beta-sarcoglycan: characterization and role in limb-girdle muscular dystrophy linked to 4q12. *Nat Genet* **11**, 257-265 (1995).
63. M. Vorgerd, P. F. van der Ven, V. Bruchertseifer, T. Löwe, R. A. Kley, R. Schröder, H. Lochmüller, M. Himmel, K. Koehler, D. O. Fürst, A. Huebner, A mutation in the dimerization domain of filamin c causes a novel type of autosomal dominant myofibrillar myopathy. *Am J Hum Genet* **77**, 297-304 (2005).
64. R. A. Kley, Y. Hellenbroich, P. F. van der Ven, D. O. Fürst, A. Huebner, V. Bruchertseifer, S. A. Peters, C. M. Heyer, J. Kirschner, R. Schröder, D. Fischer, K. Müller, K. Tolksdorf, K. Eger, A. Germing, T. Brodherr, C. Reum, M. C. Walter, H. Lochmüller, U. P. Ketelsen, M. Vorgerd, Clinical and morphological phenotype of the filamin myopathy: a study of 31 German patients. *Brain* **130**, 3250-3264 (2007).
65. P. F. van der Ven, W. M. Obermann, B. Lemke, M. Gautel, K. Weber, D. O. Fürst, Characterization of muscle filamin isoforms suggests a possible role of gamma-filamin/ABP-L in sarcomeric Z-disc formation. *Cell Motil Cytoskeleton* **45**, 149-162 (2000).

66. T. G. Thompson, Y. M. Chan, A. A. Hack, M. Brosius, M. Rajala, H. G. Lidov, E. M. McNally, S. Watkins, L. M. Kunkel, Filamin 2 (FLN2): A muscle-specific sarcoglycan interacting protein. *J Cell Biol* **148**, 115-126 (2000).
67. F. Chevessier, J. Schuld, Z. Orfanos, A. C. Plank, L. Wolf, A. Maerkens, A. Unger, U. Schlötzer-Schrehardt, R. A. Kley, S. Von Hörsten, K. Marcus, W. A. Linke, M. Vorgerd, P. F. van der Ven, D. O. Fürst, R. Schröder, Myofibrillar instability exacerbated by acute exercise in filaminopathy. *Hum Mol Genet* **24**, 7207-7220 (2015).
68. M. P. Collier, T. R. Alderson, C. P. de Villiers, D. Nicholls, H. Y. Gastall, T. M. Allison, M. T. Degiacomi, H. Jiang, G. Mlynek, D. O. Fürst, P. F. M. van der Ven, K. Djinovic-Carugo, A. J. Baldwin, H. Watkins, K. Gehmlich, J. L. P. Benesch, HspB1 phosphorylation regulates its intramolecular dynamics and mechanosensitive molecular chaperone interaction with filamin C. *Sci Adv* **5**, eaav8421 (2019).
69. V. Kumar, P. Kumar, L. Chauhan, A. Dwivedi, H. R. Ramamurthy, Novel combination of FLNC (c.5707G>A; p. Glu1903Lys) and BAG3 (c.610G>A; p.Gly204Arg) genetic variant expressing restrictive cardiomyopathy phenotype in an adolescent girl. *J Genet* **101**, (2022).
70. R. Celeghin, A. Cipriani, R. Bariani, M. Bueno Marinas, M. Cason, M. Bevilacqua, M. De Gaspari, S. Rizzo, I. Rigato, S. Da Pozzo, A. Zorzi, M. Perazzolo Marra, G. Thiene, S. Iliceto, C. Basso, D. Corrado, K. Pilichou, B. Bauce, Filamin-C variant-associated cardiomyopathy: A pooled analysis of individual patient data to evaluate the clinical profile and risk of sudden cardiac death. *Heart Rhythm* **19**, 235-243 (2022).
71. M. F. Ortiz-Genga, S. Cuenca, M. Dal Ferro, E. Zorio, R. Salgado-Aranda, V. Climent, L. Padrón-Barthe, I. Duro-Aguado, J. Jiménez-Jáimez, V. M. Hidalgo-Olivares, E. García-Campo, C. Lanzillo, M. P. Suárez-Mier, H. Yonath, S. Marcos-Alonso, J. P. Ochoa, J. L. Santomé, D. García-Giustiniani, J. L. Rodríguez-Garrido, F. Domínguez, M. Merlo, J. Palomino, M. L. Peña, J. P. Trujillo, A. Martín-Vila, D. Stolfo, P. Molina, E. Lara-Pezzi, F. E. Calvo-Iglesias, E. Nof, L. Calò, R. Barriales-Villa, J. R. Gimeno-Blanes, M. Arad, P. García-Pavía, L. Monserrat, Truncating FLNC Mutations Are Associated With High-Risk Dilated and Arrhythmogenic Cardiomyopathies. *J Am Coll Cardiol* **68**, 2440-2451 (2016).
72. D. Velardo, M. G. D'Angelo, A. Citterio, E. Panzeri, L. Napoli, C. Cinnante, M. Moggio, G. P. Comi, D. Ronchi, M. T. Bassi, Case Reports: Novel Missense Variants in the Filamin C Actin Binding Domain Cause Variable Phenotypes. *Front Neurol* **13**, 930039 (2022).
73. R. M. Duff, V. Tay, P. Hackman, G. Ravenscroft, C. McLean, P. Kennedy, A. Steinbach, W. Schöffler, P. F. M. van der Ven, D. O. Fürst, J. Song, K. Djinović-Carugo, S. Penttilä, O. Raheem, K. Reardon, A. Malandrini, S. Gambelli, M. Villanova, K. J. Nowak, D. R. Williams, J. E. Landers, R. H. Brown, Jr., B. Udd, N. G. Laing, Mutations in the N-terminal actin-binding domain of filamin C cause a distal myopathy. *Am J Hum Genet* **88**, 729-740 (2011).
74. A. Shatunov, M. Olivé, Z. Odgerel, C. Stadelmann-Nessler, K. Irlbacher, F. van Landeghem, M. Bayarsaikhan, H. S. Lee, B. Goudeau, P. F. Chinnery, V. Straub, D. Hilton-Jones, M. S. Damian, A. Kaminska, P. Vicart, K. Bushby, M. C. Dalakas, N. Sambuughin, I. Ferrer, H. H. Goebel, L. G. Goldfarb, In-frame deletion in the seventh immunoglobulin-like repeat of filamin C in a family with myofibrillar myopathy. *Eur J Hum Genet* **17**, 656-663 (2009).
75. R. Valdés-Mas, A. Gutiérrez-Fernández, J. Gómez, E. Coto, A. Astudillo, D. A. Puente, J. R. Reguero, V. Álvarez, C. Morís, D. León, M. Martín, X. S. Puente, C. López-Otín, Mutations in filamin C cause a new form of familial hypertrophic cardiomyopathy. *Nat Commun* **5**, 5326 (2014).
76. D. Avila-Smirnow, L. Gueneau, S. Batonnet-Pichon, F. Delort, H. M. Bécane, K. Claeys, M. Beuvin, B. Goudeau, J. P. Jais, I. Nelson, P. Richard, R. Ben Yaou, N. B. Romero, K. Wahbi, S. Mathis, T. Voit, D. Furst, P. van der Ven, R. Gil, P. Vicart, M. Fardeau, G. Bonne, A. Behin, Cardiac arrhythmia and late-onset muscle weakness caused by a myofibrillar myopathy with unusual histopathological features due to a novel missense mutation in FLNC. *Rev Neurol (Paris)* **172**, 594-606 (2016).
77. R. A. Kley, P. Serdaroglu-Oflazer, Y. Leber, Z. Odgerel, P. F. van der Ven, M. Olivé, I. Ferrer, A. Onipe, M. Mihaylov, J. M. Bilbao, H. S. Lee, J. Höhfeld, K. Djinović-Carugo, K. Kong, M. Tegenthoff, S. A. Peters, W. Stenzel, M. Vorgerd, L. G. Goldfarb, D. O. Fürst, Pathophysiology of protein aggregation and extended phenotyping in filaminopathy. *Brain* **135**, 2642-2660 (2012).

78. J. A. J. Verdonschot, E. K. Vanhoutte, G. R. F. Claes, A. Helderman-van den Enden, J. G. J. Hoeijmakers, D. Hellebrekers, A. de Haan, I. Christiaans, R. H. Lekanne Deprez, H. M. Boen, E. M. van Craenenbroeck, B. L. Loeys, Y. M. Hoedemaekers, C. Marcelis, M. Kempers, E. Brusse, J. I. van Waning, A. F. Baas, D. Dooijes, F. W. Asselbergs, D. Barge-Schaapveld, P. Koopman, A. van den Wijngaard, S. R. B. Heymans, I. P. C. Krapels, H. G. Brunner, A mutation update for the FLNC gene in myopathies and cardiomyopathies. *Hum Mutat* **41**, 1091-1111 (2020).
79. J. Chen, J. Wu, C. Han, Y. Li, Y. Guo, X. Tong, A mutation in the filamin c gene causes myofibrillar myopathy with lower motor neuron syndrome: a case report. *BMC Neurol* **19**, 198 (2019).
80. A. Schänzer, E. Schumann, D. Zengeler, L. Gulatz, G. Maroli, U. Ahting, A. Sprengel, S. Gräf, A. Hahn, C. Jux, T. Acker, D. O. Fürst, S. Rupp, J. Schuld, P. F. M. van der Ven, The p.Ala2430Val mutation in filamin C causes a "hypertrophic myofibrillar cardiomyopathy". *J Muscle Res Cell Motil* **42**, 381-397 (2021).
81. E. Reinstein, A. Gutierrez-Fernandez, S. Tzur, C. Bormans, S. Marcu, E. Tayeb-Fligelman, C. Vinkler, A. Raas-Rothschild, D. Irge, M. Landau, M. Shohat, X. S. Puente, D. M. Behar, C. Lopez-Otın, Congenital dilated cardiomyopathy caused by biallelic mutations in Filamin C. *Eur J Hum Genet* **24**, 1792-1796 (2016).
82. A. A. Ruparelia, M. Zhao, P. D. Currie, R. J. Bryson-Richardson, Characterization and investigation of zebrafish models of filamin-related myofibrillar myopathy. *Hum Mol Genet* **21**, 4073-4083 (2012).
83. R. L. Begay, C. A. Tharp, A. Martin, S. L. Graw, G. Sinagra, D. Miani, M. E. Sweet, D. B. Slavov, N. Stafford, M. J. Zeller, R. Alnefaie, T. J. Rowland, F. Brun, K. L. Jones, K. Gowan, L. Mestroni, D. M. Garrity, M. R. Taylor, FLNC Gene Splice Mutations Cause Dilated Cardiomyopathy. *JACC Basic Transl Sci* **1**, 344-359 (2016).
84. J. Schuld, Z. Orfanos, F. Chevessier, B. Eggers, L. Heil, J. Uszkoreit, A. Unger, G. Kirfel, P. F. M. van der Ven, K. Marcus, W. A. Linke, C. S. Clemen, R. Schröder, D. O. Fürst, Homozygous expression of the myofibrillar myopathy-associated p.W2710X filamin C variant reveals major pathomechanisms of sarcomeric lesion formation. *Acta Neuropathol Commun* **8**, 154 (2020).
85. I. Dalkilic, J. Schienda, T. G. Thompson, L. M. Kunkel, Loss of FilaminC (FLNc) results in severe defects in myogenesis and myotube structure. *Mol Cell Biol* **26**, 6522-6534 (2006).
86. Y. Zhou, Z. Chen, L. Zhang, M. Zhu, C. Tan, X. Zhou, S. M. Evans, X. Fang, W. Feng, J. Chen, Loss of Filamin C Is Catastrophic for Heart Function. *Circulation* **141**, 869-871 (2020).
87. J. D. Powers, N. J. Kirkland, C. Liu, S. S. Razu, X. Fang, A. J. Engler, J. Chen, A. D. McCulloch, Subcellular Remodeling in Filamin C Deficient Mouse Hearts Impairs Myocyte Tension Development during Progression of Dilated Cardiomyopathy. *Int J Mol Sci* **23**, (2022).
88. N. R. Tucker, M. A. McLellan, D. Hu, J. Ye, V. A. Parsons, R. W. Mills, S. Clauss, E. Dolmatova, M. A. Shea, D. J. Milan, N. S. Scott, M. Lindsay, S. A. Lubitz, I. J. Domian, J. R. Stone, H. Lin, P. T. Ellinor, Novel Mutation in FLNC (Filamin C) Causes Familial Restrictive Cardiomyopathy. *Circ Cardiovasc Genet* **10**, (2017).
89. S. N. Chen, C. K. Lam, Y. W. Wan, S. Gao, O. A. Malak, S. R. Zhao, R. Lombardi, A. V. Ambardekar, M. R. Bristow, J. Cleveland, M. Gigli, G. Sinagra, S. Graw, M. R. G. Taylor, J. C. Wu, L. Mestroni, Activation of PDGFRA signaling contributes to filamin C-related arrhythmogenic cardiomyopathy. *Sci Adv* **8**, eabk0052 (2022).
90. F. Brun, M. Gigli, S. L. Graw, D. P. Judge, M. Merlo, B. Murray, H. Calkins, G. Sinagra, M. R. Taylor, L. Mestroni, C. A. James, FLNC truncations cause arrhythmogenic right ventricular cardiomyopathy. *J Med Genet* **57**, 254-257 (2020).
91. W. Roman, H. Pinheiro, M. R. Pimentel, J. Segalés, L. M. Oliveira, E. García-Domínguez, M. C. Gómez-Cabrera, A. L. Serrano, E. R. Gomes, P. Muñoz-Cánoves, Muscle repair after physiological damage relies on nuclear migration for cellular reconstruction. *Science* **374**, 355-359 (2021).
92. Z. Orfanos, M. P. Gödderz, E. Soroka, T. Gödderz, A. Rumyantseva, P. F. van der Ven, T. J. Hawke, D. O. Fürst, Breaking sarcomeres by in vitro exercise. *Sci Rep* **6**, 19614 (2016).
93. L. Rognoni, J. Stigler, B. Pelz, J. Ylänne, M. Rief, Dynamic force sensing of filamin revealed in single-molecule experiments. *Proc Natl Acad Sci U S A* **109**, 19679-19684 (2012).

94. X. Han, K. Y. Goh, W. X. Lee, S. M. Choy, H. W. Tang, The Importance of mTORC1-Autophagy Axis for Skeletal Muscle Diseases. *Int J Mol Sci* **24**, (2022).
95. G. Sirago, A. Picca, R. Calvani, H. J. Coelho-Júnior, E. Marzetti, Mammalian Target of Rapamycin (mTOR) Signaling at the Crossroad of Muscle Fiber Fate in Sarcopenia. *Int J Mol Sci* **23**, (2022).
96. H. Tang, K. Inoki, S. V. Brooks, H. Okazawa, M. Lee, J. Wang, M. Kim, C. L. Kennedy, P. C. D. Macpherson, X. Ji, S. Van Roekel, D. A. Fraga, K. Wang, J. Zhu, Y. Wang, Z. D. Sharp, R. A. Miller, T. A. Rando, D. Goldman, K. L. Guan, J. B. Shrager, mTORC1 underlies age-related muscle fiber damage and loss by inducing oxidative stress and catabolism. *Aging Cell* **18**, e12943 (2019).
97. B. Kathage, S. Gehlert, A. Ulbricht, L. Lüdecke, V. E. Tapia, Z. Orfanos, D. Wenzel, W. Bloch, R. Volkmer, B. K. Fleischmann, D. O. Fürst, J. Höhfeld, The cochaperone BAG3 coordinates protein synthesis and autophagy under mechanical strain through spatial regulation of mTORC1. *Biochim Biophys Acta Mol Cell Res* **1864**, 62-75 (2017).
98. H. Zhu, B. A. Rothermel, J. A. Hill, Autophagy in load-induced heart disease. *Methods Enzymol* **453**, 343-363 (2009).
99. H. Zhu, P. Tannous, J. L. Johnstone, Y. Kong, J. M. Shelton, J. A. Richardson, V. Le, B. Levine, B. A. Rothermel, J. A. Hill, Cardiac autophagy is a maladaptive response to hemodynamic stress. *J Clin Invest* **117**, 1782-1793 (2007).
100. P. Tannous, H. Zhu, A. Nemchenko, J. M. Berry, J. L. Johnstone, J. M. Shelton, F. J. Miller, Jr., B. A. Rothermel, J. A. Hill, Intracellular protein aggregation is a proximal trigger of cardiomyocyte autophagy. *Circulation* **117**, 3070-3078 (2008).
101. Y. Kitajima, Y. Tashiro, N. Suzuki, H. Warita, M. Kato, M. Tateyama, R. Ando, R. Izumi, M. Yamazaki, M. Abe, K. Sakimura, H. Ito, M. Urushitani, R. Nagatomi, R. Takahashi, M. Aoki, Proteasome dysfunction induces muscle growth defects and protein aggregation. *J Cell Sci* **127**, 5204-5217 (2014).
102. L. M. Judge, J. A. Perez-Bermejo, A. Truong, A. J. Ribeiro, J. C. Yoo, C. L. Jensen, M. A. Mandegar, N. Huebsch, R. M. Kaake, P. L. So, D. Srivastava, B. L. Pruitt, N. J. Krogan, B. R. Conklin, A BAG3 chaperone complex maintains cardiomyocyte function during proteotoxic stress. *JCI Insight* **2**, (2017).
103. A. Ulbricht, S. Gehlert, B. Leciejewski, T. Schiffer, W. Bloch, J. Höhfeld, Induction and adaptation of chaperone-assisted selective autophagy CASA in response to resistance exercise in human skeletal muscle. *Autophagy* **11**, 538-546 (2015).
104. X. Fang, J. Bogomolovas, T. Wu, W. Zhang, C. Liu, J. Veevers, M. J. Stroud, Z. Zhang, X. Ma, Y. Mu, D. H. Lao, N. D. Dalton, Y. Gu, C. Wang, M. Wang, Y. Liang, S. Lange, K. Ouyang, K. L. Peterson, S. M. Evans, J. Chen, Loss-of-function mutations in co-chaperone BAG3 destabilize small HSPs and cause cardiomyopathy. *J Clin Invest* **127**, 3189-3200 (2017).
105. M. S. Willis, J. N. Min, S. Wang, H. McDonough, P. Lockyer, K. M. Wadosky, C. Patterson, Carboxyl terminus of Hsp70-interacting protein (CHIP) is required to modulate cardiac hypertrophy and attenuate autophagy during exercise. *Cell Biochem Funct* **31**, 724-735 (2013).
106. H. Qiu, P. Lizano, L. Laure, X. Sui, E. Rashed, J. Y. Park, C. Hong, S. Gao, E. Holle, D. Morin, S. K. Dhar, T. Wagner, A. Berdeaux, B. Tian, S. F. Vatner, C. Depre, H11 kinase/heat shock protein 22 deletion impairs both nuclear and mitochondrial functions of STAT3 and accelerates the transition into heart failure on cardiac overload. *Circulation* **124**, 406-415 (2011).
107. A. Hishiya, M. N. Salman, S. Carra, H. H. Kampinga, S. Takayama, BAG3 directly interacts with mutated alphaB-crystallin to suppress its aggregation and toxicity. *PLoS One* **6**, e16828 (2011).
108. Q. Zheng, H. Su, M. J. Ranek, X. Wang, Autophagy and p62 in cardiac proteinopathy. *Circ Res* **109**, 296-308 (2011).
109. W. J. Liu, L. Ye, W. F. Huang, L. J. Guo, Z. G. Xu, H. L. Wu, C. Yang, H. F. Liu, p62 links the autophagy pathway and the ubiqutin-proteasome system upon ubiquitinated protein degradation. *Cell Mol Biol Lett* **21**, 29 (2016).
110. V. I. Korolchuk, A. Mansilla, F. M. Menzies, D. C. Rubinsztein, Autophagy inhibition compromises degradation of ubiquitin-proteasome pathway substrates. *Mol Cell* **33**, 517-527 (2009).

111. R. L. Begay, S. L. Graw, G. Sinagra, A. Asimaki, T. J. Rowland, D. B. Slavov, K. Gowan, K. L. Jones, F. Brun, M. Merlo, D. Miani, M. Sweet, K. Devaraj, E. P. Wartchow, M. Gigli, I. Puggia, E. E. Salcedo, D. M. Garrity, A. V. Ambardekar, P. Buttrick, T. B. Reece, M. R. Bristow, J. E. Saffitz, L. Mestroni, M. R. G. Taylor, Filamin C Truncation Mutations Are Associated With Arrhythmogenic Dilated Cardiomyopathy and Changes in the Cell-Cell Adhesion Structures. *JACC Clin Electrophysiol* **4**, 504-514 (2018).
112. D. Selcen, K. Ohno, A. G. Engel, Myofibrillar myopathy: clinical, morphological and genetic studies in 63 patients. *Brain* **127**, 439-451 (2004).
113. D. Selcen, A. G. Engel, Myofibrillar myopathies. *Handb Clin Neurol* **101**, 143-154 (2011).
114. E. Y. Kim, D. Y. Barefield, A. H. Vo, A. M. Gacita, E. J. Schuster, E. J. Wyatt, J. L. Davis, B. Dong, C. Sun, P. Page, L. Dellefave-Castillo, A. Demonbreun, H. F. Zhang, E. M. McNally, Distinct pathological signatures in human cellular models of myotonic dystrophy subtypes. *JCI Insight* **4**, (2019).
115. P. W. Burridge, E. Matsa, P. Shukla, Z. C. Lin, J. M. Churko, A. D. Ebert, F. Lan, S. Diecke, B. Huber, N. M. Mordwinkin, J. R. Plews, O. J. Abilez, B. Cui, J. D. Gold, J. C. Wu, Chemically defined generation of human cardiomyocytes. *Nat Methods* **11**, 855-860 (2014).
116. W. Liang, P. Han, E. H. Kim, J. Mak, R. Zhang, A. G. Torrente, J. I. Goldhaber, E. Marbán, H. C. Cho, Canonical Wnt signaling promotes pacemaker cell specification of cardiac mesodermal cells derived from mouse and human embryonic stem cells. *Stem Cells* **38**, 352-368 (2020).
117. S. Mazzotta, C. Neves, R. J. Bonner, A. S. Bernardo, K. Docherty, S. Hoppler, Distinctive Roles of Canonical and Noncanonical Wnt Signaling in Human Embryonic Cardiomyocyte Development. *Stem Cell Reports* **7**, 764-776 (2016).
118. M. Gigli, D. Stolfo, S. L. Graw, M. Merlo, C. Gregorio, S. Nee Chen, M. Dal Ferro, M. A. Paldino, G. De Angelis, F. Brun, J. Jirikowic, E. E. Salcedo, S. Turja, D. Fatkin, R. Johnson, J. P. van Tintelen, A. Te Riele, A. A. M. Wilde, N. K. Lakdawala, K. Picard, D. Miani, D. Muser, G. Maria Severini, H. Calkins, C. A. James, B. Murray, C. Tichnell, V. N. Parikh, E. A. Ashley, C. Reuter, J. Song, D. P. Judge, W. J. McKenna, M. R. G. Taylor, G. Sinagra, L. Mestroni, Phenotypic Expression, Natural History, and Risk Stratification of Cardiomyopathy Caused by Filamin C Truncating Variants. *Circulation* **144**, 1600-1611 (2021).
119. J. R. Golbus, M. J. Puckelwartz, L. Dellefave-Castillo, J. P. Fahrenbach, V. Nelakuditi, L. L. Pesce, P. Pytel, E. M. McNally, Targeted analysis of whole genome sequence data to diagnose genetic cardiomyopathy. *Circ Cardiovasc Genet* **7**, 751-759 (2014).
120. S. Oz, H. Yonath, L. Visochyk, E. Ofek, N. Landa, H. Reznik-Wolf, M. Ortiz-Genga, L. Monserrat, T. Ben-Gal, O. Goitein, R. Beinart, M. Glikson, D. Freimark, E. Pras, M. Arad, E. Nof, Reduction in Filamin C transcript is associated with arrhythmogenic cardiomyopathy in Ashkenazi Jews. *Int J Cardiol* **317**, 133-138 (2020).
121. R. Goli, J. Li, J. Brandimarto, L. D. Levine, V. Riis, Q. McAfee, S. DePalma, A. Haghighi, J. G. Seidman, C. E. Seidman, D. Jacoby, G. Macones, D. P. Judge, S. Rana, K. B. Margulies, T. P. Cappola, R. Alharethi, J. Damp, E. Hsich, U. Elkayam, R. Sheppard, J. D. Alexis, J. Boehmer, C. Kamiya, F. Gustafsson, P. Damm, A. S. Ersbøll, S. Goland, D. Hilfiker-Kleiner, D. M. McNamara, Z. Arany, Genetic and Phenotypic Landscape of Peripartum Cardiomyopathy. *Circulation* **143**, 1852-1862 (2021).
122. T. G. Martin, J. A. Kirk, Under construction: The dynamic assembly, maintenance, and degradation of the cardiac sarcomere. *J Mol Cell Cardiol* **148**, 89-102 (2020).
123. R. C. Lyon, S. Lange, F. Sheikh, Breaking down protein degradation mechanisms in cardiac muscle. *Trends Mol Med* **19**, 239-249 (2013).
124. E. D. Carruth, M. Qureshi, A. Alsaid, M. A. Kelly, H. Calkins, B. Murray, C. Tichnell, A. C. Sturm, A. Baras, H. Lester Kirchner, B. K. Fornwalt, C. A. James, C. M. Haggerty, Loss-of-Function FLNC Variants Are Associated With Arrhythmogenic Cardiomyopathy Phenotypes When Identified Through Exome Sequencing of a General Clinical Population. *Circ Genom Precis Med* **15**, e003645 (2022).
125. N. A. Nafissi, J. W. Abdulrahim, L. C. Kwee, A. C. Coniglio, W. E. Kraus, J. P. Piccini, J. P. Daubert, A. Y. Sun, S. H. Shah, Prevalence and Phenotypic Burden of Monogenic Arrhythmias

Using Integration of Electronic Health Records With Genetics. *Circ Genom Precis Med* **15**, e003675 (2022).
126. S. W. Kong, Y. W. Hu, J. W. Ho, S. Ikeda, S. Polster, R. John, J. L. Hall, E. Bisping, B. Pieske, C. G. dos Remedios, W. T. Pu, Heart failure-associated changes in RNA splicing of sarcomere genes. *Circ Cardiovasc Genet* **3**, 138-146 (2010).
127. M. P. Collier, J. L. P. Benesch, Small heat-shock proteins and their role in mechanical stress. *Cell Stress Chaperones* **25**, 601-613 (2020).
128. V. Arndt, N. Dick, R. Tawo, M. Dreiseidler, D. Wenzel, M. Hesse, D. O. Fürst, P. Saftig, R. Saint, B. K. Fleischmann, M. Hoch, J. Höhfeld, Chaperone-assisted selective autophagy is essential for muscle maintenance. *Curr Biol* **20**, 143-148 (2010).
129. B. Tedesco, L. Vendredy, V. Timmerman, A. Poletti, The chaperone-assisted selective autophagy complex dynamics and dysfunctions. *Autophagy*, 1-23 (2023).
130. J. Höhfeld, T. Benzing, W. Bloch, D. O. Fürst, S. Gehlert, M. Hesse, B. Hoffmann, T. Hoppe, P. F. Huesgen, M. Köhn, W. Kolanus, R. Merkel, C. M. Niessen, W. Pokrzywa, M. M. Rinschen, D. Wachten, B. Warscheid, Maintaining proteostasis under mechanical stress. *EMBO Rep* **22**, e52507 (2021).
131. B. Del Valle-Pérez, V. G. Martínez, C. Lacasa-Salavert, A. Figueras, S. S. Shapiro, T. Takafuta, O. Casanovas, G. Capellà, F. Ventura, F. Viñals, Filamin B plays a key role in vascular endothelial growth factor-induced endothelial cell motility through its interaction with Rac-1 and Vav-2. *J Biol Chem* **285**, 10748-10760 (2010).
132. Z. Mao, F. Nakamura, Structure and Function of Filamin C in the Muscle Z-Disc. *Int J Mol Sci* **21**, (2020).
133. V. Guergueltcheva, K. Peeters, J. Baets, C. Ceuterick-de Groote, J. J. Martin, A. Suls, E. De Vriendt, V. Mihaylova, T. Chamova, L. Almeida-Souza, E. Ydens, C. Tzekov, G. Hadjidekov, M. Gospodinova, K. Storm, E. Reyniers, S. Bichev, P. F. van der Ven, D. O. Fürst, V. Mitev, H. Lochmüller, V. Timmerman, I. Tournev, P. De Jonghe, A. Jordanova, Distal myopathy with upper limb predominance caused by filamin C haploinsufficiency. *Neurology* **77**, 2105-2114 (2011).
134. M. J. O'Neill, S. N. Chen, L. Rumping, R. Johnson, M. van Slegtenhorst, A. M. Glazer, T. Yang, J. F. Solus, J. Laudeman, D. W. Mitchell, L. R. Vanags, B. M. Kroncke, K. Anderson, S. Gao, J. A. J. Verdonschot, H. Brunner, D. Hellebrekers, M. R. G. Taylor, D. M. Roden, M. W. Wessels, R. H. Lekanne Dit Deprez, D. Fatkin, L. Mestroni, M. B. Shoemaker, Multicenter Clinical and Functional Evidence Reclassifies a Recurrent Non-canonical Filamin C Splice-altering Variant. *Heart Rhythm*, (2023).
135. A. E. Goetz, M. Wilkinson, Stress and the nonsense-mediated RNA decay pathway. *Cell Mol Life Sci* **74**, 3509-3531 (2017).
136. E. Kania, B. Pająk, A. Orzechowski, Calcium homeostasis and ER stress in control of autophagy in cancer cells. *Biomed Res Int* **2015**, 352794 (2015).
137. M. Eghbali, R. Deva, A. Alioua, T. Y. Minosyan, H. Ruan, Y. Wang, L. Toro, E. Stefani, Molecular and functional signature of heart hypertrophy during pregnancy. *Circ Res* **96**, 1208-1216 (2005).
138. J. Li, S. Umar, M. Amjedi, A. Iorga, S. Sharma, R. D. Nadadur, V. Regitz-Zagrosek, M. Eghbali, New frontiers in heart hypertrophy during pregnancy. *Am J Cardiovasc Dis* **2**, 192-207 (2012).
139. D. Sellung, L. Heil, N. Daya, F. Jacobsen, J. Mertens-Rill, H. Zhuge, K. Döring, M. Piran, H. Milting, A. Unger, W. A. Linke, R. Kley, C. Preusse, A. Roos, D. O. Fürst, P. Ven, M. Vorgerd, Novel Filamin C Myofibrillar Myopathy Variants Cause Different Pathomechanisms and Alterations in Protein Quality Systems. *Cells* **12**, (2023).